

## ABSTRACT

Title of Document:                   SORPTION OF YTTRIUM AND THE RARE  
EARTH ELEMENTS ON THE MARINE  
MACROALGA *ULVA LACTUCA*

Alison M. Zoll, Ms. of Science, 2011

Directed By:                         Assistant Professor Johan Schijf, Marine  
Environmental and Estuarine Science

Trace metal interactions with organic matter are relatively poorly understood, though organic matter is ubiquitous in aquatic environments and likely instrumental in controlling metal geochemistry. To better understand the mechanisms underlying metal interactions with organic substrates, sorption of Yttrium and the Rare Earth Elements (YREEs) on *Ulva lactuca*, a marine macroalga, was studied in batch laboratory experiments at different ionic strengths over a large pH range (2.7 – 8.5). At all ionic strengths and experimental pH values, colloid-bound YREEs make up a substantial portion of sorbed metals as described by a two-site Langmuir model, which has implications for bioremediation and metal sorption studies. YREE sorption on *U. lactuca* can be modeled as a function of pH with a three-site non-electrostatic surface complexation model, and patterns of conditional YREE complexation constants were used to determine possible identities of metal-complexing functional groups.

SORPTION OF YTTRIUM AND THE RARE EARTH ELEMENTS ON THE  
MARINE MACROALGA *ULVA LACTUCA*

By

Alison M. Zoll

Thesis submitted to the Faculty of the Graduate School of the  
University of Maryland, College Park, in partial fulfillment  
of the requirements for the degree of  
Master of Science  
2011

Advisory Committee:  
Assistant Professor Johan Schijf, Chair  
Associate Professor Carys L. Mitchelmore  
Professor Neil V. Blough

© Copyright by  
Alison M. Zoll  
2011

## Acknowledgements

The completion of this thesis would not have been possible without the help and support of many special people. First I would like to extend my sincerest thanks to my committee members, Drs. Johan Schijf, Carys Mitchelmore, and Neil Blough for their thoughtful ideas, comments and insights as this project developed and came to completion. I'd especially like to thank my major advisor, Johan Schijf, for introducing me to the world of trace metal chemistry and sparking my interest for basic scientific research. His guidance and patience with my work has always been remarkably helpful for my professional and personal growth and working in his laboratory has always been very enjoyable. I would also like to thank Fredrika Moser, who ultimately steered me towards a career in environmental chemistry with the Maryland Sea Grant REU program.

My thanks go out to my fellow lab-mates, Emily Christenson and Kathleen Marshall for all their help and support in the Schijf lab, both for guidance at the lab bench and for many insightful discussions about my research. I am especially grateful to Emily Christenson for her assistance in conducting the DOC sorption experiments. I am also grateful to Nancy Kaumeyer of CBL's Nutrient Analytical Services Laboratory for conducting DOC analysis on a number of my samples. Portions of this thesis were informed by summer work from undergraduates Lauren Hunker and Alina Ebling – thank you for providing me with important background information for my own analyses.

Finally, I would like to thank my fellow students and coworkers at CBL, friends in Maryland, and family in Pennsylvania for emotional and social support during my master's work. I especially want to thank my husband, Jim, for taking a chance and moving to the Solomons area with me. Your unwavering love and encouragement continues to be a source of strength for all that I do.

## Table of Contents

|  |     |
|--|-----|
| Acknowledgements.....  | ii  |
| Table of Contents.....   | iii |
| List of Tables.....  | v   |
| List of Figures.....   | vii |
| Chapter 1: Introduction.....   | 1   |
| 1.1. Metal sorption: definitions and basic concepts.....   | 1   |
| 1.2. Metal sorption on organic matter.....   | 4   |
| 1.3. <i>Ulva lactuca</i> .....   | 8   |
| 1.3.1. <i>Morphology, ecology, and reasons for use as model organic substrate</i> .....  | 8   |
| 1.3.2. <i>Possible sorption mechanisms, surface chemistry, and trace metal interactions</i><br>.....                                   | 11  |
| 1.4. Yttrium and the rare earth elements: advantages for metal sorption studies.....   | 14  |
| 1.5. Research overview.....  | 18  |
| Chapter 2: The effect of colloids on the calculation of distribution coefficients for metal<br>sorption studies on organic matter..... | 20  |
| 2.1. Abstract.....   | 20  |
| 2.2. Introduction.....   | 21  |
| 2.3. Materials and Methods.....  | 24  |
| 2.3.1. <i>Experimental setup and materials preparations</i> .....  | 24  |
| 2.3.2. <i>Sorption experiments as a function of pH</i> .....   | 25  |
| 2.3.3. <i>Ultrafiltration and Sep-Pak C<sub>18</sub> Extractions</i> .....   | 27  |
| 2.3.4. <i>DOC analysis</i> .....   | 28  |
| 2.3.5. <i>ICP-MS analysis</i> .....  | 29  |
| 2.3.6. <i>Calculating distribution coefficients</i> .....  | 29  |
| 2.4. Results and Discussion.....   | 30  |
| 2.4.1. <i>DOC measurements and effect of colloid-bound YREEs on distribution<br/>coefficients</i> .....                                | 30  |
| 2.4.2. <i>YREE interaction with the colloidal fraction</i> .....   | 33  |
| 2.4.3. <i>Derivation and fits of the colloid correction model</i> .....  | 39  |
| 2.4.4. <i>Corrected distribution coefficients</i> .....  | 43  |
| 2.4.5. <i>Linear fits with pH</i> .....  | 49  |
| 2.5. Conclusions.....  | 52  |
| 2.6. Data Tables.....  | 54  |
| Chapter 3: Application of a non-electrostatic surface complexation model.....  | 68  |
| 3.1. Abstract.....   | 68  |
| 3.2. Introduction.....   | 69  |
| 3.3. Materials and Methods.....  | 73  |
| 3.3.1. <i>Reversibility experiment</i> .....   | 73  |
| 3.3.2. <i>Calculating distribution coefficients</i> .....  | 73  |
| 3.4. Results and Discussion.....   | 74  |
| 3.4.1. <i>Reversibility experiment</i> .....   | 74  |
| 3.4.2. <i>The non-electrostatic surface complexation model: derivation and fits</i> .....  | 75  |
| 3.4.3. <i>Interpretation of NEM best-fit parameters</i> .....  | 85  |

|   |     |
|---|-----|
| 3.4.4. <i>The modified low-ionic-strength NEM</i> .....                               | 90  |
| 3.5. Potential benefits of the NEM for biomonitoring and bioremediation efforts ..... | 94  |
| 3.6. Conclusions.....   | 96  |
| 3.7. Concluding remarks and future work .....   | 98  |
| 3.8. Data tables.....   | 101 |
| Bibliography .....  | 109 |

## List of Tables

Table 1.1. Summary of  $pK_a$  values and possible site identities from potentiometric titrations of various model organic organisms.

Table 1.2. Basic YREE properties including atomic number ( $Z$ ), atomic weight, and trivalent ionic radius for coordination number 6 (SHANNON, 1976).

Table 2.1. Dissolved organic carbon (DOC) concentrations in experimental solutions. <sup>a</sup> Sample sequentially filtered through 1  $\mu\text{m}$  GF/F filter and 0.22  $\mu\text{m}$  filter. <sup>b</sup> Short exposure test (see text for explanation).

Table 2.2. Fractions of truly dissolved metal ( $< 3$  kDa) as percentages of originally measured dissolved concentration ( $< 0.22$   $\mu\text{m}$ ). <sup>a</sup> sample extracted with Sep-Pak  $C_{18}$  columns (see text for explanation). <sup>b</sup> Fresh *U. lactuca* tissue. <sup>c</sup> Experiment performed in 0.5 M NaCl + 0.01 M  $\text{CaCl}_2$  matrix.

Table 2.3. Best-fit parameters for non-linear regressions of ultracentrifuge data (Table 2.2) using Eq. (2.12).

Table 2.4. Corrected and uncorrected  $\log K_S$  values at 0.05 M ionic strength. <sup>a</sup> Sample equilibrated for 30 minutes after adding *U. lactuca*.

Table 2.5. Corrected and uncorrected  $\log K_S$  values at 0.5 M ionic strength. <sup>a</sup> Sample equilibrated for 30 minutes after adding *U. lactuca*. <sup>b</sup> Experiment performed in 0.5 M NaCl + 0.01 M  $\text{CaCl}_2$  matrix.

Table 2.6. Corrected and uncorrected  $\log K_S$  values at 5.0 M ionic strength. <sup>a</sup> Sample equilibrated for 30 minutes after adding *U. lactuca*.

Table 2.7. Best-fit slopes from linear regressions of  $\log K_S$  vs. pH data (Tables 2.4 – 2.6).

Table 3.1. YREE hydrolysis constants ( $\log \beta_1^*$ ) and YREE-chloride stability constants ( $\log_{Cl}\beta_1$ ) calculated for  $I = 0.05, 0.5$  and  $5.0$  M ionic strength (KLUNGNESS and BYRNE, 2000; LUO and BYRNE, 2001).

Table 3.2. Acid dissociation constants as determined from potentiometric titrations of BCR-279 (SCHIJF and EBLING, 2010). These values were used to constrain NEM fits (Eq. 3.25 for 0.5 and 5.0 M data, Eq. 3.34 for 0.05 M data).

Table 3.3.  $\log K_S$  values in 0.05 M ionic strength, calculated using Eq. (3.1) and corrected for  $\text{MOH}^{2+}$  and  $\text{MCl}^{2+}$  complexation (Eq. 3.14). <sup>a</sup> Samples not included in NEM fits.

Table 3.4. Distribution coefficients in 0.5 M ionic strength, calculated using Eq. (3.1) and corrected for  $\text{MOH}^{2+}$  and  $\text{MCl}^{2+}$  complexation (Eq. 3.14). <sup>a</sup> Samples not included in NEM fits. <sup>b</sup> Fresh *U. lactuca* tissue samples.

Table 3.5. Log  $K_S$  values in 5.0 M ionic strength, calculated using Eq. (3.1) and corrected for  $\text{MOH}^{2+}$  and  $\text{MCl}^{2+}$  complexation (Eq. 3.14). <sup>a</sup> Samples not included in NEM fits.

Table 3.6. Best-fit parameters for log  $K_S$  vs. pH data (Tables 3.4 – 3.5) using the NEM (Eq. 3.25) for 0.5 and 5.0 M data, with log  $K_x$  values set equal to those found in Table 3.3.

Table 3.7. Best-fit parameters for log  $K_S$  vs. pH data (Table 3.3) using the modified NEM (Eq. 3.34) for 0.05 M data, with log  $K_C$  set equal to 9.433.

Table 3.8. Calculated YREE stability constants for  $\text{M}^{3+}$  complexation with groups A, B, and C (log  $\beta_A$ , log  $\beta_B$  and log  $\beta_C$ , respectively) and  $\text{MOH}^{2+}$  complexation with group C (log  $\beta_C^*$ ). No log  $\beta_B$  values are shown for 0.05 M ionic strength, whose model equation (Eq. 3.34) included only group C and a combined term for groups A and B (log  $\beta_a$ ).

## List of Figures

Figure 1.1. A. The most commonly identified organic functional groups responsible for metal complexation in bacteria and fungi. Shown from left to right are carboxyl, sulfonyl, phosphate, amine and carboxylic acid, the simplest of phenols. Phenols include any compound where hydroxyl groups are bound to aromatic rings. B. Structure of sulfate functional groups, which are commonly found on marine macroalgae.

Figure 1.2. A. *U. lactuca* frond collected from Dorset, England (LOUGHNANE et al., 2008). B. Cross section of *U. lactuca* thallus shows a flat 2-cell layer throughout (NORRIS, 2010).

Figure 1.3. Structure of sulfated polysaccharide units isolated from *U. lactuca* (PERCIVAL, 1979), where sulfate or carboxyl groups could participate in sorption.

Figure 2.1. Distribution coefficients as a function of pH for Sm sorption on *U. lactuca* standard BCR-279 at different ionic strengths. Separation into “dissolved” and “particulate” metal fractions was achieved with 0.22  $\mu\text{m}$  filters. Slopes from linear regressions are shown in parentheses. For 0.05 M, linear regressions were performed separately for pH < 4.6 and pH > 4.6; slope shown is for the lower pH data.

Figure 2.2. Dissolved organic carbon (DOC) concentrations in 0.05, 0.5 and 5.0 M NaCl experimental solutions containing *U. lactuca*. Sequentially filtered samples (dashed lines) were filtered through 1  $\mu\text{m}$  GF/F filter and 0.22  $\mu\text{m}$  filters. Short test samples (thick lines) were taken moments after suspending *U. lactuca* in unacidified 0.05, 0.5, or 5.0 M NaCl. Data shown at pH ~2.6 were blank samples taken before addition of *U. lactuca*.

Figure 2.3. Ultracentrifuge data for representative YREEs at all ionic strengths. The y-axis, “% [M] < 3 kDa”, is the percentage of truly dissolved metal (< 3 kDa) in the 0.22  $\mu\text{m}$  filtered sample. Hatched 0.5 M points are from the Ca/Na matrix experiment. A fresh *U. lactuca* sample in 0.5 M NaCl (open square) and Sep-Pak C<sub>18</sub> column sample in 0.05 M NaCl (open triangle) are also shown. Curves represent fits of the data (Table 2.2) with Eq. (2.12) at each ionic strength. Data from the Ca/Na matrix experiment were pooled with the 0.5 M NaCl data for fits of Eq. (2.12) at mid-ionic strength, while fresh *U. lactuca* and Sep-Pak samples were excluded from the fits

Figure 2.4. Polysaccharide structure of *U. lactuca* cell walls, where Ca<sup>2+</sup> creates cross-linkages between rhamnose subunits (WEBSTER and GADD, 1996a).

Figure 2.5. Distribution coefficients for select YREEs at 0.05 M ionic strength. Corrected log K<sub>S</sub> (closed circles) and uncorrected log K<sub>S</sub> (open circles) were calculated with and without accounting for colloid-bound metal, respectively.

Figure 2.6. Distribution coefficients for select YREEs at 0.5 M ionic strength. Corrected log K<sub>S</sub> (closed circles) and uncorrected log K<sub>S</sub> (open circles) were calculated with and without accounting for colloid-bound metal, respectively.

Figure 2.7. Distribution coefficients for select YREEs at 5.0 M ionic strength. Corrected

$\log K_S$  (closed circles) and uncorrected  $\log K_S$  (open circles) were calculated with and without accounting for colloid-bound metal, respectively.

Figure 2.8. A. YREE distribution coefficient patterns in 0.05 M NaCl. Uncorrected (open circles) and corrected (closed circles)  $\log K_S$  values are shown for comparison. B. Patterns of the fraction of colloid-bound YREEs (> 3 kDa) in 0.05 M NaCl, shown as a percentage of the < 0.22 fraction. Solution pH at the time of sampling is given to the right of each pattern.

Figure 2.9. Linear regressions of corrected  $\log K_S$  vs. pH data for Sm at 0.05 M (closed circles), 0.5 M (open circles), and 5.0 M (triangles) ionic strengths. Corrected and uncorrected slopes for Sm are shown in inset and represent the number of protons released per YREE cation sorbed, averaged over the experimental pH range.

Figure 3.1. Reversibility experiment performed in 0.5 M NaCl on *U. lactuca* dried standard. Closed triangles represent samples taken after increasing solution pH, while open triangles are samples taken after decreasing solution pH. Note that both sets of samples follow the same sorption curve.

Figure 3.2. Regressions of  $\log K_S$  vs. pH data for Samarium using the NEM (Eq. 3.26 and 3.35). Low pH data (< 3) and fresh *U. lactuca* samples (blue circles) were not included in the fits. Dashed red lines represent 95% confidence intervals.

Figure 3.3. Ratios of measured to predicted values of  $\log K_S$  for Lu, shown as a function of pH. Predicted values were calculated using Eq. (3.26) (0.5 and 5.0 M data), Eq. (3.35) (0.05 M data) and best-fit parameters from Table 3.6 – 3.7.

Figure 3.4. Functional group stability constants for  $M^{3+}$  complexation with groups A, B, and C ( $\log \beta_A$ ,  $\log \beta_B$  and  $\log \beta_C$ , respectively) and  $MOH^{2+}$  complexation with group C ( $\log \beta_C^*$ ) across the YREE series. Each panel depicts complexation with one group, shown for 0.5 and 5.0 M ionic strengths. YREE complexation with hydroxide (YREE-OH) and acetate (YREE-OAc) are shown for comparison.

Figure 3.5. Linear free-energy relations (LFER) between group A ( $\log \beta_A$ ) and acetate ( $\log OAc\beta_1$ ) stability constants and group C ( $\log \beta_C$ ) and hydroxide ( $\log \beta_1^*$ ) stability constants for 0.5 and 5.0 M ionic strengths. Dashed lines represent 95% confidence intervals.

Figure 3.6. Functional group stability constants for  $M^{3+}$  complexation with groups A and B ( $\log \beta_a$ ), group C ( $\log \beta_C$ ) and  $MOH^{2+}$  complexation with group C ( $\log \beta_C^*$ ) across the YREE series in 0.05 M NaCl. YREE complexation with hydroxide (YREE-OH) and acetate (YREE-OAc) and shown for comparison.

Figure 3.7. Linear free-energy relations (LFER) between groups A and B ( $\log \beta_a$ ) and acetate ( $\log OAc\beta_1$ ) stability constants and group C ( $\log \beta_C$ ) and hydroxide ( $\log \beta_1^*$ ) stability constants for 0.05 M ionic strength. Dashed lines represent 95% confidence intervals.

# Chapter 1: Introduction

## 1.1. Metal sorption: definitions and basic concepts

Trace metal mobility and solubility in natural waters are controlled by two opposing metal complexation processes: metal complexation with dissolved ligands in solution and metal sorption on solid surfaces. The term “sorption” refers to reversible and irreversible chemical processes at the solid-water interface, including ion exchange, surface complexation, surface precipitation and, in the case of living cells, metal uptake and internalization. The equilibrium that exists between solution complexation and surface sorption dictates a metal’s geochemistry and ultimate fate in the environment: complexation with dissolved ligands tends to solubilize metals while complexation with solid substrates tends to immobilize them in the particulate phase. This has especially important implications for toxic metals in aquatic environments, as the degree of sorption on surfaces can determine whether metals are sequestered in the sediments or remain mobile in solution to possibly contaminate additional areas. The ability to predict metal partitioning between sediments and solution not only informs a general understanding of metal geochemical cycling, but also helps scientists and policy makers in determining effective remediation strategies for contaminated environments.

Metal-ligand interactions in solution have been well studied, and the mechanisms and thermodynamics governing these processes are well understood. There are comprehensive databases of metal complex stability constants that have been measured for many different metals and a large variety of ligands (for example, SMITH and MARTELL, 2004). However, metal sorption on solid substrates, particularly organic

surfaces, is a relatively new area of study still in need of research. Metal sorption on any surface is inherently difficult to study as basic questions concerning the number, types and densities of metal-complexing functional groups, plus their degree of protonation, must be answered before sorption processes can be modeled or mechanistically explained. Even the definition of what constitutes a sorbed or dissolved metal can be difficult to determine, due to continuing improvements in filtration techniques which have allowed scientists to separate out increasingly smaller colloidal metals from particulates.

Reversible metal sorption on solid substrates (which is the focus of this project) occurs through different types of reactions and interactive forces at the solid-water interface. The intermolecular forces that govern reversible metal sorption include surface complexation reactions, which can lead to electrostatic interactions between charged metal ions and surface sites and the possible formation of coordinative bonds between metals and the surface (STUMM and MORGAN, 1996). Proton-bearing functional groups on both inorganic and organic surfaces, such as surface hydroxyl groups (S-OH) or surface amine groups (S-NH<sub>2</sub>), are the dominant participants in metal sorption. Metal sorption then occurs through functional group deprotonation, which makes them available for metal sorption. The process by which a metal ion (M) exchanges with (n) protons from a surface functional group (S-XH<sub>n</sub>) is traditionally represented with reactions of the form (XUE et al., 1988):



where the product S-XM of reaction 1.1 is the generic example of a metal ion complexing with a surface functional group.

Because the metal ions exchange with protons, pH is an essential consideration in these types of reactions and consequently in any metal sorption study. For metal cations, low pH suppresses metal sorption and increases dissolved metal concentrations, while high pH has the opposite effect. The pH above which a functional group is most likely to participate in sorption is determined by its acid dissociation constant ( $K_a$ ), shown here for the dissociation of a hydroxide group on a surface:



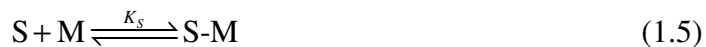
$$K_a = \frac{[\text{S-O}^-][\text{H}^+]}{[\text{S-OH}]} \quad (1.3)$$

Acid dissociation constants are equilibrium constants that represent the pH where a functional group is equally likely to be either protonated or deprotonated in solution. The degree of deprotonation will ultimately depend on the free hydrogen ion concentration ( $[\text{H}^+]$ ), or pH. For convenience,  $K_a$ s are often expressed on a logarithmic scale, as  $\text{p}K_a = -\log K_a$ .

In addition to  $\text{p}K_a$ s, distribution coefficients ( $K_s$ ) are a commonly calculated quantity in metal sorption studies. A distribution coefficient describes a metal's distribution between the solid and the solution and is calculated as the ratio of metal bound to the surface ( $[\text{S-M}]$ ) to the dissolved metal concentration in solution ( $[\text{M}]$ ). Distribution coefficients can be expressed as equilibrium constants (Eq. 1.4) when dividing by the concentration of functional groups on the solid surface available for metal binding ( $[\text{S}]$ ):

$$K_s = \frac{[\text{S-M}]}{[\text{M}][\text{S}]} \quad (1.4)$$

which corresponds to the reaction



The distribution coefficient therefore quantifies a metal's degree of sorption on a particular surface. Distribution coefficients depend on solution conditions such as ionic strength, pH, temperature, and alkalinity, all of which can enhance or suppress metal sorption.

### 1.2. Metal sorption on organic matter

In natural systems, metal sorption on organic substrates is typically more important than sorption on inorganic substrates as the majority of surfaces are either organic or coated with organic matter (LODER and LISS, 1985). BYRNE and KIM (1990) observed that glass surfaces stored in natural seawater rapidly acquired organic coatings that sorb metals in a manner similar to organic surfaces. This suggests that organic functional groups are present on inorganic and organic surfaces and play an important role in metal surface complexation. Sorption on organic surfaces is inherently difficult to study, as organic surfaces are usually poorly characterized in terms of functional group identities and properties (i.e. pK<sub>a</sub> values), whereas this information is often available for inorganic surfaces. Significant progress has been made towards describing metal sorption on inorganic surfaces such as clays (e.g., montmorillonite), ferric hydroxide, and aluminum hydroxide (for a general review of trace metal interactions with inorganic surfaces and minerals, see BROWN and PARKS, 2001). These inorganic substrates have the advantage of being relatively chemically simple in terms of their functional group identities (for example, iron oxide minerals contain hydroxide as the sole surface functional group), and the properties of these functional groups are better characterized

than those on organic substrates.

In order to better understand metal-organic interactions, two types of organic matter are commonly selected for study. Some utilize homogenized organic substrates such as natural organic matter standards or colloidal humic acid mixtures, while others focus on a single organism. Most metal-organic sorption studies in this latter category have focused on freshwater and terrestrial organisms, such as bacteria, ferns, fungi, and yeast (FOWLE and FEIN, 1999; WANG et al., 2001; BOYANOV et al., 2003; DING et al., 2005; WEI et al., 2005a, b; NAEEM et al., 2006; HA et al., 2010; MISHRA et al., 2010). These studies have focused on identifying metal-binding functional groups and determining binding-site  $pK_a$  values (Table 1.1), and many of the organisms have a high affinity for metal ions in solution, making it easy to measure relative changes in metal concentration. Sorption modeling in these studies often use empirical partitioning approaches (i.e. Freundlich isotherms), where sorption is described in terms of a generic partition between the solution and the surface, without consideration for different types of surface sites or influence from solution chemistry. Unfortunately, this approach provides only limited mechanistic and stoichiometric information about surface and solution reactions (DAVIS and KENT, 1990).

Despite the wide range of organisms studied, there is remarkable consistency in the identity and properties of the functional groups that interact with trace metals. Similar  $pK_a$  values across Gram-negative bacteria, Gram-positive bacteria (which differ fundamentally in their extracellular molecular structure), and fungal species suggest similar functional groups are present to participate in metal sorption. Authors often assign similar site identities based on the similar  $pK_a$  values, consistent with the known

composition of cellular organic matter (Table 1.1). These functional group identities in some cases have been confirmed with spectroscopic techniques (for example, as in MISHRA et al., 2010). The four main metal-complexing functional groups generally identified in freshwater and terrestrial species are sulfonyls, carboxylates, phosphates, and amines or phenols (Fig. 1.1A).

**Table 1.1: Summary of pK<sub>a</sub> values and possible site identities from potentiometric titrations of various model organic organisms.**

|                     | <i>P. agglomerans</i> <sup>a</sup><br>(Gram-negative) | <i>S. oneidensis</i> <sup>b</sup> | <i>B. subtilis</i> <sup>c</sup><br>(Gram-positive) | <i>S. cerevisiae</i> <sup>d</sup><br>(fungus) | possible<br>site identity |
|---------------------|---|-----------------------------------|--|---|---------------------------|
| pK <sub>a</sub> (1) | –   | 3.3 ± 0.2                         | 3.3  | 3.4 ± 0.4                                     | sulfonyl                  |
| pK <sub>a</sub> (2) | 4.3 ± 0.2   | 4.8 ± 0.2                         | 4.7  | 5.0 ± 0.2                                     | carboxyl                  |
| pK <sub>a</sub> (3) | 6.9 ± 0.5   | 6.7 ± 0.4                         | 6.8  | 6.8 ± 0.4                                     | phosphate                 |
| pK <sub>a</sub> (4) | 8.9 ± 0.5   | 9.4 ± 0.5                         | 8.9  | 8.9 ± 0.6                                     | amine/phenol              |

*a* NGWENYA et al. (2003); *b* MISHRA et al. (2010); *c* FEIN et al. (2005); *d* NAEEM et al. (2006)

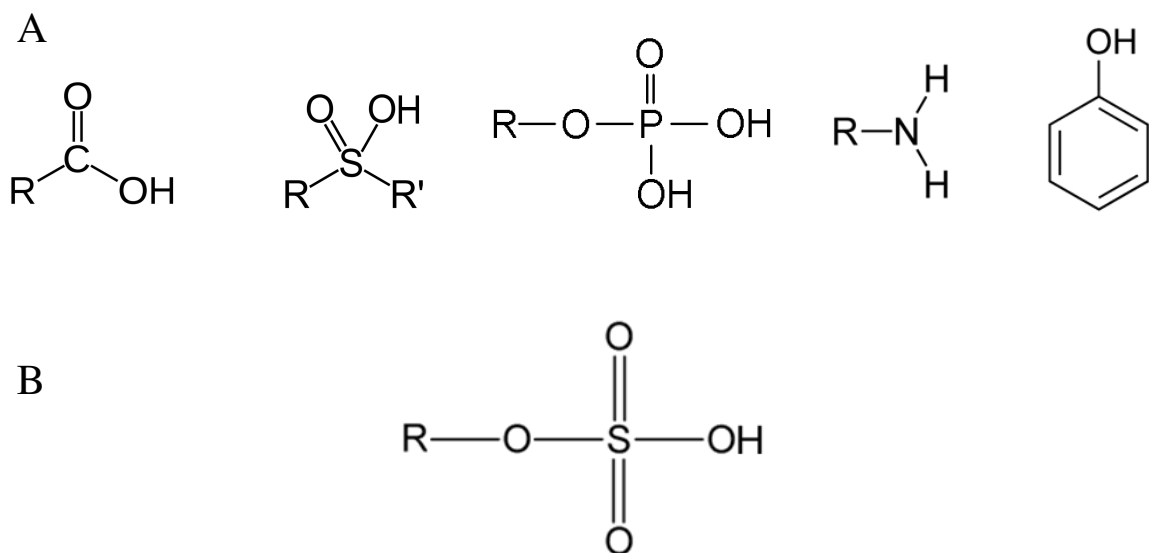


**Figure 1.1. A. The most commonly identified organic functional groups responsible for metal complexation in bacteria and fungi. Shown from left to right are carboxyl, sulfonyl, phosphate, amine and carboxylic acid, the simplest of phenols. Phenols include any compound where hydroxyl groups are bound to aromatic rings. B. Structure of sulfate functional groups, which are commonly found on marine macroalgae.**

Sulfonyl groups generally have low  $pK_{a,s}$ , and have been found in both Gram-negative and Gram-positive bacteria to participate in cadmium sorption at low pH (BOYANOV et al., 2003; HA et al., 2010; MISHRA et al., 2010). Sulfonyl groups may also be present on *Saccharomyces cerevisiae* (a fungal species), whose low  $pK_a$  matches those found in bacterial species for sulfonyl groups (NAEEM et al., 2006). Carboxylate groups participate in Cd sorption in Gram-positive and Gram-negative bacteria (*Bacillus subtilis*, *Shewanella oneidensis*, *Pantoea agglomerans*) and lead, copper and cadmium sorption on the fungal species *Aspergillus niger* (KAPOOR and VIRARAGHAVAN, 1997; BOYANOV et al., 2003; NGWENYA et al., 2003; HA et al., 2010; MISHRA et al., 2010). Carboxyl  $pK_{a,s}$  are usually found in the range of 4 – 6 on these species. Phosphate groups generally have  $pK_{a,s} \sim 6$  and have been identified in metal sorption studies on bacteria and fungi as well (BOYANOV et al., 2003; NGWENYA et al., 2003; NAEEM et al., 2006; HA et al., 2010; MISHRA et al., 2010). High  $pK_a$  (9 – 12) groups are typically attributed to nitrogen-containing amines or to phenol groups, which are common across all types of organic matter. High- $pK_a$  groups have been found to participate in sorption of many different metals (Cd, Pb, Th, U, Zn) on both bacteria and fungi (TSEZOS and VOLESKY, 1982a, b; GADD, 1990; KAPOOR and VIRARAGHAVAN, 1997; BOYANOV et al., 2003; NAEEM et al., 2006; HA et al., 2010; MISHRA et al., 2010).

Sorption studies with marine species are far less common than those for freshwater organisms, perhaps due to inherent difficulties associated in isolating and culturing organisms such as marine bacteria. The majority of marine work has focused on macroalgae, such as the brown algae *Sargassum fluitans*, *Petalonia fascia*, and *Colpomenia sinuosa*, as well as the green alga *Ulva fasciata* (SCHIEWER and VOLESKY,

1996; SCHIEWER and WONG, 2000), all of which have similar functional groups participating in metal sorption as those found in freshwater and terrestrial organisms. Both *U. fasciata* and *S. fluitans* are known to contain carboxylate and sulfate groups (Fig. 1.1B), and SCHIEWER and VOLESKY (1996) were able to model pH-dependent binding of Zn, Cu and Cd to *S. fluitans* assuming the presence of one carboxyl and one sulfate site.

### 1.3. *Ulva lactuca*

#### *1.3.1. Morphology, ecology, and reasons for use as model organic substrate*

*Ulva lactuca* L., more commonly known as “sea lettuce” (Fig. 1.2A) is a promising model of marine organic substrates in metal sorption studies. It is a hardy organism that can easily tolerate a range of solution conditions, which allows for a variety of experimental conditions. It is found throughout the world’s oceans, from temperate to tropical climates (GUIRY and GUIRY, 2010). As a benthic species, *U. lactuca* grows in coastal waters attached to rocks, pilings, and other solid substrates in shallow areas, and it grows especially well where there are high nutrient levels, such as nitrate or ammonia (NASR and ALEEM, 1948; SAWYER, 1965). It can tolerate a range of salinities (0–33 ppt) and is often found in estuaries, where it can easily cope with the rapid changes in salinity commonly found in these environments (DICKINSON et al., 1982).

Morphologically, *U. lactuca* is a simple organism. The flat undulating fronds (thalli) are typically 2–5 cm in length (though fronds may grow as long as 40–85 cm) and anywhere from 40–55 µm thick (NORRIS, 2010). The thallus may be thicker closer to the holdfast (up to 100 µm), but the fronds are only two cells thick at all points (Fig. 1.2B). This feature makes *U. lactuca* especially suited for sorption studies (STANLEY and

BYRNE, 1990). In solution, the fronds offer a large surface area available for metal sorption, yet the two-cell layer means that the organism is essentially “all surface” in that each cell is exposed to the same solution conditions. Unlike higher organisms such as vascular plants, *U. lactuca* also has cellular simplicity in that it has no specialized cells or internal structures. From a morphologic perspective, it is essentially a colony of single-cell algae making it similar to single-cell bacteria, which are often used for freshwater trace-metal sorption studies. However, unlike unicellular organisms, the large *U. lactuca* thalli can be easily handled and washed of foreign matter or trimmed to any shape or size.

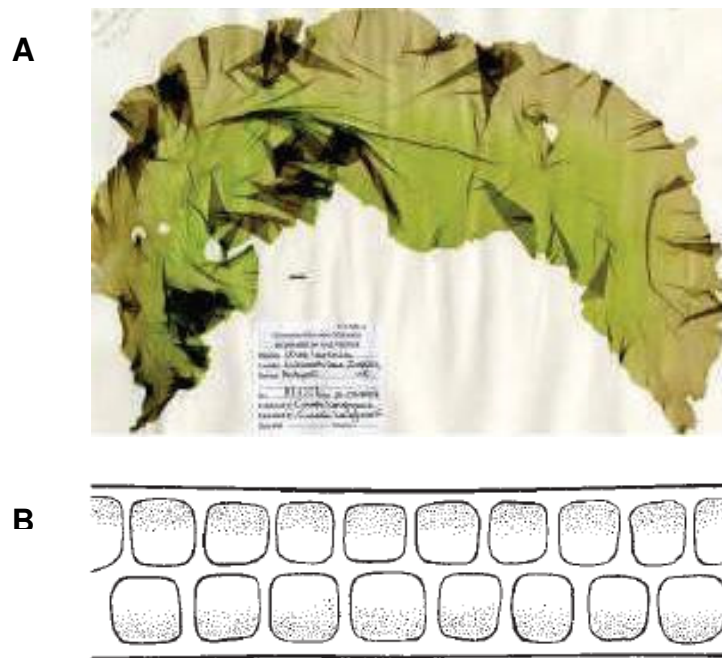


**Figure 1.2. A. *U. lactuca* frond collected from Dorset, England (LOUGHNANE et al., 2008). B. Cross section of *U. lactuca* thallus shows a flat 2-cell layer throughout (NORRIS, 2010).**

There are other characteristics of *U. lactuca* that make it an ideal candidate for controlled laboratory experiments and metal sorption studies. Perhaps most importantly, it has a high affinity for trace metals, similar to other marine algae (WONG et al., 1982;

RAINBOW, 1995). GAUDRY et al. (2007) found that *U. lactuca* not only accumulates heavy metals, but grows well in highly metal-polluted environments. Samples collected in metal polluted coastal waters near urban areas of Hong Kong showed mean Pb concentrations of  $41 \mu\text{g}\cdot\text{g}^{-1}$  (dry weight) in *U. lactuca* tissue (HO, 1990).

Due to its high affinity for trace metals, *U. lactuca* has traditionally been utilized as a trace metal biomonitor. A “trace metal biomonitor species” refers to any organism that accumulates metals in its tissues which can be analyzed to infer the concentration of metals in the organism’s surrounding environment (RAINBOW, 1995). The advantages of measuring metals in a biomonitor species, rather than directly from solution, is that the metal concentrations are generally higher than in the surrounding water (where low concentrations may put the measurement below detection limits), and the result may also suggest what portion of metals are bioavailable in an environment (PHILLIPS, 1977). *In situ* biomonitoring studies with *U. lactuca* have observed wide variation in metal uptake relative to the surrounding water, effects that authors have based on a number of factors such as seasonality, temperature, or salinity (PHILLIPS, 1977). Such variations could likely be explained if the basic chemical mechanisms and properties governing metal sorption on *U. lactuca* were better understood.

Others have looked to *U. lactuca* as a potential biosorbent for removing toxic metals from contaminated areas (SUZUKI et al., 2005; EL-SIKAILY et al., 2007), but such efforts will also be limited without a thorough understanding of the underlying metal sorption mechanisms. This includes knowledge of the functional groups interacting with metal ions and how they are influenced by various environmental parameters such as pH, ionic strength and temperature. The ability to include these parameters in a model that

can predict the extent of metal sorption would allow *U. lactuca* to be a more reliable biomonitor and for a better understanding of its properties as a biosorbent. One early attempt at elucidating the relationship between *U. lactuca* and metal sorption recognized this need by determining linear correlations between concentrations of Cu and Pb in *U. lactuca* tissue and ambient seawater (SEELIGER and EDWARDS, 1977).

### *1.3.2. Possible sorption mechanisms, surface chemistry, and trace metal interactions*

The mechanism for metal uptake in *U. lactuca* will depend on the identity of the metal, and can be either irreversible when uptake into the cell occurs through active metabolic pathways (WANG and DEI, 1999) or reversible when metals become associated with the cell wall through passive, reversible sorption processes (LAU et al., 2003). As is true for most organisms, the alkali and alkaline earth metals sodium, potassium and calcium are actively exchanged across *U. lactuca*'s cell wall (SCOTT and HAYWARD, 1953; HAUG, 1976). Na and K are used to maintain osmotic pressure and charge balance, while Ca is also used to stabilize *U. lactuca*'s polysaccharide structure on its cell wall (HAUG, 1976). It has been shown that other metals interact with live *U. lactuca* in an active manner as well. Uptake of Cu and Cd causes a loss of K ions and an increase of Na ions in live *U. lactuca* cells, which likely occurs due to an increase in the cell wall permeability (WEBSTER and GADD, 1996b). The same metal exposure to freeze dried tissue showed no measurable change in cellular sodium or potassium concentrations, and the authors suggest that metabolic activity may influence the physico-chemical microenvironment around cells and therefore indirectly affect Cu and Cd sorption.

However, for other metals it has been shown that sorption on *U. lactuca* is

consistent between live and dead tissue, suggesting that sorption for some metals occurs through passive, non-metabolically mediated sorption. Stanley and Byrne (1990) studied cerium, europium, gadolinium, ytterbium and zinc sorption on *U. lactuca*, and they state that there was no difference whether they used fresh or previously killed cells, either in relative or absolute metal uptake. As active ion transport requires metabolic energy and therefore living cells, this would suggest that sorption for these metals occurs through passive ion exchange between surface functional group protons and metals. *U. lactuca* has been shown to act as a cation exchange system, for example with Pb sorption on dried algal biomass columns consisting of *U. lactuca*, *Jania rubens* (red alga), and *Sargassum asperifolium* (brown alga) (HAMDY, 2000). These columns produced high Pb uptake capacity (281.8 mg g<sup>-1</sup> dry algal mass) that was nearly 100% reversible after eluting the column with strong acids. Mercury sorption on dried *U. lactuca* biomass columns demonstrated similar behavior with high Hg uptake capacity and full reversal after eluting the columns with sulfuric acid (ZEROUAL et al., 2003). Other algal species have demonstrated cation exchange behavior as well, for example the green macroalga *Enteromorpha intestinalis* (RITCHIE and LARKUM, 1982) and brown algae (KLOAREG et al., 1987).

Previous studies offer insight into *U. lactuca*'s surface chemistry and the functional groups that could participate in metal sorption. There are likely a wide variety of functional groups present on the cell surface, though some will have a much higher affinity for metals than others. Early work found that the cell wall is composed of sulfated polysaccharides (Fig. 1.3), which have sulfate and carboxyl groups available for metal sorption (PERCIVAL and WOLD, 1963; HAUG, 1976; PERCIVAL, 1979). WEBSTER

and GADD (1996a) looked at Cd binding to *U. lactuca* biomass and postulated that Cd was replacing Ca in the cell wall structure through binding to sulfate groups. Later work showed that Cd ions bind to oxygen (WEBSTER et al., 1997), which could be part of sulfate, carboxyl or phosphate groups (WEICH et al., 1989; GREENE and DARNALL, 1990; SHENG et al., 2004), and it has been suggested that phenol or amine groups (at high pH) could also participate in metal sorption (GREENE and DARNALL, 1990).

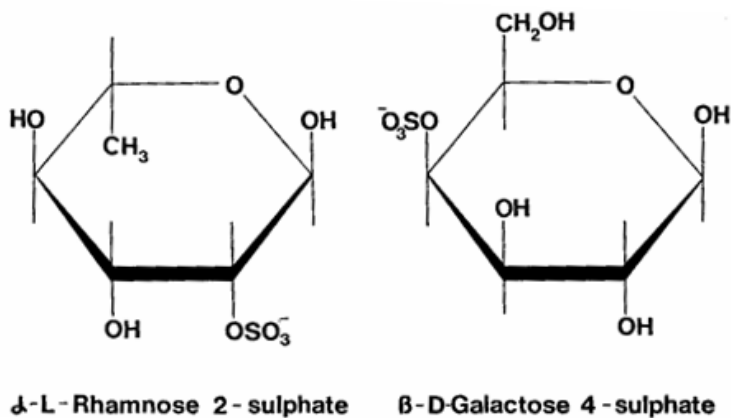


**Figure 1.3.** Structure of sulfated polysaccharide units isolated from *U. lactuca* (PERCIVAL, 1979), where sulfate or carboxyl groups could participate in metal sorption.

In contrast, there are few reports of stoichiometric metal sorption studies on *U. lactuca* under controlled solution conditions (i.e. pH, temperature, etc.) (STANLEY and BYRNE, 1990; WANG and DEI, 1999; COSDEN et al., 2003; TURNER et al., 2007; SARI and TUZEN, 2008). Kinetic sorption experiments have demonstrated that sorption of Cd, Cr, Se and Zn seems to occur through a fast process (possibly due to cation exchange), followed by a slower uptake that is attributed to diffusion into the cell interior (WANG and DEI, 1999). Rapid uptake is also observed for Pd (COSDEN et al., 2003), and other work suggests that Pd uptake is due to internalization in the cells, as sorption was not pH dependent (TURNER et al., 2007). However, sorption for platinum group metals (Rh and

Pt) in TURNER et al. (2007) were pH dependent, suggesting that sorption for these metals is occurring through ion-exchange mechanisms on the cell surface. Sorption of Pb, Cd, Ce, Eu, Gd, Yb and Zn have also been shown to be pH dependent (STANLEY and BYRNE, 1990; SARI and TUZEN, 2008). There is one attempt in the literature to model Pd, Cd, Hg and Pb sorption on *U. lactuca*, though the model assumes only a single sorption site with a  $pK_a$  and site density equivalent to standard humic acid values (TURNER et al., 2008).

#### 1.4. Yttrium and the rare earth elements: advantages for metal sorption studies

Sorption has been widely studied for the group of metals known as the Rare Earth Elements (REEs), which comprise elements from atomic number (Z) 57 through 71. Natural samples of REEs typically occur together with yttrium (Z=39) which has an ionic radius nearly identical to holmium (Z=67). As yttrium is in the same chemical group as lanthanum and exhibits similar chemical properties to the REEs, it is often included in REE sorption studies. Promethium (Z=61) is generally not included in yttrium and REE (YREE) geochemical studies, as it has no stable isotopes.

The YREEs are especially well suited for studying trace metal sorption due to their unique chemical attributes and chemical likeness across the series – for example, YREE charge is always 3+ in solution, yet for lanthanum through lutetium the ionic radii decrease systematically with increasing atomic number (Table 1.2). This gradual decrease is due to the inner 4f electron shell being progressively filled, a feature commonly known as the “lanthanide contraction”. Due to their chemical similarities, systematic changes in sorption between elements can often be explained by the consistent change in ionic radii, because other chemical properties (such as charge effects) are so similar. This makes the

YREEs sensitive probes of metal sorption processes when their relative behavior across the series is compared. Plots of stability constants and distribution coefficients for the entire YREE series give rise to distinct patterns that can be used as diagnostic tools for elucidating the nature of underlying sorption mechanisms. The large 3+ charge means that the YREEs have a high affinity for negatively charged surfaces, making it easy to measure relative changes in metal concentrations. As “hard-acid” (A-type) cations (PEARSON, 1963), the YREEs have a particular affinity for oxygen-bearing groups, which are abundant on both inorganic and organic surfaces.

**Table 1.2. Basic YREE properties including atomic number (Z), atomic weight, and trivalent ionic radius for coordination number 6 (SHANNON, 1976).**

| Element      | Symbol | Z  | Atomic Weight<br>(g·mol <sup>-1</sup> ) | Ionic Radius<br>(Å) |
|--------------|--------|----|---|---------------------|
| yttrium      | Y      | 39 | 88.91                                   | 0.900               |
| lanthanum    | La     | 57 | 138.91                                  | 1.032               |
| cerium       | Ce     | 58 | 140.12                                  | 1.01                |
| praseodymium | Pr     | 59 | 140.91                                  | 0.99                |
| neodymium    | Nd     | 60 | 144.24                                  | 0.983               |
| promethium   | Pm     | 61 | 145                                     | —                   |
| samarium     | Sm     | 62 | 150.36                                  | 0.958               |
| europium     | Eu     | 63 | 151.96                                  | 0.947               |
| gadolinium   | Gd     | 64 | 157.25                                  | 0.938               |
| terbium      | Tb     | 65 | 158.93                                  | 0.923               |
| dysprosium   | Dy     | 66 | 162.50                                  | 0.912               |
| holmium      | Ho     | 67 | 164.93                                  | 0.901               |
| erbium       | Er     | 68 | 167.27                                  | 0.890               |
| thulium      | Tm     | 69 | 168.93                                  | 0.880               |
| ytterbium    | Yb     | 70 | 173.04                                  | 0.868               |
| lutetium     | Lu     | 71 | 174.97                                  | 0.861               |

YREE complexation with both inorganic and synthetic organic ligands has been well characterized. The most important complexing inorganic ligand in seawater is CO<sub>3</sub><sup>2-</sup>, with minor contributions to YREE complexation from other anions such as fluoride,

phosphate, sulfate, hydroxide and chloride (BYRNE and SHOLKOVITZ, 1996). Complexation constants have been directly measured for YREE complexation with carbonate (LUO and BYRNE, 2004), fluoride (SCHIJF and BYRNE, 1999; LUO and BYRNE, 2000; LUO and MILLERO, 2004), hydroxide (KLUNGNESS and BYRNE, 2000), chloride (LUO and BYRNE, 2001), and sulfate (SCHIJF and BYRNE, 2004).

YREE complexation with many dissolved organic ligands has also been well characterized. Though these chemically simplistic compounds have limited bearing on natural organic material, organic ligands likely influence YREE surface chemistry as organic functional groups on particulates and in solution (BYRNE and SHOLKOVITZ, 1996). There are extensive tabulations of stability constants for many of these organic ligands summarized by BYRNE and LI (1995) from the National Institute of Standards and Technology (NIST) database of metal complex stability constants (SMITH and MARTELL, 2004). Some examples include acetate, lactate, glycolic acid, citric acid, malonate, and propionate. Unfortunately, values for many of these constants are not a result of direct measurements of the entire YREE series. Rather, one or two elements were measured and the remaining constants were estimated with linear free-energy relations (LFER). More recently, YREE complexation for the entire series has been measured for oxalate (SCHIJF and BYRNE, 2001). Such stability constants provide valuable background information, as their complexation patterns may be similar to YREE complexation patterns with organic surfaces.

There are a few studies that have looked at YREE interactions with natural organic matter and aquatic organisms, which provide some insight into YREE functional group preferences (though a review of the literature shows no studies of YREE

interactions with marine organic matter). POURRET and MARTINEZ (2009) present experimental results and a sorption model for REE sorption on humic acid, an example of a colloidal organic ligand. While they found that the lanthanides complex primarily with carboxyl groups, there were small site densities of strongly complexing phenol sites contributing to sorption under low metal loading conditions. Carboxyl groups are also important complexing groups for the YREEs in *B. subtilis*, where NGWENYA et al. (2009) found carboxyl and phosphate groups participating in sorption. They claim that light YREEs (La and Nd) bind primarily through phosphate sites while middle and heavy YREEs (Sm, Gd, Er and Yb) complex equally with carboxyl and phosphate sites. TAKAHASHI et al. (2010) found the same result with a study of the entire YREE series, concluding that phosphate sites dominate REE binding, but that with higher YREE:bacteria concentration ratios, carboxylate groups are increasingly important. Other studies have looked at YREE concentrations in terrestrial organisms, such as WEI et al. (2005a, b), who measured YREE concentrations in different cell fractions from *Dicranopteris linearis*, a YREE-hyperaccumulating fern. They found the greatest fraction of YREEs in the cell walls, with Y and La bound primarily to chlorophyll molecules. As with other trace metals, YREEs appear to bind to organic matter through a select group of organic ligands, including carboxylates, phosphates, and phenols. Additionally, because the YREEs are considered “hard” A-type metals according to the classic Pearson theory (PEARSON, 1963), it is likely that sorption will be dominated by binding to hard bases, such as oxygen-bearing hydroxyl or carboxyl groups.

### 1.5. Research overview

Although it is well known that organic matter plays an important role in sorptive processes, there are still many gaps in the literature about the details of its importance for metal sorption. What are the functional groups interacting with trace metals in marine environments? What are the distribution coefficients governing these processes? What are the mechanisms responsible for sorption? In light of the need for a better understanding of metal sorption on organic matter, *U. lactuca* was selected as a proxy for marine organic substrates and used to model YREE sorptive processes. The broad objective of this research was to understand and characterize YREE surface complexation with *U. lactuca*. This was carried out through a series of laboratory sorption experiments under different pH and ionic strength conditions. Results presented in this study will offer further insights into the nature of metal interactions with organic matter, including details about functional group identities, trace metal affinities, and sorption mechanisms. The specific research goals were as follows:

- 1) Determine how distribution coefficients vary as a function of pH and ionic strength. This topic is first addressed in Chapter 2, where it is shown that with decreasing ionic strength there is a substantial portion of sorbed metal bound to colloids, the formation of which is pH-dependent. The chemistry, presence, and nature of this colloidal fraction, as well as their implications for metal sorption experiments, are investigated and discussed.
- 2) Develop a surface complexation model for YREE sorption on *U. lactuca*. Chapter 3 covers the derivation and discussion of such a model that is able to predict and describe YREE sorption on *U. lactuca* as a function of pH and ionic strength.

3) Ascertain equilibrium coefficients (i.e. patterns of conditional surface complexation constants) to characterize and help identify *U. lactuca*'s metal-binding functional groups. The possible identity of the functional groups and their properties are discussed in Chapter 3, where it is shown that three distinct groups participate in YREE sorption.

## Chapter 2: The effect of colloids on the calculation of distribution coefficients for metal sorption studies on organic matter

The results from this chapter were submitted to *The Journal of Colloid and Interface Science* as Schijf, J. and A.M. Zoll, “When dissolved is not truly dissolved—The importance of colloids in studies of metal sorption on organic matter,” 2011, and have been accepted with minor revisions.

### 2.1. Abstract

To accurately calculate distribution coefficients in metal sorption studies, it is necessary to fully separate dissolved from particulate metal. A pH-dependent fraction of colloid-bound metals can bypass commonly used 0.22  $\mu\text{m}$  membrane filters and contribute a significant concentration of effectively sorbed metal to the dissolved fraction, an effect which has not been properly investigated in previous studies of metal sorption on organic matter. I investigated this phenomenon in the context of YREE sorption on *U. lactuca* in 0.05, 0.5 and 5.0 M NaCl, where filtration with 30 kDa and 3 kDa Amicon<sup>®</sup> ultrafiltration centrifuge tubes separated colloidal from truly dissolved metal. At all three ionic strengths, YREEs are truly dissolved (<3 kDa) at low pH, but at higher pH colloid-bound metals (3 kDa – 0.22  $\mu\text{m}$ ) make up a significant portion of the commonly defined “dissolved” fraction (<0.22  $\mu\text{m}$ ). At low ionic strength and pH > 5, distribution coefficients calculated without accounting for colloid-bound metal decrease with increasing pH, a trend which is not seen at the higher ionic strengths. Metal-colloid formation is well described with a pH-dependent two-site Langmuir sorption model, which was used to correct distribution coefficients at all ionic strengths. The correction not only removed the negative sorption trend at low ionic strength, but also revealed that sorption was originally underestimated at the higher ionic strengths, especially at pH > 6. This underestimation was not otherwise apparent in 0.5 and 5.0 M uncorrected data,

which showed the expected increase in sorption with increasing pH. Plots of corrected distribution coefficients vs. pH have similar slopes (0.4 – 0.5) for all three ionic strengths, which suggests that a single sorption mechanism is operative at all ionic strengths and for all YREEs. The presence of colloid-bound metals has implications not only for metal sorption studies, but also for biosorption and bioremediation efforts.

## 2.2. Introduction

Environmental fate and transport of trace metals is ultimately determined by their speciation. Speciation refers to the distribution of a metal among all its chemical forms, including its partitioning between dissolved, colloidal, and particulate fractions. Historically, in the classical “dissolved vs. particulate” scheme, the presence of colloids went largely unrecognized. Since colloids could not be easily separated from solution, they would generally end up in the dissolved fraction, originally defined as any form of the metal that can pass through a 0.45  $\mu\text{m}$  membrane filter (GOLDBERG et al., 1952). More recently, analytical advances allowed the dissolved fraction to be operationally redefined into a truly dissolved and a colloidal fraction, as separated by passage or retention on ultrafilters of varying size cutoffs (BUFFLE et al., 1992). The colloidal fraction consists of particles that are small enough to not be subject to gravitational forces, but large enough to provide a surface to remove trace elements from solution (GUSTAFSSON and GSCHWEND, 1997). The properties and behavior of colloids may determine the bioavailability and mobility of trace metals bound to it. Colloids can aggregate and coagulate into larger particles, causing metals associated with them to behave like particulates (NYFFELER et al., 1984; JANNASCH et al., 1988), though

depending on solution conditions aggregation can be reversible, which may give a colloid-bound metal increased mobility or bioavailability. Therefore, colloid-bound metals can exhibit characteristics of both dissolved and particulate fractions. Given these properties, separating and characterizing colloidal from dissolved metals is necessary to provide thorough descriptions of trace metal bioavailability and cycling in the environment.

It has been long known that colloids play an important role in trace metal sorption and transport (MOREL and GSCHWEND, 1987). Colloid-bound metals have been measured in a variety of aquatic systems (BENOIT et al., 1994; GUO et al., 2000; REN et al., 2010), where they can comprise a significant portion of total metals, depending on solution conditions. The need to model this behavior has been recognized (MOREL and GSCHWEND, 1987; PANKOW and MCKENZIE, 1991), and due to colloidal artifacts there are often substantial discrepancies between modeled sorption behavior and experimental data (MOREL and GSCHWEND, 1987). Even so, most metal complexation models assume that metals partition into either a particulate or dissolved fraction, while ignoring the existence of colloids. This may be due to the difficulty of separating the colloidal fraction from the truly dissolved, as ultrafiltration typically requires large sample volumes and can be a time-consuming and costly process. There are some attempts in the literature to predict the extent of colloid-bound metals in environmental settings (VIGNATI et al., 2005; REN et al., 2010), but these predictions have not been implemented in equilibrium surface complexation models, which are a powerful way to describe metal speciation, sorption mechanisms, and metal-surface interactions.

Trace metal interactions with a surface are quantified by the distribution

coefficient  $K_S$  (Eq. 1.4), which describes the binding of dissolved metals (M) to functional groups on a solid substrate (S), resulting in the formation of surface complexes (S-M):

$$K_s = \frac{[S-M]}{[M][S]} \quad (1.4)$$

Calculating meaningful values of  $K_S$  requires properly quantifying the concentrations of all species in Eq. (1.4). As outlined above, the presence of colloidal material in the dissolved phase can confound proper estimates of dissolved metal concentrations, [M]. This has substantial implications for equilibrium models, as the dissolved metal concentration is not only used directly to calculate [M], but often the concentration of surface-bound metal, [S-M], as well (see for example QUINN et al., 2006a; NGWENYA et al., 2009; HA et al., 2010; MISHRA et al., 2010). In these cases, [S-M] is calculated by subtracting the equilibrium dissolved metal concentration ([M]) from the total metal concentration ([M]<sub>init</sub>). This is generally more accurate than attempting to directly measure [S-M], so long as S is the only sorbent present in the experimental solution. The equilibrium dissolved metal concentration is usually measured by filtering with 0.22 µm syringe filters, which do not capture the colloidal fraction. Therefore, the presence of colloids will cause overestimation of [M] and underestimation of [S-M] and hence  $K_S$ . It should be noted that in metal sorption studies on inorganic surfaces, colloid-bound metals do not seem to be important, as has been demonstrated for YREE sorption on hydrous ferric oxide and manganese oxide (SCHIJF and MARSHALL, 2011; K. Marshall, pers. comm.).

I investigated the effects of colloid-bound metal formation in sorption experiments on *U. lactuca* at 0.05, 0.5 and 5.0 M ionic strength. I found that colloids

constitute a significant portion of the operationally defined “dissolved fraction ( $<0.22 \mu\text{m}$ ) and that the presence of these colloid-bound metals can be modeled as a function of pH and ionic strength. Such models can correct metal distribution coefficients for organic surfaces to properly express the distribution between truly dissolved and particulate fractions. Without this refinement, equilibrium models and distribution coefficients will not accurately reflect metal sorption processes on organic matter. The presence of colloid-bound metals could also have significant implications for bioremediation and biomonitoring studies, which are discussed below.

### 2.3. Materials and Methods

#### *2.3.1. Experimental setup and materials preparations*

All sample solution preparation took place inside a class-100 clean air laboratory or laminar flow bench. Teflon and polyethylene materials were cleaned by soaking in either cold 4 N HCl (Fisher Scientific) for one week or subboiling 8 N HNO<sub>3</sub> (Fisher Scientific) for 24 hours, followed by rinsing with Milli-Q water (Millipore Direct-Q UV-3 purification system, 18.2 M $\Omega$ ·cm ) and drying on the laminar flow bench. Solution pH was monitored by measuring free hydrogen ion concentrations (absolute mV scale) with an Orion Ross combination pH electrode and an Orion 370 pH meter. The electrode was periodically checked for Nernstian behavior by titrating 0.5 M NaCl solution with certified HCl (Brinkmann). A 66.67 mg/L mixed-YREE standard solution, used for all YREE sorption experiments, was made from individual 1000 mg/L YREE standards (SPEX CertiPrep) in 2% HNO<sub>3</sub> (excluding Pm).

For each experiment, a pH standard solution and an experimental solution of

equal ionic strength (0.05, 0.5 or 5.0 M) were prepared from NaCl salt (Reagent-Plus, Sigma-Aldrich) and Milli-Q water in Teflon wide-mouth bottles. These ionic strengths were selected to approximate to the ionic strengths of fresh water (0.05 M), seawater (0.5 M), and brines (5.0 M). The pH standard was set to a pH of 3.00 with certified HCl and was used for single-point electrode calibrations periodically throughout the experiment. The experimental solution contained 500 µg/L of each YREE. A temperature bath and jacketed beakers maintained a constant temperature of  $25.0 \pm 0.1$  °C, and stir plates and Teflon-coated floating stir bars continuously mixed both solutions. The experimental solution was bubbled with ultra-high purity grade N<sub>2</sub> gas (first passed through a Supelco CO<sub>2</sub> scrubber) to eliminate CO<sub>2</sub> and prevent YREE-carbonate complexation.

### 2.3.2. Sorption experiments as a function of pH

Algal YREE sorption was measured over a range of pH values from ~ 2.7 to 8.5. The pH electrode was equilibrated at the desired ionic strength at least 24 h before beginning the experiment. Before addition of any biomass, the experimental solution was sampled to measure initial YREE concentrations ( $[M]_{\text{init}}$ ). Approximately 0.5 g of air-dried *U. lactuca* standard (Trace Metals in Sea Lettuce, BCR-279) was added to the experimental solution and allowed to equilibrate for at least 30 min before initial sampling. This *U. lactuca* standard was used because it not only provided a consistent form of the tissue that offered reproducible experimental results, but BCR-279 is also similar to seaweed biomass tested by materials engineers as potential biosorbents (ZEROUAL et al., 2003; SUZUKI et al., 2005; HERRERO et al., 2006; EL-SIKAILY et al., 2007).

Experimental solution pH was gradually raised to predetermined values using a Gilmont micro-dispenser to deliver NaOH to the solution. At each pH point, the solution was left to equilibrate for at least 6 h before a sample was filtered for YREE concentration analysis. Each sample was passed through a 0.22  $\mu\text{m}$  PVDF membrane filter with a polypropylene syringe to remove particle-bound metals from solution. The syringe and filter were first rinsed with a 5 mL aliquot of sample solution to prevent YREE loss by saturating sorption sites on the filter. A second 5 mL aliquot was then filtered and collected in a polypropylene centrifuge tube for analysis. Filtered samples were acidified with 10  $\mu\text{L}$  of concentrated  $\text{HNO}_3$  to avoid sorption onto the wall of the centrifuge tubes.

As it has been reported that *U. lactuca* requires Ca to maintain its cell wall structure (HAUG, 1976; PERCIVAL, 1979), one sorption experiment was performed in a 0.5 M NaCl + 0.01 M  $\text{CaCl}_2$  matrix. Both the pH standard and the experimental solutions were prepared by dissolving NaCl and  $\text{CaCl}_2$  salts in Milli-Q water, and the experiment was performed in a manner identical to that described above.

Fresh *U. lactuca* specimens were studied at 0.5 M ionic strength to compare YREE sorption behavior between fresh tissue and the *U. lactuca* standard. Live fronds collected near Elms Beach Park in Lexington Park, MD were cut into  $\sim 1$  cm squares and stored in a flow-through seawater tank for 4 d before the experiment. Each piece was then rinsed briefly with Milli-Q water and 0.5 M NaCl before it was blotted dry and weighed. The fresh tissue experiment was conducted in the same manner as for the *U. lactuca* standard.

### 2.3.3. Ultrafiltration and Sep-Pak C<sub>18</sub> Extractions

To determine the extent of colloid-bound metals in the 0.22  $\mu\text{m}$  filtered samples, additional filtrates at all ionic strengths and pH ~4, 5, 6, 7, and 8 were sequentially forced through 30 kDa and 3 kDa MWCO 15-mL Amicon® Ultra-15 regenerated cellulose ultrafiltration centrifuge tubes. In a Hettich EBA 21 centrifuge, 15 mL of the 0.22  $\mu\text{m}$  filtered sample was centrifuged until the entire sample had been forced through the filter. A 5 mL aliquot of the permeate was set aside in a polypropylene tube with 10  $\mu\text{L}$  concentrated  $\text{HNO}_3$  for YREE concentration analysis. The remainder of the permeate (~10 mL) was transferred to a 3 kDa ultrafiltration tube and centrifuged. The permeate from the 3 kDa tube (~10 mL) was acidified with 20  $\mu\text{L}$   $\text{HNO}_3$  in a polypropylene tube and analyzed for YREE concentrations. The colloid-bound metals in the retentate from both the 30 and 3 kDa filters were recovered by centrifuging 10 mL 1%  $\text{HNO}_3$  through each tube, which mobilized the metals into solution and allowed them to pass through the ultrafilters. Retentate and permeates from all ultrafilters were checked for metal mass balance, and recovery was 90-105%. These values are in good agreement with recovery values for Amicon cross-flow ultrafiltrations (1 kDa MWCO), which were tested for recovery of different transition metals (Cd, Cu, Ni, Pb, Fe, Mn, Zn and Hg) (WEN et al., 1996), suggesting that YREE contamination from the ultrafilters or YREE loss due to sorption on the membrane was minor.

To quantify the fraction of hydrophobic colloid-bound metals, 100 mL of <0.22  $\mu\text{m}$  sample (~pH 8) from the 0.05 M NaCl experiment was passed through Sep-Pak C<sub>18</sub> columns, which extract hydrophobic organic species from solution on a modified silica matrix. Two columns placed in series were pre-conditioned with 10 mL acetonitrile, 10

mL Milli-Q water and 20 mL sample. A 5 mL sample of the eluate was then collected and analyzed for YREE concentrations. After the remaining 75 mL of sample had passed, each column was extracted with 10 mL of 1 M HCl to remobilize the hydrophobic extract, which was analyzed for YREE concentrations. By placing the two columns in series, it can be shown that the extraction efficiency of each column ( $\alpha$ ) may be calculated from the equation

$$\alpha = \left(1 - \frac{y}{x}\right) \quad (2.1)$$

where  $y$  is the concentration of metal in the second column, and  $x$  is the concentration of metal in the first column extract. Values of  $\alpha$  were calculated to be 20 – 40%, depending on the YREE, and corrections for extraction efficiency were applied to all results.

#### 2.3.4. DOC analysis

Additional samples from the BCR-279 sorption experiments at all ionic strengths and pH 2 – 8 were analyzed for dissolved organic carbon (DOC) as a proxy for organic colloid release to determine whether the presence of colloids was pH dependent. Chesapeake Biological Laboratory's Nutrient Analytical Services Laboratory (NASL) conducted the DOC analysis. DOC was determined using a high-temperature combustion method (SUGIMURA and SUZUKI, 1988) on a Shimadzu TOC-5000A carbon analyzer with a non-dispersive infrared detector (NDIR).

For each ionic strength, 15 mL samples were filtered with 1  $\mu\text{m}$  GF/F filters at specific pH points and analyzed for DOC. Select samples at pH ~8 and 0.5 and 5.0 M ionic strength were analyzed after sequential filtration through 1  $\mu\text{m}$  GF/F filters and 0.22  $\mu\text{m}$  membrane filters to verify that the DOC contents were not altered by the larger GF/F

pore size and that the organic PVDF membranes were not releasing additional DOC. To determine the effect of rinsing the sorbent on colloid release, a series of “short test” samples were taken at each ionic strength where ~15 mg *U. lactuca* standard was suspended in 30 mL of unacidified 0.05 M, 0.5, or 5.0 M NaCl for less than 1 minute. Samples were then immediately filtered through 1  $\mu\text{m}$  GF/F filters and analyzed for DOC.

#### 2.3.5. ICP-MS analysis

All samples were analyzed for dissolved YREE concentrations using an Agilent Technologies 7500cx inductively coupled plasma mass spectrometer (ICP-MS). Samples were generally diluted 1/100 (occasionally 1/10) with 1% HNO<sub>3</sub> in polypropylene tubes to mitigate matrix effects from high NaCl concentrations. Each diluted sample was spiked with 2 ppb <sup>115</sup>In, <sup>133</sup>Cs and <sup>187</sup>Re as an internal standard. Concentrations of YREE in each sample were calculated from linear regressions of five matrix-matched (5 mM NaCl, 1% HNO<sub>3</sub>) standards (0, 0.5, 1, 2, and 5 ppb YREE). A 1 % HNO<sub>3</sub> solution was sampled before and after the calibration line and after each sample to rinse the instrument and the autosampler. Each standard and sample was injected in triplicate and analyzed twice in random order. Ion counts were corrected for instrument drift by normalizing each sample to the internal standard (<sup>89</sup>Y to <sup>115</sup>In and all other REE isotopes to a virtual internal standard (VIS) value derived from linear interpolation between <sup>133</sup>Cs and <sup>187</sup>Re).

#### 2.3.6. Calculating distribution coefficients

Sorbed metal ([S-M]) was determined as the difference between initial ([M]<sub>init</sub>)

and dissolved ( $[M]_{\text{diss}}$ ) YREE concentrations, hence distribution coefficients ( $K_S$ ) were calculated as:

$$K_S = \frac{[M]_{\text{init}} - [M]_{\text{diss}}}{[M]_{\text{diss}} \times [S]_T} \quad (2.2)$$

where  $[S]_T$  is the total concentration of sorption sites (mol/L). This value was determined by multiplying *U. lactuca* dry weight (~0.5 g) by the sum of the site densities (~1.6 mmol·g<sup>-1</sup> *U. lactuca*, dry weight), determined from potentiometric titrations of BCR-279 (SCHIJF and EBLING, 2010).

## 2.4. Results and Discussion

### *2.4.1. DOC measurements and effect of colloid-bound YREEs on distribution coefficients*

Sorption of positively charged metal cations onto organic surfaces generally increases as pH increases. This occurs because as the pH of the solution approaches the pK<sub>a</sub> of a given acidic functional group on the surface, they are more likely to be deprotonated and negatively charged (HARDEN and HARRIS, 1953). Therefore as pH increases, an increasing concentration of functional groups are likely deprotonated and able to participate in metal sorption. This trend can be depicted with a plot of log K<sub>S</sub> vs. pH, which will show a positive correlation when metal sorption increases with increasing pH, where higher values of log K<sub>S</sub> indicate enhanced sorption. Examples of such plots can be found in SCHIJF and MARSHALL (2011) or QUINN et al. (2006a), demonstrating the expected positive correlation for YREE sorption on hydrous ferric oxides. The system studied here also shows the same behavior at 0.5 and 5.0 M ionic strength (Fig. 2.1), where YREE sorption on *U. lactuca* consistently increases as pH increases and linear

regressions of  $\log K_S$  and pH data give positive slopes ( $\sim 0.3$ ).

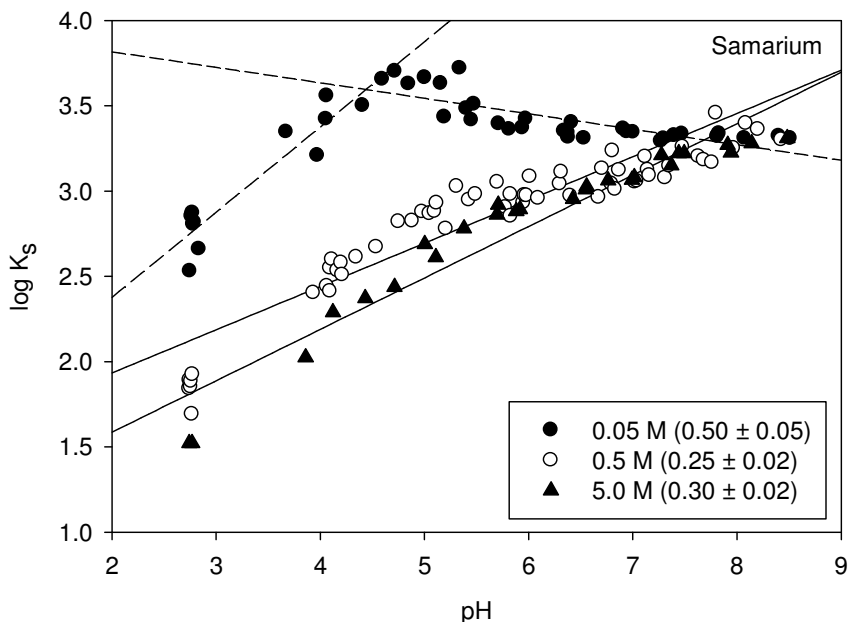


**Figure 2.1. Distribution coefficients as a function of pH for Sm sorption on *U. lactuca* standard BCR-279 at different ionic strengths. Separation into “dissolved” and “particulate” metal fractions was achieved with 0.22  $\mu\text{m}$  filters. Slopes from linear regressions are shown in parentheses. For 0.05 M, linear regressions were performed separately for  $\text{pH} < 4.6$  and  $\text{pH} > 4.6$ ; slope shown is for the lower pH data.**

However, this trend is not repeated at the lowest ionic strength studied, 0.05 M NaCl (Fig. 2.1, closed circles). At low pH (2 – 5) sorption increases with increasing pH (though with a somewhat higher slope than the 0.5 and 5.0 M data), but above pH  $\sim 5$ , the trend reverses. For some YREEs (such as La) there appears to be no correlation between  $\log K_S$  and pH above pH  $\sim 5$ , but for other YREEs (such as Sm), the correlation is actually negative at higher pHs. This unexpected behavior is likely an indication that there are other competing ligands or surfaces in the experimental solution participating in metal sorption. Because the experiments were carried out under controlled conditions (i.e. exclusion of  $\text{CO}_2$ , trace-metal clean Teflon containers where sorption loss is negligible), it may be reasonably assumed that *U. lactuca* was the only surface available for metal

sorption. This supports the idea that colloids, which are able to bypass the 0.22  $\mu\text{m}$  filters, might be participating in metal sorption. These colloids are unaccounted for in Fig. 2.1, and their presence would result in overestimation of dissolved metal concentrations and subsequent underestimation of  $\log K_S$  values.

To determine if organic ligands were present in the experimental solutions, DOC was measured as a proxy for the presence of organic colloids. According to the method used, DOC is defined as any dissolved organic carbon detected after filtering with a 1  $\mu\text{m}$  GF/F filter. It was not possible to isolate only colloidal organic carbon with the ultrafiltration units, as they are known to leach DOC, even after rinsing (GHORPADE, 2010). Instead, it was assumed that a proportion of DOC would occur as colloidal compounds, and DOC could therefore serve as a proxy for organic colloid presence. There is  $\sim 30 \text{ mg DOC}\cdot\text{L}^{-1}$  present in solution at all ionic strengths, over the entire pH range studied (Fig. 2.2, Table 2.1). The “short test” data, which were sampled moments after *U. lactuca* was suspended in unacidified solution, show that more than half of the DOC is immediately present in solution (Fig. 2.2, thick lines). As the DOC samples were taken with a larger pore-size filter (1  $\mu\text{m}$ ) than the PVDF filters (0.22  $\mu\text{m}$ ), there was a possibility that the DOC data were representing carbon concentrations from the size fraction 0.22–1  $\mu\text{m}$  rather than the colloidal pool (< 0.22  $\mu\text{m}$ ). It was also possible that the PVDF filters were contributing DOC to the samples. This was clearly not the case, as the dashed lines in Fig. 2.2 indicate consistent DOC concentrations when the samples were sequentially forced through the 1  $\mu\text{m}$  GF/F and 0.22  $\mu\text{m}$  PVDF filters.

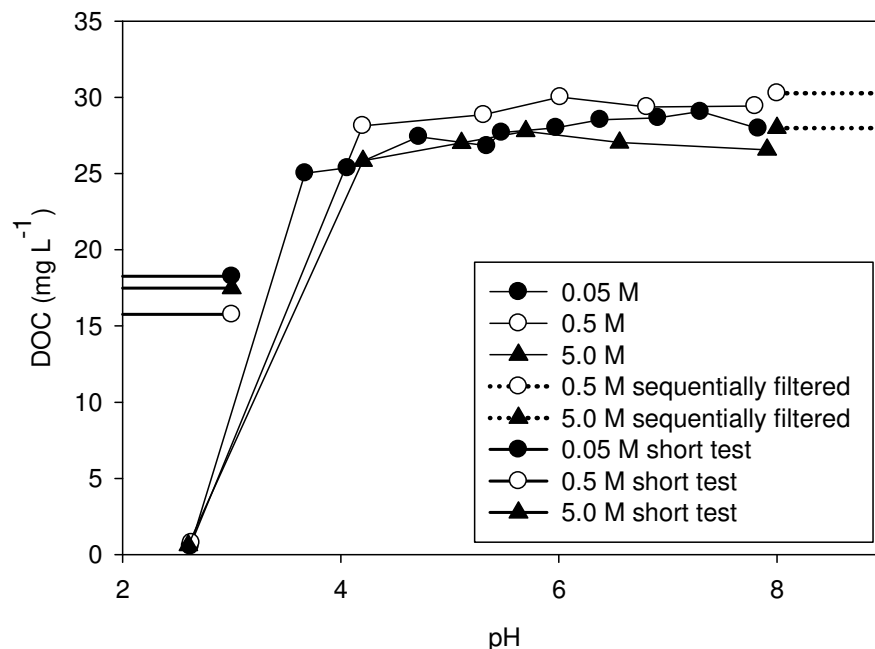


**Figure 2.2.** Dissolved organic carbon (DOC) concentrations in 0.05, 0.5 and 5.0 M NaCl experimental solutions containing *U. lactuca*. Sequentially filtered samples (dashed lines) were filtered through 1  $\mu\text{m}$  GF/F filter and 0.22  $\mu\text{m}$  filters. Short test samples (thick lines) were taken moments after suspending *U. lactuca* in unacidified 0.05, 0.5, or 5.0 M NaCl. Data shown at pH  $\sim$ 2.6 were blank samples taken before addition of *U. lactuca*.

#### 2.4.2. YREE interaction with the colloidal fraction

To determine what portion of the  $< 0.22 \mu\text{m}$  metal fraction was colloid-bound, ultracentrifuge filters were used on select 0.22  $\mu\text{m}$  filtered samples to separate colloid-bound from truly dissolved metal. These data are summarized for Y, La, Sm and Lu in Fig. 2.3 (data for other YREEs are given in Table 2.2), which confirms that metal binding to a colloidal fraction increases with increasing pH. The percentage of truly dissolved YREE (% [M]  $< 3 \text{ kDa}$ ) on the y-axis was calculated as the percentage of metal measured in a 3 kDa permeate out of total dissolved metal  $< 0.22 \mu\text{m}$ . The 3 kDa molecular weight cutoff (rather than 30 kDa) was selected as a conservative cutoff point, although there was typically  $< 5\%$  colloidal YREE contained in the size class 3 – 30 kDa. At low pH

(< 4), most YREE passing through the 0.22  $\mu\text{m}$  filters (93 – 97%) is truly dissolved, but as pH increases an increasing fraction of the YREEs are present as colloids. These metal-colloid interactions were found at all ionic strengths, though the effect is most substantial at the lowest ionic strength, where at pH ~6 only about 20% of YREEs passing through the 0.22  $\mu\text{m}$  filter are truly dissolved. For the higher ionic strengths studied, at pH ~6 roughly 50% of 0.22  $\mu\text{m}$  filtered metal is truly dissolved, resulting in an overestimation of the dissolved metal pool for the higher ionic strengths as well. The presence of colloids is not apparent in the 0.5 and 5.0 M  $\log K_s$  data (Fig. 2.1), which show increasing sorption with increasing pH. In order to better understand the colloidal fraction's origin, additional experiments were conducted, including a calcium matrix experiment and Sep-Pak C<sub>18</sub> column extractions. Data from these experiments are also shown in Fig. 2.3 and Table 2.1.

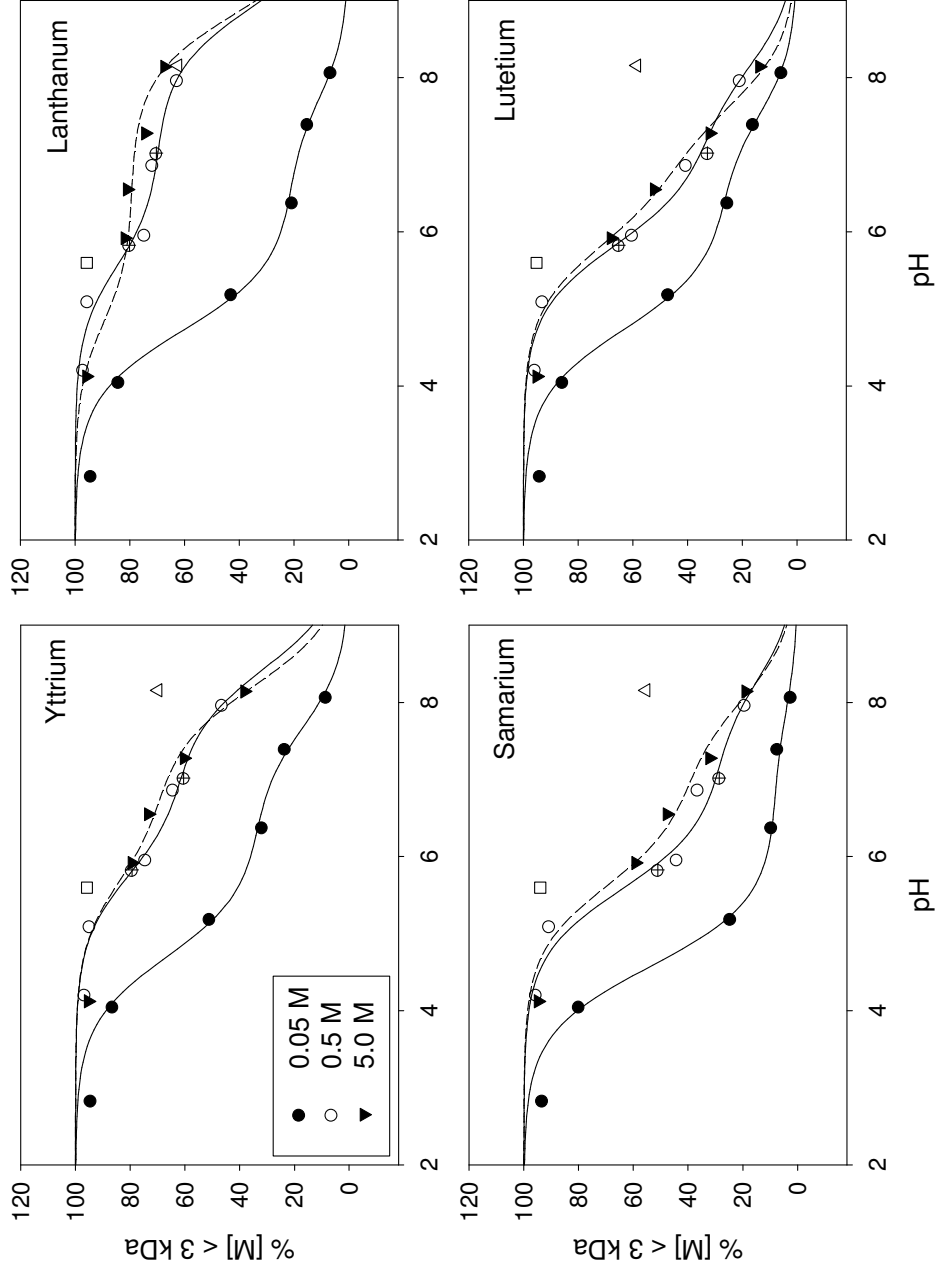


**Figure 2.3.** Ultracentrifuge data for representative YREs at all ionic strengths. The y-axis, “%  $[M] < 3 \text{ kDa}$ ”, is the percentage of truly dissolved metal ( $< 3 \text{ kDa}$ ) in the  $0.22 \mu\text{m}$  filtered sample. Hatched  $0.5 \text{ M}$  points are from the Ca/Na matrix experiment. A fresh *U. lactuca* sample in  $0.5 \text{ M}$  NaCl (open square) and Sep-Pak  $C_{18}$  column sample in  $0.05 \text{ M}$  NaCl (open triangle) are also shown. Curves represent fits of the data (Table 2.2) with Eq. (2.12) at each ionic strength. Data from the Ca/Na matrix experiment were pooled with the  $0.5 \text{ M}$  NaCl data for fits of Eq. (2.12) at mid-ionic strength, while fresh *U. lactuca* and Sep-Pak samples were excluded from the fits.

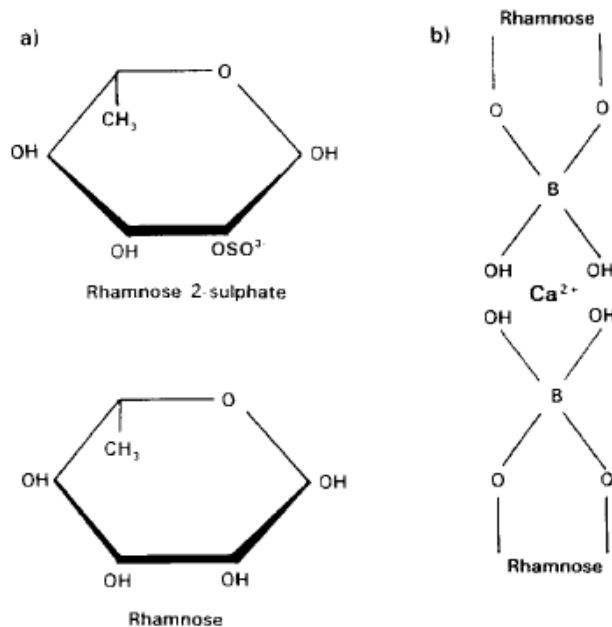


**Figure 2.4. Polysaccharide structure of *U. lactuca* cell walls, where  $\text{Ca}^{2+}$  creates cross-linkages between rhamnose subunits (WEBSTER and GADD, 1996a).**

Certain studies have indicated that calcium is an essential element in *U. lactuca*'s cell wall structure. HAUG (1976) found that  $\text{Ca}^{2+}$  complexed with borate esters formed at the hydroxide groups on rhamnose subunits (Fig. 2.4). As my experiments were conducted in NaCl solutions, it was possible that the lack of  $\text{Ca}^{2+}$  in the surrounding solution caused a breakdown of the cell wall structure and led to release of the colloidal material. I hypothesized that the presence of  $\text{Ca}^{2+}$  in solution could reduce colloid release. The sorption experiment conducted in the 0.5 M NaCl + 0.01 M  $\text{CaCl}_2$  matrix more closely represented *U. lactuca*'s natural environment and provided the typical Ca concentration *U. lactuca* would encounter in natural seawater. However, the ultracentrifuge data in the Ca/Na matrix experiment indicated no difference in metal-colloid formation from that in the NaCl matrix (Fig. 2.3, hatched and open circles), and data from both experiments were pooled and fit together in Fig. 2.3. This result shows that additional  $\text{Ca}^{2+}$  in solution is insufficient to prevent colloid release. The fact that no

change was observed may be due to the absence of borate (HAUG, 1976), which could not be added as it interferes with pH control and is a weak YREE complexing ligand.

The Sep-Pak C<sub>18</sub> extraction (Fig. 2.3, open triangles) is a measure of what fraction of the colloid-bound metal at high pH (~8) is hydrophobic. Sep-Pak C<sub>18</sub> columns isolate non-polar, hydrophobic compounds and are commonly used in field studies to determine trace-metal complexation with organic material (MILLS and QUINN, 1981; YOON et al., 1999). The data points in Fig. 2.3 (open triangles) indicate that the Sep-Pak C<sub>18</sub> extractions captured only ~50% of the colloid-bound YREEs < 0.22 μm. It is important to note that the Sep-Pak C<sub>18</sub> columns provide a chemical (rather than size) characterization of all material < 0.22 μm, which includes the colloidal (3 kDa - 0.22 μm) and the dissolved (< 3 kDa) fractions. Therefore, this result suggests that only a portion of the colloidal fraction is hydrophobic, especially because the C<sub>18</sub> columns also extract truly dissolved organic YREE complexes that are not removed by the Amicon® units.

Though the fresh *U. lactuca* sorption experiment provided just a single sample for ultrafiltration (Fig. 2.3, open squares), it is still useful to compare its behavior to the dried standard. The fresh sample demonstrates that fresh tissue releases less colloidal material than the dried standard, at least in 0.5 M NaCl at pH 5.5. This could be due to the lower surface area of the intact fresh *U. lactuca* thalli (per mass unit) and a lower portion of cellular fragments as compared to BCR-279. Additionally, the fresh *U. lactuca* specimens were rinsed prior to use in the experiment to remove adhering particles and epibiota, whereas the dried standard was not rinsed in order to minimize disturbance of the material and maximize the presence of colloids for the purpose of this study. The DOC analysis (Fig. 2.2, thick lines) reveals that only 50% of the DOC present in these

solutions is released almost immediately from the dried *U. lactuca* in the “short test” experiments. Therefore, it is possible that rinsing the dried standard may only remove a portion of the colloidal material. As metal sorption experiments may use either fresh or dried biomass (TEXIER et al., 2000; TURNER et al., 2007, 2008; MISHRA et al., 2010), it is prudent to always check for the presence of colloid-bound metals.

In addition to metal sorption studies, both living and dried *U. lactuca* have also been used in bioremediation and biomonitoring studies (SUZUKI et al., 2005; EL-SIKAILY et al., 2007), where colloidal artifacts have been typically unaccounted for and unrecognized. The presence of colloid-bound metals could have serious implications for these efforts. Macroalgae such as *U. lactuca* have high surface reactivity, worldwide distribution, and a natural ability to grow well in polluted environments, making them ideal biomonitors for dissolved metals in coastal systems. Biomonitors can be used to monitor water quality and the bioavailability of dissolved metals by measuring metal concentrations from an organism’s tissue. If *U. lactuca* or other biomonitors release organic colloids that interact strongly with trace metals, it will greatly influence the relationship between tissue and ambient water concentrations. Metal-bound colloids could also have an effect on the bioavailability of the metals to other organisms in the surrounding area. Those who wish to use *U. lactuca* in bioremediation studies will also need to determine whether colloid-bound metals are present. Materials engineers have proposed using dried *U. lactuca* biomass as a biofilter in packed columns to treat metal-contaminated environments (ZEROUAL et al., 2003; SUZUKI et al., 2005; HERRERO et al., 2006; EL-SIKAILY et al., 2007), as a potential alternative to more expensive synthetic cation-exchange resins. BCR-279 is very similar to the biomass used in these studies, and

the possibility of colloid-bound metal could subvert such efforts. Labile, colloid-bound metal could cause premature column break-through and substantially decrease column efficiency. Extended exposure to harsh, polluted waters could also cause structural damage to the packed biomass and increase the amount of colloids released, which would ultimately make columns less durable.

#### 2.4.3. Derivation and fits of the colloid correction model

The data in Fig. 2.3 demonstrate sorption-edge type behavior (i.e. a sharp increase in sorption as a function of pH), where there are two inflection points at pH ~5 and 7.5 in 0.05 M NaCl and similar transitions at pH ~ 6 and 8 for 0.5 and 5.0 M NaCl. These shapes are common in metal sorption studies, and suggests the presence of at least two metal complexing sites on the colloids, each with different  $pK_{a,s}$  (KULIK et al., 2000). The sorption edges are not a result of pH-dependent release of organic carbon from the *U. lactuca* tissue, as the DOC measurements demonstrate constant DOC concentrations present in solution (Fig. 2.2, Table 2.1). Samples taken directly after *U. lactuca* was suspended in unacidified solution show that more than half of the DOC is immediately released (Fig. 2.2, thick lines), suggesting that gradual DOC release over time is also not responsible for the sorption-edge behavior. Therefore, the pH-sorption edges do not appear to be a result of either progressive or pH-dependent DOC release. Rather, the metal interaction with the colloids is a result of pH-dependent sorption with a fixed colloidal fraction. This insight supports the idea of developing a colloid correction model, which is able to predict the extent of metal sorption onto colloids as a function of pH at each of the three ionic strengths studied.

In view of the presence of colloid-bound metals in the 0.22  $\mu\text{m}$  filtered samples, a model was developed to correct all 0.22  $\mu\text{m}$  filtered samples to reflect truly dissolved metal concentrations. Though it would be ideal to ultracentrifuge every sample, time and financial constraints make it impractical to use ultracentrifuge filtration on large numbers of samples. However, ultracentrifuging a limited number of samples allowed for development of a correction model which can be used to calculate the extent of colloid-bound metal in all 0.22  $\mu\text{m}$  filtered samples. The model is derived from a “Langmuir” treatment of the species involved whereby the colloidal functional group (L) is treated as the sorbent and protons (H) are treated as the sorbate. A similar derivation of these terms can also be found in STROES-GASCOYNE et al. (1986), where a single-site Langmuir model was derived for Cu sorption on manganese oxide. Potentiometric titrations of the *U. lactuca* standard used here (BCR-279) identified non-amphoteric, monoprotic functional groups (SCHIJF and EBLING, 2010), and as the curves in Fig. 2.3 show the unmistakable presence of two sorption edges (and therefore two functional groups), the model derived below assumes the presence of two acidic, monoprotic functional groups. For a 1-site cation exchange reaction between protons and colloid-bound metal (ML):



The corresponding equilibrium constant is

$$Q = \frac{[\text{HL}][\text{M}]}{[\text{H}][\text{ML}]} \quad (2.4)$$

I assumed that the functional groups were always occupied by either protons or metal, which would imply little or no free ligand at any pH. This is consistent with arguments for use of non-electrostatic complexation models, which assume that the electric double-layer charge on a surface is largely eliminated due to the complete

occupation of active sites (KULIK et al., 2000). In the system studied here, this assumption results in total site concentration  $[L_T] \approx [ML] + [HL]$ . By combining this assumption with Eq. (2.4), one can derive

$$\frac{[HL]}{L_T} = \left( \frac{[M]}{[H]Q} + 1 \right)^{-1} \quad (2.5)$$

This describes the sorption of a cation ( $H^+$ ) onto an active surface site (L). Assuming a 1-site Langmuir model (STUMM and MORGAN, 1996) where  $[HL] = \Gamma_H$  and  $L_T = \Gamma_{\max}$ , Eq. (2.5) takes the form of a Langmuir isotherm:

$$\Gamma_H = \frac{\Gamma_{\max}}{1 + \frac{[M]}{[H]Q}} \quad (2.6)$$

If a 2-site model with two independent monoprotic sites ( $L_1$  and  $L_2$ ) is assumed, the analogous 2-site Langmuir model is:

$$\Gamma_H = \frac{\Gamma_1}{1 + \frac{[M]}{[H]Q_1}} + \frac{\Gamma_2}{1 + \frac{[M]}{[H]Q_2}} \quad (2.7)$$

By dividing both sides by  $\Gamma_{\max}$ , where  $\Gamma_1/\Gamma_{\max} = F$  and  $\Gamma_2/\Gamma_{\max} = 1-F$ :

$$\frac{\Gamma_H}{\Gamma_{\max}} = \frac{[HL]}{[L_T]} = \frac{F}{1 + \frac{[M]}{[H]Q_1}} + \frac{1-F}{1 + \frac{[M]}{[H]Q_2}} \quad (2.8)$$

$F$  and  $1-F$  are the fractions of the total site density represented by  $L_1$  and  $L_2$ , respectively, and

$$[HL] = [HL_1] + [HL_2] \quad (2.9)$$

$$L_T \approx [ML_1] + [ML_2] + [HL] \quad (2.10)$$

$$M_T = [M] + [ML_1] + [ML_2] \quad (2.11)$$

Combining Eq. (2.8) with Eqs. (2.9) – (2.11) and simplifying terms gives the

equation used to fit the data in Fig. 2.3 and Table 2.2:

$$\% [M](< 3\text{kDa}) = 100 \times \left[ \frac{F}{1 + 10^{pH - \log Q_1}} + \frac{1 - F}{1 + 10^{pH - \log Q_2}} \right] \quad (2.12)$$

where

$$Q_1 = \frac{[ML_1][H]}{[HL_1]} \quad (2.13)$$

$$Q_2 = \frac{[ML_2][H]}{[HL_2]} \quad (2.14)$$

The parameters  $\log Q_1$  and  $\log Q_2$  represent pH values at which the concentration of protonated ligand is equal to the concentration of sites occupied by metal ions (i.e.  $[HL_1] = [ML_1]$  and  $[HL_2] = [ML_2]$ ). As the model assumes sites  $L_1$  and  $L_2$  are always occupied,  $\log Q_1$  and  $\log Q_2$  represent the point at which  $L_1$  and  $L_2$ , respectively, reach 50% of their final metal saturation for each individual element (in the presence of all YREEs), and are related to the  $pK_a$  values of  $L_1$  and  $L_2$ .

Eq. (2.12) was separately fit to the ultracentrifuge data (Table 2.2) for each YREE and each ionic strength, using  $\log Q_1$ ,  $\log Q_2$ , and  $F$  as adjustable parameters (the fresh *U. lactuca* and Sep-Pak data were excluded from the fits). Parameters and fit statistics for all YREEs are given in Table 2.3, and fits are shown as solid and dashed lines for Y, La, Sm and Lu in Fig. 2.3. Fits are quite good ( $r^2 > 0.97$ ) for all elements, and the parameters have low standard errors. In 0.05 M NaCl, the first functional group ( $L_1$ ) contributes 70 – 90% of total YREE binding with a corresponding  $\log Q_1$  value of  $\sim 4.6$ . The  $L_2$  group is responsible for the second minor sorption edge at  $pH \sim 7.7$  ( $\log Q_2$ ). At higher ionic strength, the sorption edges shift to slightly higher pH ( $\log Q_1 \sim 5.7$  and  $\log Q_2 \sim 8.3$ ), and  $L_1$  and  $L_2$  contribute more equally to YREE sorption for most

elements. The differences between the low (0.05 M) and higher (0.5 and 5.0 M) ionic strengths could be a result of different YREE affinities for the functional groups at each ionic strength, which is likely due to a combination of different ionic strength effects on each functional group's stability constants and  $pK_a$  values (see also Ch. 3).

The curves in Fig. 2.3 show two distinct sorption edges and were fit with the assumption that two functional groups are participating in metal sorption. SCHIJF and EBLING (2010) found three acidic functional groups on BCR-279 with  $pK_{a,s}$  of  $\sim 4$ , 6 and 9 and similar site densities. There are a few possible reasons for the difference between the results from these experiments and the potentiometric titrations. First, the colloids may be chemically different from the *U. lactuca* standard and only have two functional groups present. It is also possible that one of the three groups does not participate in YREE sorption. However, the most likely explanation is that only two groups could be distinguished with the relatively low resolution ( $\sim 1$  pH unit) in Fig. 2.3. The values of  $\log Q_1$  and  $\log Q_2$  are about midway between the first and second and second and third  $pK_{a,s}$  in SCHIJF and EBLING (2010) though, as stated above, even though  $\log Q_1$  and  $\log Q_2$  are related to the functional group  $pK_{a,s}$ , this relation is not a trivial one. It should be kept in mind that while Eq. (2.12) is derived from first principles, an exact interpretation is not crucial for its main purpose, which is to provide an analytical equation to correct  $0.22 \mu\text{m}$  filtered samples to reflect truly dissolved YREE concentrations.

#### 2.4.4. Corrected distribution coefficients

With Eq. (2.12) and the best-fit parameters in Table 2.3, it is possible to correct “dissolved” concentrations from the  $< 0.22 \mu\text{m}$  filtrates for the presence of colloid-bound

metals. The concentration of truly dissolved YREE ( $[M]_{\text{diss}}$ ) out of all metal filtered through the 0.22  $\mu\text{m}$  filters was calculated by multiplying  $< 0.22 \mu\text{m}$  filtrate values by the right side of Eq. (2.12). The calculated values of truly dissolved metal were then used in Eq. (2.2) (as  $[M]_{\text{diss}}$ ) to calculate corrected distribution coefficients.

Corrected and uncorrected distribution coefficients are plotted as a function of pH in Figs. 2.5 – 2.7 (data for all YREEs in Tables 2.4 – 2.6). The effect of the correction is most striking at the lowest ionic strength (Fig. 2.5), where at  $\text{pH} > 5$  the negative trend in the uncorrected data has been completely reversed. The data now show the expected behavior where sorption increases consistently with increasing pH. The corrected distribution coefficients at 0.5 and 5.0 M NaCl show that the uncorrected distribution coefficients were underestimated without the colloid correction, especially at  $\text{pH} > 5$ .

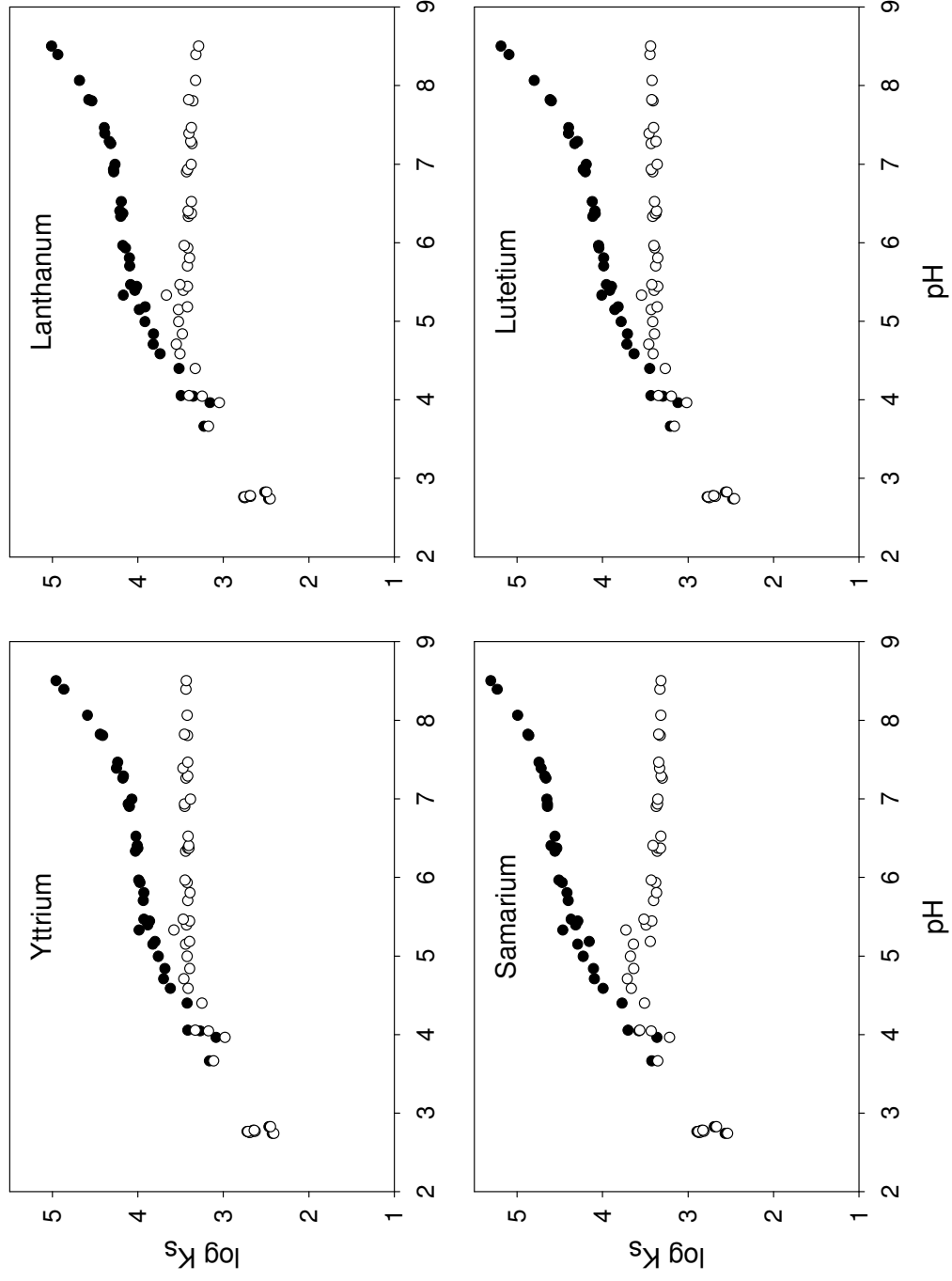


Figure 2.5. Distribution coefficients for select YREEs at 0.05 M ionic strength. Corrected  $\log K_s$  (closed circles) and uncorrected  $\log K_s$  (open circles) were calculated with and without accounting for colloid-bound metal, respectively.

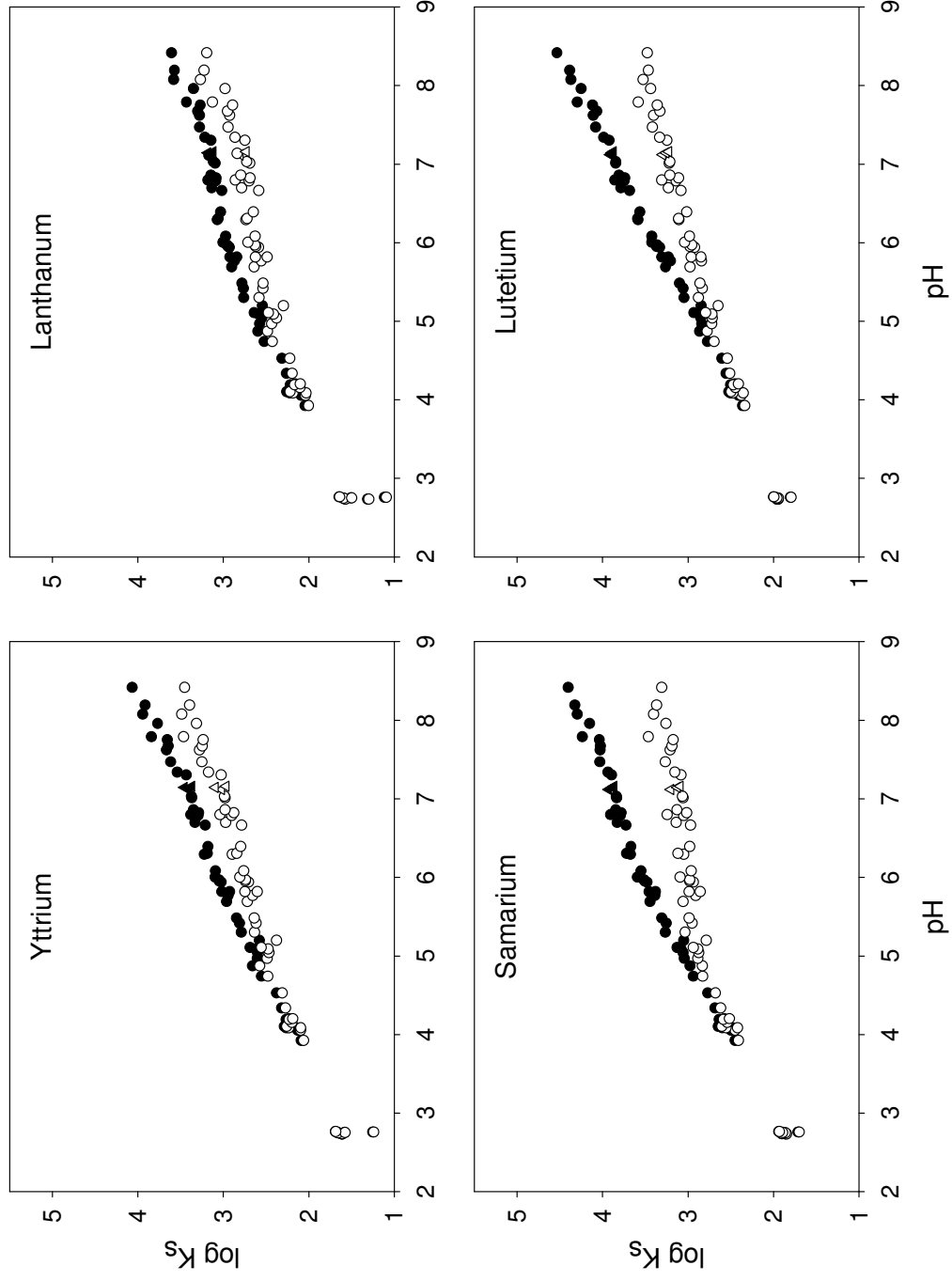
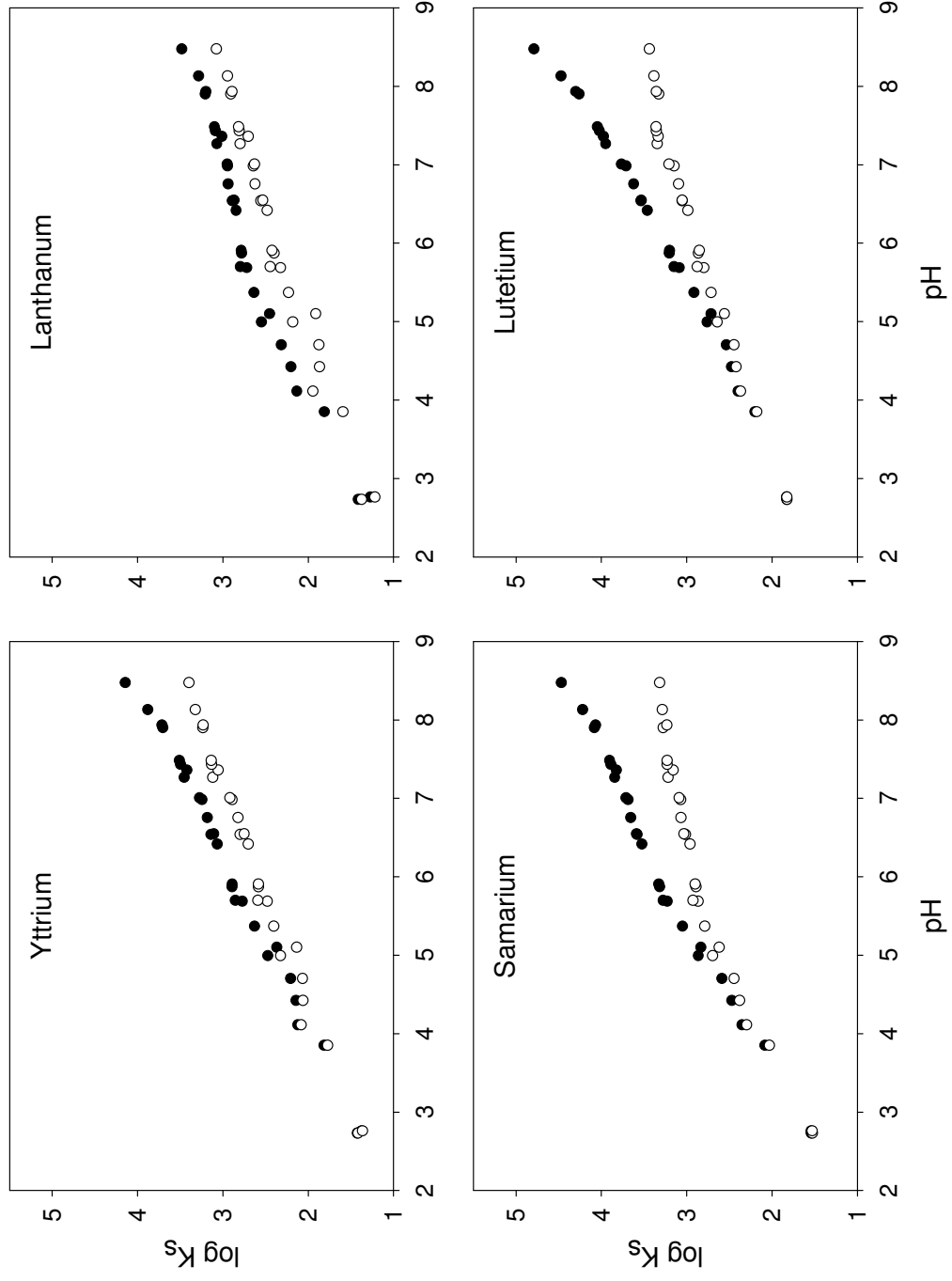
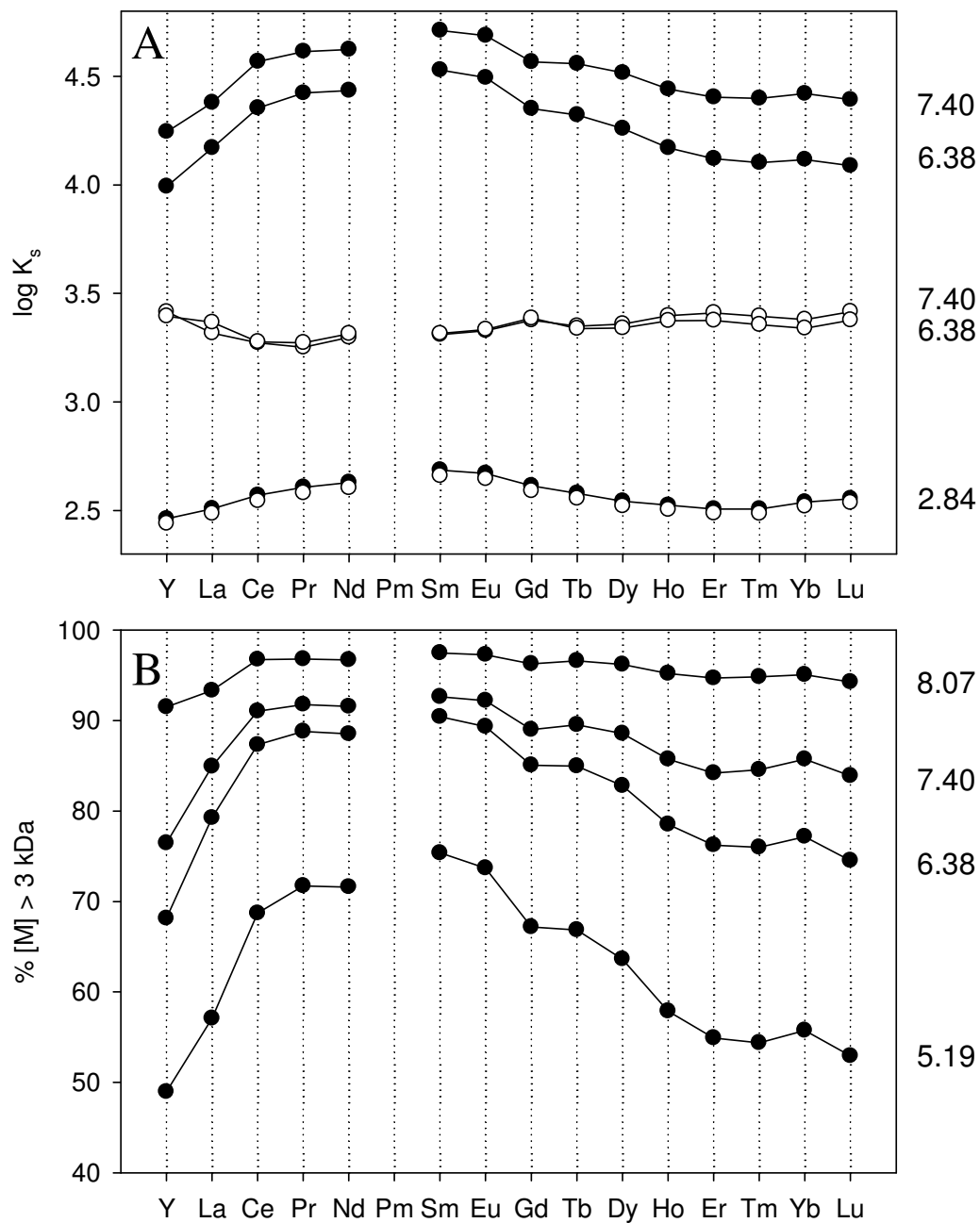


Figure 2.6. Distribution coefficients for select YREEs at 0.5 M ionic strength. Corrected  $\log K_s$  (closed circles) and uncorrected  $\log K_s$  (open circles) were calculated with and without accounting for colloid-bound metal, respectively.



**Figure 2.7.** Distribution coefficients for select YREEs at 5.0 M ionic strength. Corrected  $\log K_s$  (closed circles) and uncorrected  $\log K_s$  (open circles) were calculated with and without accounting for colloid-bound metal, respectively.



**Figure 2.8. A.** YREE distribution coefficient patterns in 0.05 M NaCl. Uncorrected (open circles) and corrected (closed circles) log  $K_s$  values are shown for comparison. **B.** Patterns of the fraction of colloid-bound YREEs (> 3 kDa) in 0.05 M NaCl, shown as a percentage of the < 0.22 fraction. Solution pH at the time of sampling is given to the right of each pattern.

Comparative  $\log K_S$  values and colloid-bound YREE percentages across the YREE series are shown in Fig. 2.8 for 0.05 M ionic strength, demonstrating that the colloid correction is unique to each individual metal. YREE patterns are often used as a diagnostic tool to gain mechanistic insights into YREE solution chemistry (see Chapter 3 for further discussion, or for example OHTA and KAWABE, 2000; SCHIJF and MARSHALL, 2011). Clearly, the presence of colloids affects relative as well as absolute YREE concentrations, which can be seen in the differences between the uncorrected and corrected  $\log K_S$  values (Fig. 2.8A). At pH 2.8, the uncorrected (open circles) and corrected distribution coefficients (closed circles) have similar relative values (i.e. shape of the pattern), but at pH 6.4 and 7.4, the data exhibits different shapes due to the colloid interaction (Fig. 2.8B), which makes up a growing component of the  $< 0.22 \mu\text{m}$  fraction as pH increases. The uncorrected distribution coefficients are rather flat, and there is little change from element to element. Corrected distribution coefficients are much more fractionated, where  $\log K_S$  values are higher around Sm-Eu. This fractionation is due to the increasing presence of colloid-bound YREEs which also shows a similar pattern across the YREE series (Fig. 2.8B). The shape of the pattern in Fig. 2.8B appears to be somewhat pH-dependent and becomes slightly flatter as pH increases, which could be due to the presence of the different functional groups, which will likely have different patterns of YREE affinities.

#### 2.4.5. *Linear fits with pH*

Linear regressions of distribution coefficients and pH can be used as a diagnostic tool to determine the pH dependence of YREE sorption (QUINN et al., 2006a; SCHIJF and

MARSHALL, 2011). While the data in Fig. 2.9 is not strictly linear, there is an overall positive trend, and the slope of a linear regression equals the number of protons released per metal ion sorbed, averaged over the entire pH range of the experiment. Linear regressions of the corrected  $\log K_S$  vs. pH data for Sm are shown in Fig. 2.9 (all elements shown in Table 2.7), where all three ionic strengths now have similar slopes of  $\sim 0.4 - 0.5$  and all data shows an increasing trend over the entire pH range. The slopes are also more consistent for individual elements over all three ionic strengths, suggesting that a single mechanism is responsible for sorption of all YREEs. However, as the slope does represent total sorption, its value actually represents a mixture of surface complexation reactions with different functional groups, and this mixture is not necessarily the same for all YREEs or at all ionic strengths (also see Ch. 3).

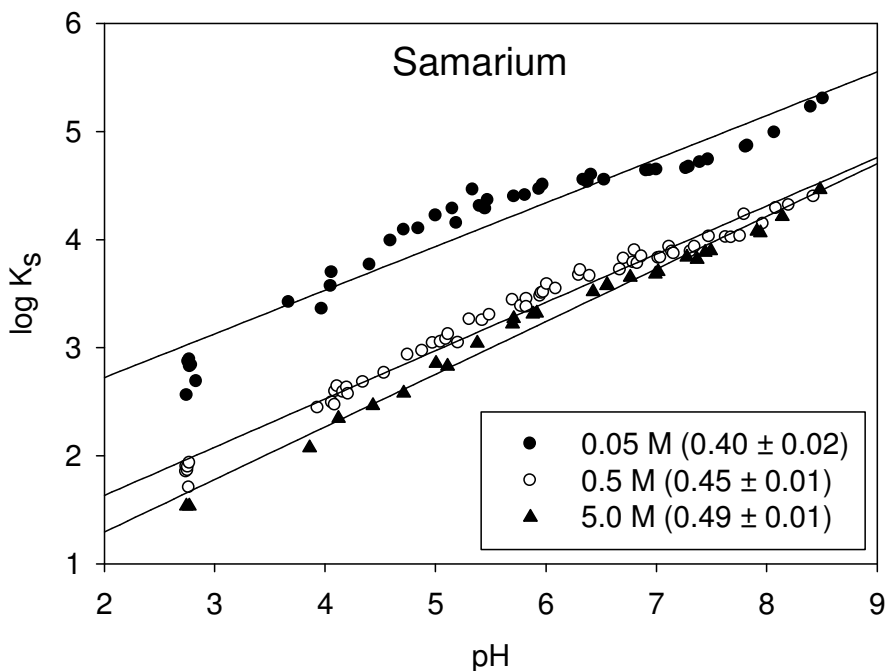


**Figure 2.9. Linear regressions of corrected  $\log K_S$  vs. pH data for Sm at 0.05 M (closed circles), 0.5 M (open circles), and 5.0 M (triangles) ionic strengths. Corrected slopes for Sm are shown in inset and represent the number of protons released per YREE cation sorbed, averaged over the experimental pH range.**

Slopes are  $< 1$  for all YREEs and all ionic strengths (Table 2.7), implying on average one proton is released for every two YREEs sorbed. These values agree well with slopes found in LEAD et al. (1999), where a similar metal-proton stoichiometry was found for Cu and Cd sorption to natural organic colloidal material collected from the River Mersey in NW England. Metal to proton ratios were  $\sim 0.5$  and  $\sim 0.6$  for  $\text{Cd}^{2+}$  and  $\text{Cu}^{2+}$ , respectively (LEAD et al., 1999). For YREE sorption on hydrous ferric oxides, linear regressions of distribution coefficient vs. pH also give slopes of  $< 1$  when ionic strength is increased from 0.025 M to 0.5 M (SCHIJF and MARSHALL, 2011).

Ionic strength appears to have an effect on the overall strength of YREE sorption, which is suppressed at the highest ionic strength (indicated by lower  $\log K_S$  values). Sorption is enhanced at the lowest ionic strength, (indicated by higher  $\log K_S$  values) and is consistent with the idea that there is decreased interference from  $\text{Na}^+$  ions. However, the average slope for each ionic strength subtly increases from low to high ionic strength (Table 2.7), which is somewhat counterintuitive and opposite the trend for hydrous ferric oxide, where increasing ionic strength causes a decrease in the slope (SCHIJF and MARSHALL, 2011). While there is only one type of functional group present on amorphous hydrous ferric oxide surfaces (hydroxides), there are multiple types of functional groups participating in sorption on *U. lactuca*. The metal affinity and  $\text{pK}_a$  of each group likely have different ionic strength dependencies, which could enhance or suppress one another in the overall  $\log K_S$  data.

## 2.5. Conclusions

A colloidal fraction is consistently present at all ionic strengths over the pH range studied, even though initial distribution coefficients at 0.5 and 5.0 M NaCl did not obviously reveal metal-colloid interactions. YREE interactions with colloids demonstrate pH sorption-edge type behavior, and DOC analysis suggests that the colloid sorption edges are not due to either gradual or pH-dependent DOC release. Rather, the sorption edges are the result of pH-dependent YREE sorption onto a consistently present colloidal fraction. This conclusion led to the development of a metal-colloid interaction model which is able to correct 0.22  $\mu\text{m}$  filtered samples as a function of pH and ionic strength to calculate truly dissolved YREE concentrations ( $< 3$  kDa). This model was used to calculate corrected distribution coefficients, which reverse the negative sorption trends seen in the uncorrected 0.05 M NaCl data. Corrected distribution coefficients in 0.5 and 5.0 M NaCl revealed that sorption at  $\text{pH} > 6$  was underestimated without the colloid correction, an effect that is not otherwise apparent from graphs of distribution coefficients vs. pH, which demonstrate the expected increase in metal sorption with increasing pH. Corrected  $\log K_s$  vs. pH plots show similar slopes at all three ionic strengths, suggesting that they are representing a single sorption mechanism. Failing to account for colloid-bound metals can lead to misinterpretation of experimental results and colloids should be anticipated as a significant portion of the commonly defined “dissolved” metals ( $< 0.22$   $\mu\text{m}$ ), especially in sorption studies on organic matter. By accounting for the colloidal fraction, more accurate equilibrium models can be developed that will provide insights into metal interactions with organic surfaces. Additionally, these results have implications for *U. lactuca* (and possibly other organic substrates)

when they are used as biosorbents in packed columns or biomonitors for metal contaminated sites, as colloids could subvert cleanup efforts by remobilizing toxic metals, altering their bioavailability, or decreasing column durability.

2.6. Data Tables

**Table 2.1. Dissolved organic carbon (DOC) concentrations in experimental solutions. <sup>a</sup> Sample sequentially filtered through 1 µm GF/F filter and 0.22 µm filter. <sup>b</sup> Short exposure test (see text for explanation).**

| <b>0.05 M NaCl</b> |                           | <b>0.5 M NaCl</b> |                           | <b>5.0 M NaCl</b> |                           |
|--------------------|---------------------------|-------------------|---------------------------|-------------------|---------------------------|
| pH                 | DOC (mg·L <sup>-1</sup> ) | pH                | DOC (mg·L <sup>-1</sup> ) | pH                | DOC (mg·L <sup>-1</sup> ) |
| 2.62               | 0.54                      | 2.63              | 0.77                      | 2.60              | 0.62                      |
| 3.67               | 25.0                      | 4.20              | 28.1                      | 4.20              | 25.8                      |
| 4.06               | 25.4                      | 5.31              | 28.9                      | 5.11              | 27.0                      |
| 4.72               | 27.4                      | 6.01              | 30.0                      | 5.70              | 27.8                      |
| 5.34               | 26.8                      | 6.81              | 29.4                      | 6.56              | 27.0                      |
| 5.47               | 27.7                      | 7.80              | 29.4                      | 7.91              | 26.6                      |
| 5.97               | 28.0                      | 7.80              | 30.3 <sup>a</sup>         | 7.91              | 28.0 <sup>a</sup>         |
| 6.38               | 28.5                      | —                 | 15.8 <sup>b</sup>         | —                 | 17.5 <sup>b</sup>         |
| 6.91               | 28.7                      |                   |                           |                   |                           |
| 7.30               | 29.1                      |                   |                           |                   |                           |
| 7.83               | 28.0                      |                   |                           |                   |                           |
| —                  | 18.3 <sup>b</sup>         |                   |                           |                   |                           |

Table 2.2. Fractions of truly dissolved metal (< 3 kDa) as percentages of originally measured dissolved concentration (< 0.22 μm).<sup>a</sup> sample extracted with Sep-Pak C<sub>18</sub> columns (see text for explanation).<sup>b</sup> Fresh *U. lactuca* tissue. <sup>c</sup> Experiment performed in 0.5 M NaCl + 0.01 M CaCl<sub>2</sub> matrix.

| pH                 | Y    | La   | Ce   | Pr   | Nd   | Sm   | Eu   | Gd   | Tb   | Dy   | Ho   | Er   | Tm   | Yb   | Lu   |
|--------------------|------|------|------|------|------|------|------|------|------|------|------|------|------|------|------|
| <b>0.05 M NaCl</b> |      |      |      |      |      |      |      |      |      |      |      |      |      |      |      |
| 2.84               | 94.5 | 94.3 | 94.1 | 93.9 | 93.3 | 93.3 | 93.5 | 93.4 | 93.6 | 94.0 | 94.0 | 94.2 | 94.1 | 94.1 | 94.0 |
| 4.05               | 86.5 | 84.2 | 82.5 | 82.1 | 81.7 | 80.0 | 81.1 | 82.6 | 83.6 | 84.7 | 85.4 | 85.9 | 86.0 | 85.9 | 85.8 |
| 5.19               | 51.0 | 42.9 | 31.3 | 28.3 | 28.4 | 24.6 | 26.3 | 32.8 | 33.2 | 36.4 | 42.1 | 45.1 | 45.6 | 44.3 | 47.1 |
| 6.38               | 31.9 | 20.7 | 12.7 | 11.2 | 11.5 | 9.6  | 10.7 | 14.9 | 15.0 | 17.2 | 21.5 | 23.8 | 24.0 | 22.8 | 25.5 |
| 7.40               | 23.5 | 15.1 | 9.0  | 8.2  | 8.4  | 7.4  | 7.8  | 11.0 | 10.5 | 11.4 | 14.3 | 15.8 | 15.4 | 14.3 | 16.1 |
| 8.07               | 8.5  | 6.7  | 3.2  | 3.2  | 3.3  | 2.5  | 2.7  | 3.7  | 3.4  | 3.8  | 4.8  | 5.3  | 5.2  | 4.9  | 5.7  |
| 8.16 <sup>a</sup>  | 69.8 | 62.5 | 39.4 | 48.1 | 55.8 | 55.4 | 57.9 | 65.0 | 61.9 | 62.0 | 64.5 | 64.2 | 59.4 | 58.2 | 58.6 |
| <b>0.5 M NaCl</b>  |      |      |      |      |      |      |      |      |      |      |      |      |      |      |      |
| 4.21               | 96.7 | 97.0 | 96.7 | 96.5 | 96.3 | 95.6 | 95.5 | 96.1 | 96.3 | 96.2 | 96.1 | 96.3 | 96.4 | 95.8 | 95.8 |
| 5.10               | 94.9 | 95.5 | 94.1 | 93.2 | 93.0 | 90.7 | 91.2 | 92.8 | 92.3 | 92.8 | 93.7 | 93.9 | 93.6 | 92.7 | 93.0 |
| 5.60 <sup>b</sup>  | 95.8 | 95.7 | 95.2 | 95.0 | 95.1 | 94.0 | 94.3 | 94.6 | 95.0 | 94.7 | 95.3 | 95.9 | 95.3 | 95.6 | 95.2 |
| 5.83 <sup>c</sup>  | 79.4 | 80.2 | 66.7 | 61.1 | 60.2 | 51.0 | 52.5 | 61.9 | 59.4 | 61.4 | 66.8 | 68.2 | 66.4 | 62.5 | 65.1 |
| 5.96               | 74.5 | 74.7 | 60.3 | 54.5 | 53.7 | 44.2 | 46.0 | 55.6 | 53.1 | 55.4 | 61.1 | 62.9 | 61.0 | 57.2 | 60.3 |
| 6.87               | 64.3 | 71.7 | 55.5 | 49.1 | 47.8 | 36.5 | 36.9 | 46.0 | 41.2 | 42.0 | 46.6 | 46.9 | 42.8 | 37.8 | 40.6 |
| 7.02 <sup>c</sup>  | 60.5 | 70.3 | 47.7 | 42.1 | 40.5 | 28.6 | 29.1 | 38.9 | 33.6 | 34.3 | 39.4 | 39.6 | 35.0 | 30.0 | 32.7 |
| 7.97               | 46.5 | 62.7 | 39.8 | 32.1 | 30.3 | 19.4 | 19.6 | 26.8 | 21.7 | 22.1 | 25.9 | 26.0 | 22.4 | 19.0 | 21.0 |
| <b>5.0 M NaCl</b>  |      |      |      |      |      |      |      |      |      |      |      |      |      |      |      |
| 4.12               | 95.3 | 95.8 | 95.7 | 95.6 | 95.3 | 94.8 | 95.1 | 95.5 | 95.3 | 95.2 | 95.3 | 95.2 | 95.3 | 95.2 | 95.1 |
| 5.92               | 79.4 | 81.8 | 72.5 | 68.5 | 68.0 | 59.2 | 59.1 | 66.3 | 63.1 | 64.6 | 69.3 | 70.5 | 68.5 | 65.2 | 68.0 |
| 6.55               | 73.4 | 80.9 | 66.8 | 61.4 | 60.2 | 47.6 | 47.5 | 56.7 | 51.3 | 52.2 | 57.5 | 58.1 | 54.4 | 49.3 | 52.2 |
| 7.28               | 60.3 | 74.3 | 55.8 | 48.4 | 46.6 | 32.1 | 31.7 | 40.9 | 33.7 | 34.0 | 38.9 | 39.0 | 34.5 | 29.4 | 31.9 |
| 8.14               | 38.3 | 67.3 | 42.1 | 35.8 | 33.2 | 19.0 | 17.9 | 24.3 | 17.6 | 17.0 | 19.4 | 18.6 | 15.3 | 12.3 | 13.7 |

Table 2.1. Dissolved organic carbon (DOC) concentrations in experimental solutions. <sup>a</sup> Sample sequentially filtered through 1 µm GF/F filter and 0.22 µm filter. <sup>b</sup> Short exposure test (see text for explanation).

| 0.05 M NaCl |                           | 0.5 M NaCl |                           | 5.0 M NaCl |                           |
|-------------|---------------------------|------------|---------------------------|------------|---------------------------|
| pH          | DOC (mg·L <sup>-1</sup> ) | pH         | DOC (mg·L <sup>-1</sup> ) | pH         | DOC (mg·L <sup>-1</sup> ) |
| 2.62        | 0.54                      | 2.63       | 0.77                      | 2.60       | 0.62                      |
| 3.67        | 25.0                      | 4.20       | 28.1                      | 4.20       | 25.8                      |
| 4.06        | 25.4                      | 5.31       | 28.9                      | 5.11       | 27.0                      |
| 4.72        | 27.4                      | 6.01       | 30.0                      | 5.70       | 27.8                      |
| 5.34        | 26.8                      | 6.81       | 29.4                      | 6.56       | 27.0                      |
| 5.47        | 27.7                      | 7.80       | 29.4                      | 7.91       | 26.6                      |
| 5.97        | 28.0                      | 7.80       | 30.3 <sup>a</sup>         | 7.91       | 28.0 <sup>a</sup>         |
| 6.38        | 28.5                      | —          | 15.8 <sup>b</sup>         | —          | 17.5 <sup>b</sup>         |
| 6.91        | 28.7                      |            |                           |            |                           |
| 7.30        | 29.1                      |            |                           |            |                           |
| 7.83        | 28.0                      |            |                           |            |                           |
| —           | 18.3 <sup>b</sup>         |            |                           |            |                           |

Table 2.3. Best-fit parameters for non-linear regressions of ultracentrifuge data (Table 2.2) using Eq. (2.12).

| YREE | 0.05 M NaCl |                    |                    |                | 0.5 M NaCl  |                    |                    |                | 5.0 M NaCl  |                    |                    |                |
|------|-------------|--------------------|--------------------|----------------|-------------|--------------------|--------------------|----------------|-------------|--------------------|--------------------|----------------|
|      | F           | log Q <sub>1</sub> | log Q <sub>2</sub> | r <sup>2</sup> | F           | log Q <sub>1</sub> | log Q <sub>2</sub> | r <sup>2</sup> | F           | log Q <sub>1</sub> | log Q <sub>2</sub> | r <sup>2</sup> |
| Y    | 0.66 ± 0.04 | 4.7 ± 0.1          | 7.7 ± 0.2          | 0.995          | 0.38 ± 0.02 | 5.7 ± 0.1          | 8.4 ± 0.1          | 0.993          | 0.31 ± 0.05 | 5.7 ± 0.3          | 8.2 ± 0.1          | 0.986          |
| La   | 0.79 ± 0.04 | 4.7 ± 0.1          | 7.7 ± 0.3          | 0.996          | 0.30 ± 0.02 | 5.6 ± 0.1          | 8.9 ± 0.3          | 0.973          | 0.21 ± 0.02 | 4.8 ± 0.4          | 8.9 ± 0.1          | 0.968          |
| Ce   | 0.88 ± 0.03 | 4.6 ± 0.1          | 7.7 ± 0.4          | 0.997          | 0.51 ± 0.05 | 5.6 ± 0.2          | 8.6 ± 0.4          | 0.971          | 0.39 ± 0.04 | 5.5 ± 0.3          | 8.5 ± 0.1          | 0.986          |
| Pr   | 0.90 ± 0.03 | 4.6 ± 0.1          | 7.9 ± 0.5          | 0.997          | 0.57 ± 0.05 | 5.6 ± 0.2          | 8.5 ± 0.4          | 0.971          | 0.46 ± 0.05 | 5.6 ± 0.2          | 8.4 ± 0.2          | 0.986          |
| Nd   | 0.90 ± 0.03 | 4.6 ± 0.1          | 7.8 ± 0.6          | 0.996          | 0.59 ± 0.05 | 5.6 ± 0.2          | 8.4 ± 0.4          | 0.972          | 0.47 ± 0.05 | 5.6 ± 0.2          | 8.3 ± 0.2          | 0.986          |
| Sm   | 0.92 ± 0.03 | 4.6 ± 0.1          | 7.9 ± 0.7          | 0.996          | 0.71 ± 0.06 | 5.6 ± 0.1          | 8.3 ± 0.6          | 0.973          | 0.60 ± 0.06 | 5.6 ± 0.2          | 8.0 ± 0.2          | 0.991          |
| Eu   | 0.91 ± 0.03 | 4.6 ± 0.1          | 7.8 ± 0.6          | 0.996          | 0.71 ± 0.06 | 5.6 ± 0.1          | 8.3 ± 0.5          | 0.976          | 0.60 ± 0.06 | 5.6 ± 0.2          | 8.0 ± 0.2          | 0.992          |
| Gd   | 0.86 ± 0.03 | 4.6 ± 0.1          | 7.7 ± 0.4          | 0.996          | 0.60 ± 0.05 | 5.6 ± 0.1          | 8.3 ± 0.3          | 0.982          | 0.51 ± 0.06 | 5.7 ± 0.2          | 8.1 ± 0.2          | 0.990          |
| Tb   | 0.86 ± 0.03 | 4.7 ± 0.1          | 7.7 ± 0.4          | 0.996          | 0.65 ± 0.05 | 5.7 ± 0.1          | 8.2 ± 0.3          | 0.984          | 0.56 ± 0.07 | 5.7 ± 0.2          | 7.9 ± 0.2          | 0.992          |
| Dy   | 0.83 ± 0.03 | 4.7 ± 0.1          | 7.6 ± 0.3          | 0.997          | 0.64 ± 0.05 | 5.7 ± 0.1          | 8.2 ± 0.3          | 0.986          | 0.55 ± 0.07 | 5.7 ± 0.2          | 7.8 ± 0.2          | 0.992          |
| Ho   | 0.78 ± 0.04 | 4.7 ± 0.1          | 7.6 ± 0.3          | 0.996          | 0.59 ± 0.04 | 5.7 ± 0.1          | 8.2 ± 0.2          | 0.989          | 0.49 ± 0.07 | 5.7 ± 0.2          | 7.9 ± 0.2          | 0.991          |
| Er   | 0.75 ± 0.04 | 4.7 ± 0.1          | 7.6 ± 0.2          | 0.996          | 0.59 ± 0.04 | 5.8 ± 0.1          | 8.2 ± 0.2          | 0.991          | 0.49 ± 0.08 | 5.8 ± 0.2          | 7.8 ± 0.2          | 0.992          |
| Tm   | 0.75 ± 0.04 | 4.7 ± 0.1          | 7.5 ± 0.2          | 0.996          | 0.64 ± 0.04 | 5.8 ± 0.1          | 8.2 ± 0.2          | 0.992          | 0.52 ± 0.08 | 5.8 ± 0.2          | 7.7 ± 0.2          | 0.993          |
| Yb   | 0.76 ± 0.04 | 4.7 ± 0.1          | 7.5 ± 0.3          | 0.996          | 0.69 ± 0.04 | 5.8 ± 0.1          | 8.2 ± 0.3          | 0.992          | 0.56 ± 0.09 | 5.7 ± 0.2          | 7.6 ± 0.2          | 0.994          |
| Lu   | 0.73 ± 0.04 | 4.7 ± 0.1          | 7.5 ± 0.2          | 0.995          | 0.66 ± 0.04 | 5.8 ± 0.1          | 8.2 ± 0.2          | 0.992          | 0.55 ± 0.09 | 5.8 ± 0.2          | 7.7 ± 0.2          | 0.993          |

Table 2.4. Corrected and uncorrected log  $K_S$  values at 0.05 M ionic strength. <sup>a</sup> Sample equilibrated for 30 minutes after adding *U. lactuca*.

| pH                | Y    | La   | Ce   | Pr   | Nd   | Sm   | Eu   | Gd   | Tb   | Dy   | Ho   | Er   | Tm   | Yb   | Lu   |
|-------------------|------|------|------|------|------|------|------|------|------|------|------|------|------|------|------|
| 2.75 <sup>a</sup> | 2.42 | 2.46 | 2.50 | 2.51 | 2.53 | 2.56 | 2.54 | 2.50 | 2.48 | 2.46 | 2.45 | 2.44 | 2.44 | 2.45 | 2.47 |
| 2.76 <sup>a</sup> | 2.69 | 2.75 | 2.81 | 2.82 | 2.84 | 2.87 | 2.85 | 2.81 | 2.78 | 2.76 | 2.73 | 2.72 | 2.72 | 2.74 | 2.75 |
| 2.77 <sup>a</sup> | 2.72 | 2.76 | 2.83 | 2.84 | 2.85 | 2.89 | 2.87 | 2.82 | 2.79 | 2.77 | 2.75 | 2.74 | 2.74 | 2.76 | 2.77 |
| 2.78 <sup>a</sup> | 2.64 | 2.69 | 2.75 | 2.77 | 2.78 | 2.82 | 2.80 | 2.75 | 2.71 | 2.69 | 2.67 | 2.65 | 2.66 | 2.67 | 2.69 |
| 2.79 <sup>a</sup> | 2.65 | 2.69 | 2.75 | 2.78 | 2.80 | 2.84 | 2.81 | 2.77 | 2.74 | 2.71 | 2.69 | 2.68 | 2.67 | 2.69 | 2.71 |
| 2.84              | 2.46 | 2.51 | 2.57 | 2.61 | 2.63 | 2.69 | 2.67 | 2.61 | 2.58 | 2.54 | 2.52 | 2.51 | 2.51 | 2.54 | 2.55 |
| 3.67              | 3.16 | 3.22 | 3.31 | 3.34 | 3.36 | 3.42 | 3.40 | 3.34 | 3.30 | 3.26 | 3.22 | 3.19 | 3.18 | 3.20 | 3.20 |
| 3.97              | 3.08 | 3.15 | 3.24 | 3.28 | 3.30 | 3.36 | 3.33 | 3.27 | 3.23 | 3.19 | 3.14 | 3.12 | 3.10 | 3.12 | 3.11 |
| 4.05              | 3.27 | 3.35 | 3.44 | 3.48 | 3.51 | 3.57 | 3.54 | 3.47 | 3.43 | 3.38 | 3.33 | 3.30 | 3.28 | 3.29 | 3.29 |
| 4.06              | 3.41 | 3.49 | 3.58 | 3.62 | 3.64 | 3.70 | 3.67 | 3.60 | 3.56 | 3.52 | 3.47 | 3.44 | 3.42 | 3.43 | 3.43 |
| 4.41              | 3.42 | 3.51 | 3.63 | 3.67 | 3.70 | 3.77 | 3.73 | 3.66 | 3.61 | 3.56 | 3.50 | 3.46 | 3.44 | 3.45 | 3.44 |
| 4.60              | 3.61 | 3.73 | 3.85 | 3.90 | 3.92 | 3.99 | 3.95 | 3.87 | 3.82 | 3.77 | 3.70 | 3.66 | 3.63 | 3.63 | 3.62 |
| 4.72              | 3.69 | 3.81 | 3.95 | 4.00 | 4.02 | 4.09 | 4.05 | 3.97 | 3.92 | 3.86 | 3.79 | 3.74 | 3.72 | 3.72 | 3.71 |
| 4.85              | 3.68 | 3.81 | 3.95 | 4.01 | 4.03 | 4.10 | 4.07 | 3.97 | 3.92 | 3.86 | 3.79 | 3.74 | 3.71 | 3.72 | 3.70 |
| 5.00              | 3.75 | 3.91 | 4.06 | 4.12 | 4.14 | 4.22 | 4.18 | 4.08 | 4.02 | 3.96 | 3.87 | 3.82 | 3.79 | 3.80 | 3.78 |
| 5.16              | 3.82 | 3.98 | 4.13 | 4.19 | 4.21 | 4.28 | 4.25 | 4.15 | 4.10 | 4.03 | 3.95 | 3.90 | 3.87 | 3.87 | 3.85 |
| 5.19              | 3.79 | 3.91 | 4.02 | 4.06 | 4.09 | 4.15 | 4.12 | 4.05 | 4.01 | 3.95 | 3.89 | 3.85 | 3.82 | 3.82 | 3.81 |
| 5.34              | 3.98 | 4.16 | 4.32 | 4.37 | 4.39 | 4.46 | 4.42 | 4.31 | 4.27 | 4.20 | 4.11 | 4.05 | 4.02 | 4.03 | 4.00 |
| 5.40              | 3.88 | 4.03 | 4.16 | 4.21 | 4.24 | 4.31 | 4.28 | 4.19 | 4.14 | 4.08 | 4.00 | 3.95 | 3.92 | 3.93 | 3.91 |
| 5.45              | 3.86 | 4.01 | 4.14 | 4.19 | 4.21 | 4.28 | 4.25 | 4.16 | 4.12 | 4.05 | 3.98 | 3.93 | 3.90 | 3.91 | 3.89 |
| 5.47              | 3.92 | 4.08 | 4.22 | 4.27 | 4.29 | 4.36 | 4.33 | 4.23 | 4.19 | 4.12 | 4.05 | 3.99 | 3.96 | 3.97 | 3.95 |
| 5.71              | 3.93 | 4.09 | 4.24 | 4.30 | 4.32 | 4.40 | 4.36 | 4.25 | 4.22 | 4.15 | 4.07 | 4.02 | 3.99 | 4.00 | 3.98 |
| 5.81              | 3.92 | 4.09 | 4.25 | 4.31 | 4.33 | 4.41 | 4.38 | 4.26 | 4.22 | 4.16 | 4.07 | 4.02 | 4.00 | 4.00 | 3.98 |
| 5.94              | 3.97 | 4.14 | 4.30 | 4.37 | 4.38 | 4.46 | 4.43 | 4.31 | 4.27 | 4.21 | 4.12 | 4.07 | 4.05 | 4.06 | 4.03 |
| 5.97              | 3.99 | 4.17 | 4.34 | 4.41 | 4.42 | 4.50 | 4.47 | 4.33 | 4.30 | 4.23 | 4.13 | 4.08 | 4.05 | 4.06 | 4.04 |
| 6.34              | 4.02 | 4.19 | 4.38 | 4.45 | 4.46 | 4.55 | 4.52 | 4.38 | 4.35 | 4.28 | 4.19 | 4.14 | 4.12 | 4.14 | 4.11 |
| 6.38              | 4.00 | 4.19 | 4.37 | 4.44 | 4.45 | 4.54 | 4.51 | 4.36 | 4.33 | 4.27 | 4.17 | 4.12 | 4.10 | 4.11 | 4.08 |
| 6.38              | 3.99 | 4.17 | 4.35 | 4.42 | 4.44 | 4.53 | 4.49 | 4.35 | 4.32 | 4.26 | 4.17 | 4.12 | 4.10 | 4.12 | 4.09 |

Table 2.4 (cont.). Corrected and uncorrected log  $K_S$  values at 0.05 M ionic strength. <sup>a</sup> Sample equilibrated for 30 minutes after adding *U. lactuca*.

| pH                | Y    | La   | Ce   | Pr   | Nd   | Sm   | Eu   | Gd   | Tb   | Dy   | Ho   | Er   | Tm   | Yb   | Lu   |
|-------------------|------|------|------|------|------|------|------|------|------|------|------|------|------|------|------|
| 6.41              | 4.00 | 4.20 | 4.41 | 4.49 | 4.50 | 4.60 | 4.55 | 4.39 | 4.36 | 4.28 | 4.18 | 4.13 | 4.10 | 4.12 | 4.08 |
| 6.53              | 4.02 | 4.19 | 4.37 | 4.45 | 4.46 | 4.55 | 4.51 | 4.37 | 4.35 | 4.28 | 4.19 | 4.15 | 4.13 | 4.15 | 4.11 |
| 6.91              | 4.09 | 4.28 | 4.47 | 4.54 | 4.54 | 4.64 | 4.60 | 4.45 | 4.43 | 4.36 | 4.27 | 4.23 | 4.21 | 4.23 | 4.19 |
| 6.94              | 4.11 | 4.28 | 4.47 | 4.54 | 4.55 | 4.64 | 4.61 | 4.46 | 4.44 | 4.38 | 4.29 | 4.25 | 4.23 | 4.25 | 4.22 |
| 7.00              | 4.07 | 4.26 | 4.47 | 4.54 | 4.55 | 4.64 | 4.60 | 4.45 | 4.43 | 4.36 | 4.26 | 4.21 | 4.20 | 4.22 | 4.18 |
| 7.27              | 4.17 | 4.31 | 4.50 | 4.55 | 4.56 | 4.66 | 4.63 | 4.50 | 4.49 | 4.44 | 4.37 | 4.33 | 4.33 | 4.35 | 4.32 |
| 7.30              | 4.16 | 4.33 | 4.52 | 4.57 | 4.58 | 4.67 | 4.64 | 4.51 | 4.49 | 4.44 | 4.36 | 4.31 | 4.30 | 4.32 | 4.29 |
| 7.40              | 4.24 | 4.38 | 4.57 | 4.61 | 4.62 | 4.71 | 4.69 | 4.57 | 4.56 | 4.52 | 4.44 | 4.40 | 4.40 | 4.42 | 4.39 |
| 7.47              | 4.23 | 4.39 | 4.59 | 4.64 | 4.65 | 4.74 | 4.71 | 4.58 | 4.57 | 4.53 | 4.44 | 4.40 | 4.40 | 4.42 | 4.39 |
| 7.81              | 4.41 | 4.53 | 4.74 | 4.76 | 4.78 | 4.86 | 4.84 | 4.73 | 4.74 | 4.70 | 4.63 | 4.60 | 4.60 | 4.62 | 4.59 |
| 7.83              | 4.43 | 4.57 | 4.77 | 4.78 | 4.79 | 4.87 | 4.85 | 4.75 | 4.75 | 4.72 | 4.65 | 4.61 | 4.62 | 4.64 | 4.61 |
| 8.07              | 4.58 | 4.68 | 4.90 | 4.89 | 4.91 | 4.99 | 4.98 | 4.89 | 4.91 | 4.88 | 4.82 | 4.79 | 4.80 | 4.82 | 4.79 |
| 8.40              | 4.86 | 4.93 | 5.16 | 5.14 | 5.15 | 5.22 | 5.23 | 5.15 | 5.18 | 5.16 | 5.11 | 5.08 | 5.09 | 5.12 | 5.09 |
| 8.51              | 4.95 | 5.00 | 5.25 | 5.21 | 5.23 | 5.30 | 5.31 | 5.24 | 5.26 | 5.25 | 5.20 | 5.17 | 5.19 | 5.21 | 5.18 |
| (Uncorrected)     |      |      |      |      |      |      |      |      |      |      |      |      |      |      |      |
| 2.75 <sup>a</sup> | 2.40 | 2.44 | 2.48 | 2.49 | 2.51 | 2.53 | 2.51 | 2.48 | 2.46 | 2.44 | 2.43 | 2.42 | 2.42 | 2.43 | 2.45 |
| 2.76 <sup>a</sup> | 2.68 | 2.74 | 2.80 | 2.81 | 2.82 | 2.85 | 2.84 | 2.79 | 2.77 | 2.74 | 2.72 | 2.71 | 2.71 | 2.73 | 2.74 |
| 2.77 <sup>a</sup> | 2.70 | 2.74 | 2.81 | 2.83 | 2.84 | 2.87 | 2.85 | 2.81 | 2.78 | 2.76 | 2.74 | 2.72 | 2.73 | 2.75 | 2.76 |
| 2.78 <sup>a</sup> | 2.62 | 2.68 | 2.73 | 2.75 | 2.76 | 2.81 | 2.78 | 2.73 | 2.70 | 2.68 | 2.65 | 2.64 | 2.64 | 2.66 | 2.67 |
| 2.79 <sup>a</sup> | 2.63 | 2.68 | 2.74 | 2.76 | 2.78 | 2.82 | 2.80 | 2.75 | 2.72 | 2.69 | 2.68 | 2.67 | 2.66 | 2.68 | 2.69 |
| 2.84              | 2.44 | 2.49 | 2.54 | 2.58 | 2.60 | 2.66 | 2.65 | 2.59 | 2.56 | 2.52 | 2.50 | 2.49 | 2.49 | 2.52 | 2.54 |
| 3.67              | 3.11 | 3.17 | 3.24 | 3.27 | 3.30 | 3.35 | 3.33 | 3.28 | 3.24 | 3.20 | 3.17 | 3.15 | 3.13 | 3.15 | 3.15 |
| 3.97              | 2.97 | 3.04 | 3.11 | 3.14 | 3.16 | 3.21 | 3.19 | 3.14 | 3.10 | 3.07 | 3.03 | 3.01 | 3.00 | 3.01 | 3.01 |
| 4.05              | 3.17 | 3.24 | 3.31 | 3.35 | 3.37 | 3.42 | 3.40 | 3.35 | 3.30 | 3.27 | 3.23 | 3.20 | 3.18 | 3.18 | 3.19 |
| 4.06              | 3.32 | 3.39 | 3.46 | 3.49 | 3.52 | 3.56 | 3.54 | 3.49 | 3.45 | 3.41 | 3.38 | 3.35 | 3.33 | 3.34 | 3.34 |
| 4.41              | 3.24 | 3.32 | 3.39 | 3.43 | 3.46 | 3.50 | 3.48 | 3.43 | 3.39 | 3.35 | 3.31 | 3.28 | 3.25 | 3.26 | 3.26 |
| 4.60              | 3.40 | 3.50 | 3.56 | 3.60 | 3.62 | 3.66 | 3.64 | 3.59 | 3.54 | 3.50 | 3.46 | 3.43 | 3.41 | 3.40 | 3.40 |
| 4.72              | 3.45 | 3.54 | 3.61 | 3.64 | 3.66 | 3.70 | 3.69 | 3.64 | 3.60 | 3.56 | 3.52 | 3.48 | 3.46 | 3.46 | 3.45 |
| 4.85              | 3.39 | 3.47 | 3.53 | 3.57 | 3.59 | 3.63 | 3.61 | 3.57 | 3.53 | 3.49 | 3.45 | 3.42 | 3.39 | 3.39 | 3.38 |

Table 2.4 (cont.). Corrected and uncorrected log  $K_S$  values at 0.05 M ionic strength. <sup>a</sup> Sample equilibrated for 30 minutes after adding *U. lactuca*.

| pH   | Y    | La   | Ce   | Pr   | Nd   | Sm   | Eu   | Gd   | Tb   | Dy   | Ho   | Er   | Tm   | Yb   | Lu   |
|------|------|------|------|------|------|------|------|------|------|------|------|------|------|------|------|
| 5.00 | 3.42 | 3.52 | 3.57 | 3.61 | 3.63 | 3.67 | 3.65 | 3.61 | 3.56 | 3.52 | 3.48 | 3.44 | 3.41 | 3.41 | 3.41 |
| 5.16 | 3.44 | 3.52 | 3.55 | 3.58 | 3.61 | 3.63 | 3.62 | 3.60 | 3.55 | 3.51 | 3.48 | 3.46 | 3.43 | 3.42 | 3.42 |
| 5.19 | 3.39 | 3.41 | 3.38 | 3.39 | 3.43 | 3.43 | 3.44 | 3.46 | 3.41 | 3.39 | 3.39 | 3.38 | 3.35 | 3.34 | 3.35 |
| 5.34 | 3.57 | 3.66 | 3.68 | 3.69 | 3.71 | 3.72 | 3.71 | 3.70 | 3.65 | 3.62 | 3.60 | 3.57 | 3.54 | 3.54 | 3.54 |
| 5.40 | 3.42 | 3.46 | 3.43 | 3.44 | 3.47 | 3.48 | 3.49 | 3.51 | 3.45 | 3.44 | 3.43 | 3.42 | 3.38 | 3.37 | 3.39 |
| 5.45 | 3.39 | 3.41 | 3.37 | 3.37 | 3.41 | 3.42 | 3.42 | 3.45 | 3.40 | 3.38 | 3.38 | 3.37 | 3.34 | 3.33 | 3.35 |
| 5.47 | 3.46 | 3.50 | 3.47 | 3.47 | 3.50 | 3.51 | 3.52 | 3.53 | 3.48 | 3.46 | 3.46 | 3.44 | 3.41 | 3.40 | 3.42 |
| 5.71 | 3.41 | 3.41 | 3.35 | 3.35 | 3.39 | 3.40 | 3.41 | 3.44 | 3.39 | 3.38 | 3.40 | 3.39 | 3.36 | 3.34 | 3.37 |
| 5.81 | 3.38 | 3.39 | 3.32 | 3.32 | 3.36 | 3.36 | 3.38 | 3.41 | 3.36 | 3.35 | 3.37 | 3.36 | 3.34 | 3.32 | 3.35 |
| 5.94 | 3.42 | 3.41 | 3.33 | 3.33 | 3.37 | 3.37 | 3.39 | 3.43 | 3.38 | 3.38 | 3.40 | 3.39 | 3.36 | 3.35 | 3.38 |
| 5.97 | 3.44 | 3.45 | 3.39 | 3.39 | 3.43 | 3.42 | 3.43 | 3.46 | 3.41 | 3.40 | 3.42 | 3.41 | 3.38 | 3.36 | 3.39 |
| 6.34 | 3.43 | 3.40 | 3.32 | 3.31 | 3.35 | 3.35 | 3.37 | 3.42 | 3.38 | 3.38 | 3.41 | 3.41 | 3.39 | 3.37 | 3.41 |
| 6.38 | 3.41 | 3.39 | 3.31 | 3.31 | 3.34 | 3.34 | 3.36 | 3.41 | 3.36 | 3.35 | 3.38 | 3.38 | 3.35 | 3.34 | 3.37 |
| 6.38 | 3.40 | 3.37 | 3.28 | 3.27 | 3.31 | 3.32 | 3.33 | 3.39 | 3.34 | 3.34 | 3.37 | 3.38 | 3.36 | 3.34 | 3.38 |
| 6.41 | 3.40 | 3.40 | 3.35 | 3.36 | 3.39 | 3.40 | 3.41 | 3.43 | 3.38 | 3.36 | 3.38 | 3.37 | 3.34 | 3.33 | 3.36 |
| 6.53 | 3.41 | 3.37 | 3.27 | 3.27 | 3.31 | 3.31 | 3.33 | 3.39 | 3.34 | 3.34 | 3.38 | 3.39 | 3.37 | 3.35 | 3.38 |
| 6.91 | 3.44 | 3.42 | 3.34 | 3.33 | 3.37 | 3.37 | 3.38 | 3.43 | 3.38 | 3.38 | 3.41 | 3.41 | 3.39 | 3.37 | 3.41 |
| 6.94 | 3.45 | 3.41 | 3.31 | 3.31 | 3.35 | 3.35 | 3.37 | 3.42 | 3.38 | 3.38 | 3.41 | 3.42 | 3.40 | 3.38 | 3.42 |
| 7.00 | 3.38 | 3.37 | 3.30 | 3.30 | 3.34 | 3.35 | 3.35 | 3.39 | 3.34 | 3.33 | 3.35 | 3.36 | 3.33 | 3.32 | 3.35 |
| 7.27 | 3.43 | 3.36 | 3.26 | 3.25 | 3.29 | 3.29 | 3.32 | 3.38 | 3.34 | 3.35 | 3.40 | 3.41 | 3.40 | 3.38 | 3.43 |
| 7.30 | 3.41 | 3.38 | 3.28 | 3.27 | 3.31 | 3.31 | 3.32 | 3.38 | 3.33 | 3.33 | 3.37 | 3.38 | 3.36 | 3.34 | 3.37 |
| 7.40 | 3.47 | 3.39 | 3.29 | 3.29 | 3.32 | 3.33 | 3.35 | 3.41 | 3.37 | 3.38 | 3.43 | 3.44 | 3.42 | 3.41 | 3.45 |
| 7.47 | 3.41 | 3.37 | 3.29 | 3.29 | 3.33 | 3.34 | 3.35 | 3.39 | 3.35 | 3.36 | 3.39 | 3.40 | 3.38 | 3.36 | 3.40 |
| 7.81 | 3.41 | 3.35 | 3.28 | 3.28 | 3.31 | 3.32 | 3.34 | 3.38 | 3.35 | 3.35 | 3.39 | 3.40 | 3.38 | 3.37 | 3.40 |
| 7.83 | 3.45 | 3.40 | 3.31 | 3.30 | 3.34 | 3.34 | 3.35 | 3.40 | 3.37 | 3.37 | 3.41 | 3.42 | 3.40 | 3.38 | 3.42 |
| 8.07 | 3.42 | 3.32 | 3.27 | 3.25 | 3.30 | 3.31 | 3.33 | 3.38 | 3.35 | 3.36 | 3.40 | 3.41 | 3.40 | 3.38 | 3.42 |
| 8.40 | 3.43 | 3.31 | 3.28 | 3.26 | 3.30 | 3.32 | 3.34 | 3.39 | 3.37 | 3.38 | 3.42 | 3.43 | 3.41 | 3.40 | 3.44 |
| 8.51 | 3.43 | 3.28 | 3.28 | 3.24 | 3.29 | 3.31 | 3.33 | 3.38 | 3.36 | 3.37 | 3.41 | 3.42 | 3.41 | 3.40 | 3.43 |

Table 2.5. Corrected and uncorrected log  $K_S$  values at 0.5 M ionic strength. <sup>a</sup> Sample equilibrated for 30 minutes after adding *U. lactuca*. <sup>b</sup> Experiment performed in 0.5 M NaCl + 0.01 M CaCl<sub>2</sub> matrix.

| pH                 | Y    | La   | Ce   | Pr   | Nd   | Sm   | Eu   | Gd   | Tb   | Dy   | Ho   | Er   | Tm   | Yb   | Lu   |
|--------------------|------|------|------|------|------|------|------|------|------|------|------|------|------|------|------|
| 2.74 <sup>a</sup>  | 1.61 | 1.31 | 1.66 | 1.61 | 1.69 | 1.85 | 1.84 | 1.78 | 1.79 | 1.69 | 1.72 | 1.72 | 1.71 | 1.89 | 1.95 |
| 2.74 <sup>a</sup>  | 1.61 | 1.57 | 1.80 | 1.74 | 1.76 | 1.90 | 1.91 | 1.84 | 1.81 | 1.78 | 1.73 | 1.72 | 1.77 | 1.89 | 1.94 |
| 2.76 <sup>ab</sup> | 1.65 | 1.59 | 1.75 | 1.75 | 1.78 | 1.86 | 1.87 | 1.81 | 1.77 | 1.78 | 1.72 | 1.72 | 1.76 | 1.88 | 1.94 |
| 2.76 <sup>a</sup>  | 1.58 | 1.50 | 1.74 | 1.75 | 1.76 | 1.89 | 1.88 | 1.82 | 1.81 | 1.78 | 1.71 | 1.75 | 1.77 | 1.89 | 1.96 |
| 2.77 <sup>a</sup>  | 1.25 | 1.11 | 1.46 | 1.45 | 1.51 | 1.70 | 1.71 | 1.57 | 1.55 | 1.55 | 1.46 | 1.44 | 1.56 | 1.70 | 1.79 |
| 2.77 <sup>a</sup>  | 1.68 | 1.64 | 1.73 | 1.72 | 1.82 | 1.93 | 1.93 | 1.86 | 1.83 | 1.82 | 1.78 | 1.80 | 1.87 | 1.93 | 1.99 |
| 3.93               | 2.08 | 2.04 | 2.20 | 2.28 | 2.31 | 2.44 | 2.43 | 2.34 | 2.32 | 2.29 | 2.24 | 2.22 | 2.25 | 2.32 | 2.36 |
| 4.06               | 2.12 | 2.08 | 2.26 | 2.34 | 2.36 | 2.49 | 2.49 | 2.38 | 2.36 | 2.34 | 2.30 | 2.28 | 2.30 | 2.38 | 2.40 |
| 4.09 <sup>b</sup>  | 2.13 | 2.08 | 2.24 | 2.31 | 2.35 | 2.47 | 2.46 | 2.36 | 2.36 | 2.33 | 2.28 | 2.26 | 2.28 | 2.35 | 2.38 |
| 4.09               | 2.26 | 2.22 | 2.37 | 2.44 | 2.47 | 2.59 | 2.59 | 2.50 | 2.50 | 2.45 | 2.39 | 2.39 | 2.41 | 2.48 | 2.50 |
| 4.11               | 2.28 | 2.25 | 2.42 | 2.50 | 2.53 | 2.64 | 2.63 | 2.55 | 2.54 | 2.51 | 2.46 | 2.45 | 2.45 | 2.51 | 2.52 |
| 4.16               | 2.23 | 2.15 | 2.34 | 2.41 | 2.43 | 2.59 | 2.57 | 2.48 | 2.47 | 2.43 | 2.37 | 2.36 | 2.37 | 2.44 | 2.47 |
| 4.20               | 2.26 | 2.21 | 2.41 | 2.46 | 2.49 | 2.63 | 2.62 | 2.52 | 2.51 | 2.47 | 2.41 | 2.39 | 2.40 | 2.48 | 2.50 |
| 4.21               | 2.22 | 2.15 | 2.32 | 2.41 | 2.45 | 2.57 | 2.55 | 2.46 | 2.45 | 2.41 | 2.36 | 2.34 | 2.36 | 2.43 | 2.44 |
| 4.35               | 2.31 | 2.26 | 2.44 | 2.52 | 2.56 | 2.68 | 2.67 | 2.59 | 2.57 | 2.54 | 2.48 | 2.45 | 2.46 | 2.53 | 2.55 |
| 4.54               | 2.37 | 2.31 | 2.50 | 2.59 | 2.63 | 2.76 | 2.75 | 2.65 | 2.64 | 2.61 | 2.54 | 2.53 | 2.53 | 2.59 | 2.60 |
| 4.75               | 2.55 | 2.52 | 2.68 | 2.77 | 2.80 | 2.93 | 2.92 | 2.82 | 2.80 | 2.77 | 2.71 | 2.69 | 2.70 | 2.76 | 2.76 |
| 4.88               | 2.65 | 2.59 | 2.76 | 2.83 | 2.86 | 2.97 | 2.96 | 2.89 | 2.89 | 2.86 | 2.82 | 2.80 | 2.81 | 2.86 | 2.86 |
| 4.98               | 2.60 | 2.57 | 2.76 | 2.86 | 2.90 | 3.04 | 3.02 | 2.90 | 2.90 | 2.86 | 2.79 | 2.77 | 2.78 | 2.84 | 2.83 |
| 5.05               | 2.59 | 2.54 | 2.71 | 2.87 | 2.89 | 3.05 | 3.04 | 2.92 | 2.91 | 2.87 | 2.79 | 2.77 | 2.78 | 2.84 | 2.84 |
| 5.10               | 2.61 | 2.58 | 2.80 | 2.89 | 2.93 | 3.07 | 3.06 | 2.94 | 2.93 | 2.89 | 2.81 | 2.79 | 2.80 | 2.87 | 2.86 |
| 5.12               | 2.68 | 2.63 | 2.84 | 2.94 | 2.99 | 3.12 | 3.11 | 2.98 | 2.98 | 2.95 | 2.88 | 2.85 | 2.86 | 2.93 | 2.93 |
| 5.21 <sup>b</sup>  | 2.57 | 2.54 | 2.76 | 2.86 | 2.90 | 3.04 | 3.03 | 2.90 | 2.90 | 2.86 | 2.79 | 2.76 | 2.78 | 2.85 | 2.84 |
| 5.31               | 2.78 | 2.76 | 2.98 | 3.08 | 3.11 | 3.26 | 3.24 | 3.11 | 3.12 | 3.08 | 3.00 | 2.97 | 2.99 | 3.05 | 3.04 |
| 5.43               | 2.81 | 2.76 | 2.97 | 3.08 | 3.11 | 3.25 | 3.23 | 3.11 | 3.12 | 3.08 | 3.01 | 2.98 | 3.00 | 3.06 | 3.05 |
| 5.49               | 2.84 | 2.77 | 3.00 | 3.12 | 3.15 | 3.30 | 3.28 | 3.16 | 3.16 | 3.13 | 3.05 | 3.03 | 3.04 | 3.11 | 3.09 |
| 5.70               | 2.96 | 2.90 | 3.15 | 3.25 | 3.29 | 3.44 | 3.43 | 3.30 | 3.32 | 3.28 | 3.21 | 3.19 | 3.21 | 3.28 | 3.26 |
| 5.78               | 2.94 | 2.86 | 3.11 | 3.20 | 3.24 | 3.38 | 3.37 | 3.25 | 3.26 | 3.23 | 3.16 | 3.13 | 3.16 | 3.21 | 3.20 |
| 5.83               | 3.01 | 2.92 | 3.16 | 3.26 | 3.30 | 3.45 | 3.44 | 3.32 | 3.34 | 3.31 | 3.24 | 3.22 | 3.25 | 3.31 | 3.30 |
| 5.83 <sup>b</sup>  | 2.92 | 2.84 | 3.09 | 3.19 | 3.22 | 3.37 | 3.36 | 3.23 | 3.26 | 3.23 | 3.16 | 3.14 | 3.17 | 3.24 | 3.22 |

Table 2.5 (cont.). Corrected and uncorrected log  $K_S$  values at 0.5 M ionic strength. <sup>a</sup> Sample equilibrated for 30 minutes after adding *U. lactuca*.  
<sup>b</sup> Experiment performed in 0.5 M NaCl + 0.01 M CaCl<sub>2</sub> matrix.

| pH                | Y    | La   | Ce   | Pr   | Nd   | Sm   | Eu   | Gd   | Tb   | Dy   | Ho   | Er   | Tm   | Yb   | Lu   |
|-------------------|------|------|------|------|------|------|------|------|------|------|------|------|------|------|------|
| 5.95              | 3.02 | 2.92 | 3.18 | 3.28 | 3.31 | 3.47 | 3.46 | 3.34 | 3.36 | 3.34 | 3.26 | 3.25 | 3.28 | 3.35 | 3.33 |
| 5.96              | 3.04 | 2.94 | 3.19 | 3.30 | 3.34 | 3.50 | 3.49 | 3.36 | 3.39 | 3.36 | 3.29 | 3.28 | 3.31 | 3.38 | 3.36 |
| 5.98              | 3.05 | 2.95 | 3.20 | 3.31 | 3.35 | 3.51 | 3.50 | 3.37 | 3.39 | 3.36 | 3.29 | 3.28 | 3.31 | 3.38 | 3.36 |
| 6.01              | 3.09 | 3.00 | 3.27 | 3.37 | 3.41 | 3.58 | 3.57 | 3.43 | 3.46 | 3.43 | 3.35 | 3.33 | 3.37 | 3.44 | 3.42 |
| 6.09              | 3.09 | 2.97 | 3.23 | 3.33 | 3.38 | 3.54 | 3.53 | 3.40 | 3.43 | 3.41 | 3.34 | 3.33 | 3.37 | 3.44 | 3.42 |
| 6.30              | 3.22 | 3.06 | 3.34 | 3.45 | 3.49 | 3.67 | 3.66 | 3.53 | 3.57 | 3.55 | 3.49 | 3.49 | 3.53 | 3.60 | 3.58 |
| 6.31              | 3.18 | 3.05 | 3.36 | 3.48 | 3.52 | 3.71 | 3.70 | 3.55 | 3.60 | 3.58 | 3.49 | 3.48 | 3.53 | 3.61 | 3.58 |
| 6.40              | 3.17 | 3.03 | 3.32 | 3.43 | 3.47 | 3.66 | 3.65 | 3.50 | 3.55 | 3.53 | 3.45 | 3.44 | 3.50 | 3.58 | 3.56 |
| 6.67 <sup>b</sup> | 3.21 | 3.01 | 3.34 | 3.46 | 3.50 | 3.72 | 3.71 | 3.55 | 3.62 | 3.61 | 3.54 | 3.54 | 3.61 | 3.70 | 3.68 |
| 6.71              | 3.33 | 3.13 | 3.44 | 3.56 | 3.61 | 3.82 | 3.82 | 3.66 | 3.73 | 3.71 | 3.65 | 3.65 | 3.71 | 3.80 | 3.78 |
| 6.79              | 3.29 | 3.08 | 3.40 | 3.52 | 3.57 | 3.79 | 3.78 | 3.62 | 3.69 | 3.68 | 3.61 | 3.61 | 3.68 | 3.77 | 3.74 |
| 6.81              | 3.38 | 3.17 | 3.51 | 3.63 | 3.67 | 3.90 | 3.89 | 3.72 | 3.80 | 3.79 | 3.71 | 3.72 | 3.79 | 3.88 | 3.85 |
| 6.83              | 3.28 | 3.08 | 3.40 | 3.51 | 3.56 | 3.78 | 3.77 | 3.61 | 3.68 | 3.67 | 3.59 | 3.60 | 3.67 | 3.76 | 3.73 |
| 6.87              | 3.34 | 3.14 | 3.47 | 3.58 | 3.62 | 3.84 | 3.83 | 3.67 | 3.74 | 3.73 | 3.66 | 3.67 | 3.74 | 3.83 | 3.80 |
| 7.02 <sup>b</sup> | 3.36 | 3.09 | 3.45 | 3.55 | 3.60 | 3.83 | 3.83 | 3.67 | 3.76 | 3.76 | 3.69 | 3.70 | 3.78 | 3.87 | 3.84 |
| 7.04              | 3.37 | 3.11 | 3.44 | 3.56 | 3.61 | 3.83 | 3.83 | 3.68 | 3.75 | 3.75 | 3.69 | 3.70 | 3.77 | 3.86 | 3.84 |
| 7.12              | 3.40 | 3.16 | 3.51 | 3.64 | 3.69 | 3.93 | 3.93 | 3.76 | 3.84 | 3.84 | 3.76 | 3.77 | 3.85 | 3.95 | 3.91 |
| 7.14              | 3.46 | 3.18 | 3.51 | 3.62 | 3.67 | 3.89 | 3.89 | 3.74 | 3.82 | 3.82 | 3.76 | 3.77 | 3.84 | 3.92 | 3.90 |
| 7.16              | 3.37 | 3.12 | 3.46 | 3.58 | 3.63 | 3.87 | 3.87 | 3.70 | 3.79 | 3.78 | 3.72 | 3.72 | 3.80 | 3.90 | 3.87 |
| 7.31              | 3.43 | 3.14 | 3.48 | 3.60 | 3.65 | 3.89 | 3.88 | 3.73 | 3.82 | 3.82 | 3.76 | 3.77 | 3.85 | 3.94 | 3.92 |
| 7.35              | 3.53 | 3.21 | 3.54 | 3.65 | 3.71 | 3.93 | 3.94 | 3.80 | 3.88 | 3.88 | 3.84 | 3.85 | 3.92 | 4.00 | 3.98 |
| 7.48              | 3.61 | 3.27 | 3.63 | 3.74 | 3.79 | 4.03 | 4.03 | 3.89 | 3.98 | 3.98 | 3.93 | 3.94 | 4.01 | 4.10 | 4.07 |
| 7.63              | 3.66 | 3.27 | 3.63 | 3.74 | 3.79 | 4.02 | 4.03 | 3.91 | 4.00 | 4.01 | 3.96 | 3.98 | 4.05 | 4.12 | 4.10 |
| 7.68              | 3.64 | 3.29 | 3.63 | 3.74 | 3.80 | 4.02 | 4.02 | 3.89 | 3.98 | 3.98 | 3.93 | 3.95 | 4.01 | 4.08 | 4.06 |
| 7.76              | 3.65 | 3.26 | 3.63 | 3.74 | 3.80 | 4.03 | 4.04 | 3.92 | 4.01 | 4.02 | 3.97 | 3.98 | 4.05 | 4.13 | 4.11 |
| 7.80              | 3.83 | 3.43 | 3.81 | 3.93 | 3.99 | 4.23 | 4.24 | 4.10 | 4.21 | 4.21 | 4.16 | 4.17 | 4.24 | 4.31 | 4.29 |
| 7.97              | 3.76 | 3.34 | 3.70 | 3.84 | 3.90 | 4.14 | 4.16 | 4.03 | 4.14 | 4.14 | 4.10 | 4.11 | 4.19 | 4.26 | 4.24 |
| 8.08              | 3.94 | 3.58 | 3.90 | 4.02 | 4.08 | 4.29 | 4.30 | 4.19 | 4.29 | 4.29 | 4.24 | 4.25 | 4.31 | 4.39 | 4.36 |
| 8.20              | 3.91 | 3.57 | 3.90 | 4.04 | 4.09 | 4.32 | 4.33 | 4.21 | 4.31 | 4.31 | 4.25 | 4.26 | 4.33 | 4.41 | 4.38 |
| 8.43              | 4.06 | 3.60 | 3.96 | 4.09 | 4.16 | 4.40 | 4.41 | 4.31 | 4.43 | 4.44 | 4.39 | 4.41 | 4.48 | 4.54 | 4.53 |

Table 2.5 (cont.). Corrected and uncorrected log  $K_S$  values at 0.5 M ionic strength. <sup>a</sup> Sample equilibrated for 30 minutes after adding *U. lactuca*.  
<sup>b</sup> Experiment performed in 0.5 M NaCl + 0.01 M CaCl<sub>2</sub> matrix.

| pH                 | Y    | La   | Ce   | Pr   | Nd   | Sm   | Eu   | Gd   | Tb   | Dy   | Ho   | Er   | Tm   | Yb   | Lu   |
|--------------------|------|------|------|------|------|------|------|------|------|------|------|------|------|------|------|
| 2.74 <sup>a</sup>  | 1.60 | 1.29 | 1.65 | 1.60 | 1.68 | 1.84 | 1.83 | 1.77 | 1.78 | 1.68 | 1.72 | 1.71 | 1.71 | 1.88 | 1.95 |
| 2.74 <sup>a</sup>  | 1.60 | 1.56 | 1.80 | 1.73 | 1.76 | 1.89 | 1.90 | 1.84 | 1.80 | 1.77 | 1.72 | 1.71 | 1.76 | 1.89 | 1.94 |
| 2.76 <sup>ab</sup> | 1.65 | 1.59 | 1.74 | 1.75 | 1.77 | 1.85 | 1.86 | 1.80 | 1.76 | 1.77 | 1.71 | 1.72 | 1.75 | 1.87 | 1.94 |
| 2.76 <sup>a</sup>  | 1.57 | 1.49 | 1.73 | 1.74 | 1.75 | 1.89 | 1.88 | 1.81 | 1.81 | 1.77 | 1.70 | 1.74 | 1.77 | 1.88 | 1.95 |
| 2.77 <sup>a</sup>  | 1.23 | 1.09 | 1.45 | 1.43 | 1.49 | 1.69 | 1.70 | 1.56 | 1.53 | 1.53 | 1.45 | 1.43 | 1.55 | 1.70 | 1.79 |
| 2.77 <sup>a</sup>  | 1.68 | 1.63 | 1.72 | 1.71 | 1.82 | 1.92 | 1.92 | 1.85 | 1.82 | 1.81 | 1.77 | 1.80 | 1.86 | 1.92 | 1.99 |
| 3.93               | 2.05 | 2.00 | 2.15 | 2.23 | 2.27 | 2.40 | 2.40 | 2.31 | 2.29 | 2.25 | 2.21 | 2.19 | 2.22 | 2.29 | 2.33 |
| 4.06               | 2.09 | 2.03 | 2.21 | 2.29 | 2.31 | 2.44 | 2.44 | 2.34 | 2.31 | 2.30 | 2.26 | 2.25 | 2.26 | 2.35 | 2.37 |
| 4.09 <sup>b</sup>  | 2.09 | 2.02 | 2.18 | 2.25 | 2.29 | 2.41 | 2.41 | 2.32 | 2.31 | 2.29 | 2.23 | 2.22 | 2.24 | 2.31 | 2.35 |
| 4.09               | 2.23 | 2.18 | 2.32 | 2.39 | 2.43 | 2.55 | 2.54 | 2.46 | 2.46 | 2.42 | 2.36 | 2.36 | 2.38 | 2.44 | 2.47 |
| 4.11               | 2.25 | 2.21 | 2.38 | 2.46 | 2.49 | 2.60 | 2.59 | 2.51 | 2.51 | 2.47 | 2.43 | 2.42 | 2.42 | 2.48 | 2.49 |
| 4.16               | 2.19 | 2.10 | 2.28 | 2.35 | 2.38 | 2.53 | 2.52 | 2.44 | 2.42 | 2.38 | 2.33 | 2.32 | 2.33 | 2.40 | 2.44 |
| 4.20               | 2.22 | 2.16 | 2.36 | 2.40 | 2.44 | 2.58 | 2.57 | 2.48 | 2.47 | 2.43 | 2.37 | 2.35 | 2.37 | 2.44 | 2.46 |
| 4.21               | 2.18 | 2.09 | 2.26 | 2.34 | 2.39 | 2.51 | 2.49 | 2.40 | 2.39 | 2.36 | 2.31 | 2.29 | 2.31 | 2.39 | 2.40 |
| 4.35               | 2.27 | 2.19 | 2.37 | 2.45 | 2.50 | 2.61 | 2.61 | 2.53 | 2.51 | 2.48 | 2.42 | 2.40 | 2.41 | 2.48 | 2.50 |
| 4.54               | 2.30 | 2.22 | 2.40 | 2.49 | 2.54 | 2.67 | 2.67 | 2.57 | 2.55 | 2.53 | 2.47 | 2.46 | 2.46 | 2.52 | 2.53 |
| 4.75               | 2.47 | 2.42 | 2.58 | 2.66 | 2.69 | 2.82 | 2.81 | 2.72 | 2.70 | 2.68 | 2.62 | 2.60 | 2.62 | 2.67 | 2.69 |
| 4.88               | 2.57 | 2.48 | 2.63 | 2.70 | 2.73 | 2.83 | 2.82 | 2.78 | 2.76 | 2.74 | 2.72 | 2.71 | 2.72 | 2.76 | 2.77 |
| 4.98               | 2.48 | 2.43 | 2.61 | 2.70 | 2.75 | 2.88 | 2.87 | 2.76 | 2.76 | 2.71 | 2.66 | 2.65 | 2.65 | 2.71 | 2.72 |
| 5.05               | 2.46 | 2.37 | 2.51 | 2.69 | 2.71 | 2.87 | 2.86 | 2.76 | 2.74 | 2.70 | 2.64 | 2.63 | 2.63 | 2.70 | 2.71 |
| 5.10               | 2.47 | 2.41 | 2.62 | 2.69 | 2.74 | 2.88 | 2.87 | 2.77 | 2.75 | 2.72 | 2.65 | 2.63 | 2.65 | 2.71 | 2.71 |
| 5.12               | 2.55 | 2.47 | 2.65 | 2.75 | 2.80 | 2.93 | 2.92 | 2.82 | 2.81 | 2.78 | 2.72 | 2.70 | 2.71 | 2.77 | 2.79 |
| 5.21 <sup>b</sup>  | 2.37 | 2.29 | 2.49 | 2.59 | 2.65 | 2.78 | 2.77 | 2.66 | 2.65 | 2.62 | 2.57 | 2.55 | 2.56 | 2.63 | 2.64 |
| 5.31               | 2.63 | 2.58 | 2.78 | 2.86 | 2.89 | 3.03 | 3.02 | 2.92 | 2.91 | 2.88 | 2.82 | 2.80 | 2.81 | 2.87 | 2.87 |
| 5.43               | 2.61 | 2.53 | 2.70 | 2.79 | 2.83 | 2.95 | 2.94 | 2.86 | 2.85 | 2.82 | 2.78 | 2.76 | 2.77 | 2.82 | 2.83 |
| 5.49               | 2.63 | 2.53 | 2.71 | 2.82 | 2.86 | 2.98 | 2.98 | 2.89 | 2.87 | 2.85 | 2.80 | 2.79 | 2.79 | 2.85 | 2.85 |
| 5.70               | 2.71 | 2.63 | 2.82 | 2.90 | 2.95 | 3.05 | 3.05 | 2.98 | 2.98 | 2.95 | 2.91 | 2.90 | 2.91 | 2.97 | 2.97 |
| 5.78               | 2.65 | 2.55 | 2.70 | 2.77 | 2.81 | 2.91 | 2.91 | 2.86 | 2.84 | 2.82 | 2.79 | 2.77 | 2.78 | 2.81 | 2.83 |
| 5.83               | 2.74 | 2.62 | 2.77 | 2.84 | 2.89 | 2.98 | 2.98 | 2.94 | 2.93 | 2.91 | 2.89 | 2.88 | 2.89 | 2.94 | 2.96 |
| 5.83 <sup>b</sup>  | 2.60 | 2.48 | 2.64 | 2.71 | 2.76 | 2.85 | 2.86 | 2.80 | 2.80 | 2.79 | 2.76 | 2.75 | 2.77 | 2.82 | 2.84 |

Table 2.5 (cont.). Corrected and uncorrected log  $K_S$  values at 0.5 M ionic strength. <sup>a</sup> Sample equilibrated for 30 minutes after adding *U. lactuca*.  
<sup>b</sup> Experiment performed in 0.5 M NaCl + 0.01 M CaCl<sub>2</sub> matrix.

| pH                | Y    | La   | Ce   | Pr   | Nd   | Sm   | Eu   | Gd   | Tb   | Dy   | Ho   | Er   | Tm   | Yb   | Lu   |
|-------------------|------|------|------|------|------|------|------|------|------|------|------|------|------|------|------|
| 5.95              | 2.70 | 2.58 | 2.73 | 2.80 | 2.84 | 2.93 | 2.94 | 2.90 | 2.89 | 2.87 | 2.85 | 2.85 | 2.86 | 2.90 | 2.92 |
| 5.96              | 2.74 | 2.61 | 2.76 | 2.84 | 2.89 | 2.98 | 2.98 | 2.94 | 2.93 | 2.92 | 2.90 | 2.90 | 2.92 | 2.96 | 2.97 |
| 5.98              | 2.73 | 2.63 | 2.76 | 2.84 | 2.89 | 2.97 | 2.98 | 2.93 | 2.92 | 2.91 | 2.89 | 2.89 | 2.90 | 2.93 | 2.95 |
| 6.01              | 2.80 | 2.70 | 2.88 | 2.95 | 2.98 | 3.09 | 3.09 | 3.03 | 3.02 | 3.01 | 2.97 | 2.96 | 2.98 | 3.02 | 3.03 |
| 6.09              | 2.76 | 2.62 | 2.75 | 2.83 | 2.88 | 2.96 | 2.97 | 2.93 | 2.92 | 2.91 | 2.90 | 2.90 | 2.92 | 2.96 | 2.98 |
| 6.30              | 2.89 | 2.73 | 2.86 | 2.93 | 2.97 | 3.04 | 3.05 | 3.03 | 3.03 | 3.03 | 3.04 | 3.05 | 3.06 | 3.09 | 3.10 |
| 6.31              | 2.84 | 2.72 | 2.89 | 2.97 | 3.03 | 3.11 | 3.12 | 3.07 | 3.07 | 3.06 | 3.03 | 3.03 | 3.05 | 3.09 | 3.10 |
| 6.40              | 2.79 | 2.64 | 2.79 | 2.85 | 2.89 | 2.97 | 2.98 | 2.95 | 2.94 | 2.94 | 2.92 | 2.93 | 2.95 | 2.99 | 3.01 |
| 6.67 <sup>b</sup> | 2.78 | 2.58 | 2.75 | 2.82 | 2.87 | 2.96 | 2.98 | 2.95 | 2.96 | 2.97 | 2.97 | 2.98 | 3.01 | 3.06 | 3.08 |
| 6.71              | 2.97 | 2.78 | 2.94 | 3.01 | 3.05 | 3.13 | 3.15 | 3.12 | 3.13 | 3.13 | 3.13 | 3.14 | 3.17 | 3.20 | 3.22 |
| 6.79              | 2.90 | 2.69 | 2.84 | 2.91 | 2.97 | 3.04 | 3.06 | 3.03 | 3.04 | 3.05 | 3.05 | 3.06 | 3.09 | 3.11 | 3.13 |
| 6.81              | 3.03 | 2.85 | 3.03 | 3.10 | 3.14 | 3.24 | 3.24 | 3.20 | 3.22 | 3.22 | 3.21 | 3.22 | 3.25 | 3.29 | 3.30 |
| 6.83              | 2.87 | 2.68 | 2.83 | 2.89 | 2.93 | 3.01 | 3.03 | 3.01 | 3.01 | 3.01 | 3.01 | 3.02 | 3.05 | 3.08 | 3.11 |
| 6.87              | 2.97 | 2.79 | 2.96 | 3.00 | 3.05 | 3.12 | 3.13 | 3.11 | 3.11 | 3.12 | 3.12 | 3.13 | 3.16 | 3.18 | 3.21 |
| 7.02 <sup>b</sup> | 2.97 | 2.68 | 2.89 | 2.92 | 2.98 | 3.05 | 3.07 | 3.07 | 3.09 | 3.11 | 3.12 | 3.14 | 3.17 | 3.19 | 3.22 |
| 7.04              | 2.98 | 2.72 | 2.87 | 2.93 | 2.99 | 3.06 | 3.08 | 3.07 | 3.08 | 3.09 | 3.11 | 3.13 | 3.16 | 3.18 | 3.21 |
| 7.12              | 3.02 | 2.80 | 2.99 | 3.07 | 3.11 | 3.20 | 3.22 | 3.19 | 3.20 | 3.21 | 3.20 | 3.22 | 3.25 | 3.28 | 3.30 |
| 7.14              | 3.09 | 2.83 | 2.98 | 3.02 | 3.07 | 3.12 | 3.14 | 3.15 | 3.16 | 3.17 | 3.19 | 3.22 | 3.22 | 3.23 | 3.26 |
| 7.16              | 2.97 | 2.73 | 2.89 | 2.96 | 3.01 | 3.09 | 3.11 | 3.09 | 3.10 | 3.12 | 3.12 | 3.14 | 3.17 | 3.20 | 3.23 |
| 7.31              | 3.02 | 2.74 | 2.90 | 2.95 | 2.99 | 3.08 | 3.09 | 3.10 | 3.11 | 3.12 | 3.14 | 3.16 | 3.19 | 3.21 | 3.24 |
| 7.35              | 3.17 | 2.86 | 3.00 | 3.04 | 3.10 | 3.15 | 3.17 | 3.19 | 3.20 | 3.22 | 3.25 | 3.28 | 3.29 | 3.29 | 3.32 |
| 7.48              | 3.24 | 2.94 | 3.11 | 3.15 | 3.19 | 3.26 | 3.28 | 3.29 | 3.30 | 3.31 | 3.34 | 3.36 | 3.37 | 3.38 | 3.41 |
| 7.63              | 3.27 | 2.92 | 3.09 | 3.10 | 3.15 | 3.20 | 3.23 | 3.27 | 3.28 | 3.30 | 3.33 | 3.36 | 3.37 | 3.36 | 3.40 |
| 7.68              | 3.24 | 2.95 | 3.08 | 3.10 | 3.15 | 3.18 | 3.20 | 3.23 | 3.23 | 3.25 | 3.28 | 3.30 | 3.30 | 3.29 | 3.32 |
| 7.76              | 3.23 | 2.88 | 3.05 | 3.07 | 3.12 | 3.17 | 3.19 | 3.23 | 3.24 | 3.26 | 3.29 | 3.31 | 3.32 | 3.32 | 3.35 |
| 7.80              | 3.46 | 3.12 | 3.32 | 3.36 | 3.40 | 3.46 | 3.47 | 3.48 | 3.50 | 3.52 | 3.54 | 3.55 | 3.56 | 3.55 | 3.58 |
| 7.97              | 3.31 | 2.97 | 3.11 | 3.16 | 3.20 | 3.25 | 3.28 | 3.30 | 3.31 | 3.33 | 3.37 | 3.39 | 3.40 | 3.40 | 3.43 |
| 8.08              | 3.48 | 3.26 | 3.35 | 3.36 | 3.39 | 3.40 | 3.42 | 3.46 | 3.45 | 3.46 | 3.49 | 3.50 | 3.49 | 3.49 | 3.52 |
| 8.20              | 3.39 | 3.22 | 3.31 | 3.33 | 3.36 | 3.36 | 3.38 | 3.41 | 3.40 | 3.41 | 3.43 | 3.44 | 3.43 | 3.44 | 3.46 |
| 8.43              | 3.45 | 3.19 | 3.26 | 3.25 | 3.29 | 3.30 | 3.32 | 3.37 | 3.37 | 3.39 | 3.43 | 3.45 | 3.44 | 3.43 | 3.47 |

Table 2.6. Corrected and uncorrected log  $K_S$  values at 5.0 M ionic strength. <sup>a</sup> Sample equilibrated for 30 minutes after adding *U. lactuca*.

| pH                | Y    | La   | Ce   | Pr   | Nd   | Sm   | Eu   | Gd   | Tb   | Dy   | Ho   | Er   | Tm   | Yb   | Lu   |
|-------------------|------|------|------|------|------|------|------|------|------|------|------|------|------|------|------|
| 2.74 <sup>a</sup> | 1.42 | 1.41 | 1.49 | 1.39 | 1.44 | 1.53 | 1.61 | 1.57 | 1.58 | 1.55 | 1.49 | 1.51 | 1.58 | 1.77 | 1.82 |
| 2.77 <sup>a</sup> | 1.37 | 1.27 | 1.41 | 1.35 | 1.39 | 1.54 | 1.53 | 1.46 | 1.46 | 1.40 | 1.43 | 1.50 | 1.62 | 1.76 | 1.82 |
| 3.86              | 1.81 | 1.80 | 1.81 | 1.88 | 1.91 | 2.08 | 2.09 | 2.01 | 2.01 | 2.00 | 1.94 | 1.97 | 2.04 | 2.15 | 2.20 |
| 4.12              | 2.12 | 2.13 | 2.14 | 2.20 | 2.22 | 2.35 | 2.35 | 2.27 | 2.30 | 2.28 | 2.23 | 2.22 | 2.28 | 2.36 | 2.39 |
| 4.43              | 2.14 | 2.20 | 2.19 | 2.27 | 2.30 | 2.47 | 2.48 | 2.38 | 2.41 | 2.37 | 2.30 | 2.29 | 2.33 | 2.44 | 2.47 |
| 4.71              | 2.20 | 2.31 | 2.29 | 2.37 | 2.40 | 2.58 | 2.59 | 2.48 | 2.51 | 2.48 | 2.41 | 2.38 | 2.42 | 2.52 | 2.53 |
| 5.00              | 2.47 | 2.54 | 2.58 | 2.66 | 2.69 | 2.86 | 2.86 | 2.76 | 2.78 | 2.75 | 2.67 | 2.65 | 2.68 | 2.76 | 2.75 |
| 5.11              | 2.36 | 2.45 | 2.53 | 2.60 | 2.64 | 2.83 | 2.83 | 2.70 | 2.73 | 2.70 | 2.60 | 2.58 | 2.62 | 2.72 | 2.71 |
| 5.38              | 2.62 | 2.63 | 2.74 | 2.83 | 2.86 | 3.04 | 3.05 | 2.93 | 2.95 | 2.92 | 2.83 | 2.81 | 2.84 | 2.92 | 2.91 |
| 5.70              | 2.77 | 2.71 | 2.91 | 3.00 | 3.04 | 3.22 | 3.23 | 3.10 | 3.13 | 3.10 | 3.02 | 2.99 | 3.03 | 3.10 | 3.08 |
| 5.71              | 2.85 | 2.79 | 2.97 | 3.06 | 3.09 | 3.27 | 3.28 | 3.16 | 3.19 | 3.16 | 3.08 | 3.06 | 3.09 | 3.16 | 3.14 |
| 5.88              | 2.89 | 2.77 | 2.99 | 3.09 | 3.13 | 3.31 | 3.32 | 3.19 | 3.24 | 3.21 | 3.13 | 3.11 | 3.14 | 3.22 | 3.20 |
| 5.92              | 2.88 | 2.78 | 2.99 | 3.09 | 3.13 | 3.32 | 3.33 | 3.20 | 3.24 | 3.21 | 3.13 | 3.10 | 3.14 | 3.22 | 3.19 |
| 6.43              | 3.06 | 2.84 | 3.14 | 3.26 | 3.30 | 3.52 | 3.53 | 3.39 | 3.45 | 3.43 | 3.36 | 3.34 | 3.39 | 3.47 | 3.45 |
| 6.55              | 3.13 | 2.88 | 3.21 | 3.32 | 3.36 | 3.58 | 3.58 | 3.45 | 3.52 | 3.50 | 3.43 | 3.42 | 3.47 | 3.55 | 3.53 |
| 6.56              | 3.10 | 2.86 | 3.19 | 3.31 | 3.36 | 3.58 | 3.59 | 3.45 | 3.51 | 3.50 | 3.42 | 3.41 | 3.46 | 3.54 | 3.53 |
| 6.76              | 3.18 | 2.93 | 3.25 | 3.38 | 3.43 | 3.65 | 3.66 | 3.52 | 3.59 | 3.58 | 3.50 | 3.49 | 3.55 | 3.63 | 3.62 |
| 6.99              | 3.24 | 2.94 | 3.27 | 3.40 | 3.45 | 3.68 | 3.69 | 3.55 | 3.64 | 3.63 | 3.56 | 3.56 | 3.63 | 3.72 | 3.70 |
| 7.02              | 3.27 | 2.94 | 3.28 | 3.41 | 3.46 | 3.70 | 3.72 | 3.58 | 3.68 | 3.67 | 3.61 | 3.61 | 3.68 | 3.77 | 3.76 |
| 7.28              | 3.45 | 3.06 | 3.41 | 3.54 | 3.59 | 3.84 | 3.86 | 3.73 | 3.83 | 3.84 | 3.78 | 3.79 | 3.87 | 3.96 | 3.94 |
| 7.37              | 3.42 | 3.00 | 3.37 | 3.50 | 3.56 | 3.82 | 3.84 | 3.71 | 3.82 | 3.84 | 3.78 | 3.79 | 3.88 | 3.99 | 3.97 |
| 7.44              | 3.49 | 3.08 | 3.44 | 3.56 | 3.62 | 3.88 | 3.91 | 3.77 | 3.89 | 3.90 | 3.84 | 3.86 | 3.94 | 4.04 | 4.02 |
| 7.49              | 3.50 | 3.09 | 3.45 | 3.57 | 3.63 | 3.90 | 3.93 | 3.79 | 3.91 | 3.92 | 3.86 | 3.88 | 3.96 | 4.07 | 4.04 |
| 7.91              | 3.70 | 3.20 | 3.60 | 3.72 | 3.78 | 4.08 | 4.11 | 3.97 | 4.11 | 4.13 | 4.07 | 4.08 | 4.18 | 4.30 | 4.25 |
| 7.94              | 3.71 | 3.19 | 3.57 | 3.70 | 3.76 | 4.06 | 4.10 | 3.96 | 4.11 | 4.13 | 4.08 | 4.11 | 4.21 | 4.33 | 4.29 |
| 8.14              | 3.88 | 3.28 | 3.73 | 3.82 | 3.89 | 4.21 | 4.26 | 4.11 | 4.29 | 4.31 | 4.26 | 4.29 | 4.39 | 4.51 | 4.47 |
| 8.48              | 4.14 | 3.47 | 3.91 | 4.03 | 4.11 | 4.46 | 4.52 | 4.37 | 4.56 | 4.60 | 4.55 | 4.58 | 4.70 | 4.83 | 4.78 |

Table 2.6 (cont.). Corrected and uncorrected log  $K_S$  values at 5.0 M ionic strength. <sup>a</sup> Sample equilibrated for 30 minutes after adding *U. lactuca*.

| pH                | Y    | La   | Ce   | Pr   | Nd   | Sm   | Eu   | Gd   | Tb   | Dy   | Ho   | Er   | Tm   | Yb   | Lu   |
|-------------------|------|------|------|------|------|------|------|------|------|------|------|------|------|------|------|
| 2.74 <sup>a</sup> | 1.41 | 1.37 | 1.48 | 1.37 | 1.42 | 1.52 | 1.59 | 1.56 | 1.57 | 1.54 | 1.48 | 1.50 | 1.57 | 1.77 | 1.82 |
| 2.77 <sup>a</sup> | 1.36 | 1.21 | 1.40 | 1.33 | 1.37 | 1.52 | 1.52 | 1.44 | 1.45 | 1.38 | 1.42 | 1.49 | 1.62 | 1.75 | 1.82 |
| 3.86              | 1.77 | 1.59 | 1.74 | 1.82 | 1.86 | 2.02 | 2.04 | 1.96 | 1.97 | 1.96 | 1.90 | 1.93 | 2.00 | 2.12 | 2.17 |
| 4.12              | 2.08 | 1.94 | 2.07 | 2.14 | 2.16 | 2.29 | 2.30 | 2.22 | 2.25 | 2.23 | 2.19 | 2.18 | 2.24 | 2.32 | 2.36 |
| 4.43              | 2.05 | 1.86 | 2.07 | 2.17 | 2.20 | 2.37 | 2.39 | 2.30 | 2.32 | 2.29 | 2.22 | 2.21 | 2.26 | 2.37 | 2.41 |
| 4.71              | 2.06 | 1.87 | 2.10 | 2.21 | 2.25 | 2.44 | 2.45 | 2.35 | 2.38 | 2.34 | 2.28 | 2.27 | 2.30 | 2.41 | 2.44 |
| 5.00              | 2.32 | 2.17 | 2.38 | 2.48 | 2.52 | 2.69 | 2.70 | 2.60 | 2.62 | 2.59 | 2.53 | 2.51 | 2.53 | 2.62 | 2.63 |
| 5.11              | 2.13 | 1.90 | 2.26 | 2.36 | 2.41 | 2.61 | 2.62 | 2.50 | 2.52 | 2.49 | 2.41 | 2.39 | 2.42 | 2.53 | 2.55 |
| 5.38              | 2.40 | 2.22 | 2.45 | 2.56 | 2.61 | 2.78 | 2.79 | 2.69 | 2.70 | 2.67 | 2.61 | 2.60 | 2.62 | 2.69 | 2.71 |
| 5.70              | 2.47 | 2.32 | 2.56 | 2.66 | 2.71 | 2.86 | 2.87 | 2.78 | 2.79 | 2.77 | 2.71 | 2.69 | 2.71 | 2.78 | 2.79 |
| 5.71              | 2.58 | 2.44 | 2.64 | 2.73 | 2.78 | 2.92 | 2.94 | 2.86 | 2.86 | 2.84 | 2.79 | 2.78 | 2.79 | 2.85 | 2.87 |
| 5.88              | 2.58 | 2.39 | 2.60 | 2.70 | 2.75 | 2.88 | 2.90 | 2.83 | 2.84 | 2.82 | 2.77 | 2.76 | 2.78 | 2.84 | 2.86 |
| 5.92              | 2.58 | 2.42 | 2.61 | 2.70 | 2.76 | 2.89 | 2.90 | 2.83 | 2.83 | 2.82 | 2.77 | 2.76 | 2.78 | 2.83 | 2.85 |
| 6.43              | 2.70 | 2.47 | 2.69 | 2.78 | 2.83 | 2.95 | 2.97 | 2.92 | 2.93 | 2.92 | 2.90 | 2.89 | 2.91 | 2.96 | 2.98 |
| 6.55              | 2.79 | 2.55 | 2.79 | 2.85 | 2.89 | 3.01 | 3.02 | 2.98 | 2.99 | 2.99 | 2.97 | 2.97 | 2.99 | 3.03 | 3.05 |
| 6.56              | 2.74 | 2.53 | 2.76 | 2.84 | 2.90 | 3.03 | 3.04 | 2.98 | 2.99 | 2.99 | 2.96 | 2.95 | 2.98 | 3.03 | 3.05 |
| 6.76              | 2.82 | 2.62 | 2.81 | 2.90 | 2.95 | 3.06 | 3.08 | 3.03 | 3.04 | 3.03 | 3.01 | 3.01 | 3.02 | 3.07 | 3.09 |
| 6.99              | 2.88 | 2.64 | 2.82 | 2.91 | 2.96 | 3.07 | 3.08 | 3.05 | 3.06 | 3.06 | 3.05 | 3.06 | 3.08 | 3.12 | 3.14 |
| 7.02              | 2.91 | 2.62 | 2.83 | 2.92 | 2.97 | 3.08 | 3.10 | 3.07 | 3.10 | 3.10 | 3.10 | 3.10 | 3.13 | 3.17 | 3.20 |
| 7.28              | 3.11 | 2.79 | 3.00 | 3.07 | 3.12 | 3.21 | 3.23 | 3.22 | 3.24 | 3.25 | 3.26 | 3.27 | 3.29 | 3.31 | 3.34 |
| 7.37              | 3.05 | 2.69 | 2.91 | 3.00 | 3.05 | 3.15 | 3.18 | 3.16 | 3.19 | 3.21 | 3.22 | 3.23 | 3.26 | 3.29 | 3.33 |
| 7.44              | 3.13 | 2.80 | 3.01 | 3.08 | 3.13 | 3.22 | 3.25 | 3.23 | 3.25 | 3.26 | 3.27 | 3.28 | 3.30 | 3.32 | 3.35 |
| 7.49              | 3.13 | 2.81 | 3.01 | 3.08 | 3.13 | 3.22 | 3.25 | 3.24 | 3.25 | 3.26 | 3.27 | 3.29 | 3.30 | 3.32 | 3.35 |
| 7.91              | 3.23 | 2.90 | 3.12 | 3.17 | 3.22 | 3.27 | 3.28 | 3.29 | 3.28 | 3.28 | 3.30 | 3.30 | 3.29 | 3.29 | 3.32 |
| 7.94              | 3.22 | 2.89 | 3.06 | 3.12 | 3.16 | 3.23 | 3.25 | 3.26 | 3.25 | 3.26 | 3.29 | 3.31 | 3.31 | 3.31 | 3.35 |
| 8.14              | 3.32 | 2.94 | 3.18 | 3.19 | 3.23 | 3.28 | 3.30 | 3.32 | 3.32 | 3.33 | 3.35 | 3.36 | 3.36 | 3.35 | 3.38 |
| 8.48              | 3.39 | 3.07 | 3.21 | 3.24 | 3.29 | 3.31 | 3.33 | 3.37 | 3.35 | 3.36 | 3.40 | 3.41 | 3.40 | 3.39 | 3.43 |

(Uncorrected)

Table 2.7. Best-fit slopes from linear regressions of log  $K_S$  vs. pH data (Tables 2.4 – 2.6).

|         | <b>0.05 M NaCl</b> | <b>0.5 M NaCl</b> | <b>5.0 M NaCl</b> |
|---------|--------------------|-------------------|-------------------|
| Y       | 0.35 ± 0.02        | 0.42 ± 0.01       | 0.45 ± 0.01       |
| La      | 0.37 ± 0.02        | 0.36 ± 0.01       | 0.33 ± 0.02       |
| Ce      | 0.40 ± 0.02        | 0.40 ± 0.01       | 0.42 ± 0.01       |
| Pr      | 0.40 ± 0.02        | 0.42 ± 0.01       | 0.44 ± 0.01       |
| Nd      | 0.40 ± 0.02        | 0.42 ± 0.01       | 0.45 ± 0.01       |
| Sm      | 0.40 ± 0.02        | 0.45 ± 0.01       | 0.49 ± 0.01       |
| Eu      | 0.41 ± 0.02        | 0.45 ± 0.01       | 0.49 ± 0.01       |
| Gd      | 0.39 ± 0.02        | 0.44 ± 0.01       | 0.48 ± 0.01       |
| Tb      | 0.40 ± 0.02        | 0.46 ± 0.01       | 0.51 ± 0.01       |
| Dy      | 0.40 ± 0.02        | 0.47 ± 0.01       | 0.52 ± 0.01       |
| Ho      | 0.39 ± 0.01        | 0.47 ± 0.01       | 0.52 ± 0.01       |
| Er      | 0.38 ± 0.01        | 0.47 ± 0.01       | 0.52 ± 0.01       |
| Tm      | 0.38 ± 0.01        | 0.48 ± 0.01       | 0.52 ± 0.01       |
| Yb      | 0.39 ± 0.01        | 0.48 ± 0.01       | 0.52 ± 0.01       |
| Lu      | 0.38 ± 0.01        | 0.46 ± 0.01       | 0.50 ± 0.01       |
| Average | 0.39 ± 0.004       | 0.44 ± 0.01       | 0.48 ± 0.01       |

## Chapter 3: Application of a non-electrostatic surface complexation model

### 3.1. Abstract

The sorption of the YREEs on *U. lactuca* was investigated by determining distribution coefficients ( $K_S$ ) in solutions containing all YREEs and dehydrated *U. lactuca* tissue. These values were calculated over a wide pH range (2.7 – 8.5) and at three different ionic strengths (0.05, 0.5 and 5.0 M NaCl). All  $K_S$  values also account for the presence of colloid-bound metals  $< 0.22 \mu\text{m}$  with a colloid correction (Ch. 2).

As linear regressions (Fig. 2.9) are insufficient to fully capture sorption behavior, a non-electrostatic surface complexation model (NEM) was developed to describe the equilibrium between dissolved and sorbed YREE. The model assumes three independent metal-complexing groups with approximate  $\text{pK}_a$ s of 4, 6 and 9 and is able to precisely describe YREE sorption as a function of pH ( $r^2 > 0.98$  in most cases). Low ionic strength data could not resolve the first two groups independently, so a modified NEM with one combined term for the first two groups was required to fit the data. The model contains several conditional stability constants ( $\beta_x$ ) that describe free metal and hydrolyzed metal sorption on the monoprotic surface groups. Using known YREE stability constants and linear free-energy relations (LFER), the first of these groups is identified as a carboxyl group and the third as a phenol. The second group did not match any known YREE stability constant patterns, but could possibly be a phosphate moiety. NEMs appear to be a productive approach for modeling metal sorption on organic matter and can help inform bioremediation and biomonitoring efforts, as well as a general understanding of trace

metal geochemistry in natural waters.

### 3.2. Introduction

Because the majority of particles that participate in metal sorption in the open ocean are organic, the ability to model the chemical mechanisms governing metal-organic sorption is an important goal of trace metal geochemistry. To this end, various models have been developed and utilized to predict metal sorption on organic matter. Initial work by Stumm et al. (1970) laid the groundwork for equilibrium descriptions of metal sorption onto particles. These surface complexation models (SCMs) were first developed to describe sorption on amphoteric mineral surfaces, and they have been extended to describe sorption on organic matter as well (DAVIS and KENT, 1990). SCMs differ in their derivations and assumptions, but there are a few general guidelines that all metal SCMs follow (DZOMBAK and MOREL, 1990; DAVIS et al., 1998). First, they assume that the surface is composed of discrete functional groups capable of interacting with dissolved metals in solution. These functional groups form surface complexes with metal ions, analogous to metal complexation with dissolved ligands in solution. Second, the equilibrium sorption reactions can be described with mass law equations. Third, surface charge on the particle is a result of the sorption reactions and acid-base reactions, which are described by equilibrium constants (i.e.  $K_S$  and  $K_a$ ).

As a result of these tenets, there are two types of SCMs commonly used in the literature. Electrostatic SCMs treat metal sorption as an intrinsic process, independent of influence from solution effects such as ionic strength or pH, and calculate intrinsic equilibrium constants ( $K_S(\text{int})$ ) by correcting apparent equilibrium constants ( $K_S(\text{app})$ )

with a Coulombic energy term (STUMM and MORGAN, 1996):

$$K_s(\text{app}) = K_s(\text{int}) \exp\left(-\frac{\Delta Z F \Psi_0}{RT}\right) \quad (3.1)$$

where  $\Delta Z$  is the change in surface charge due to the reaction that  $K_s$  describes,  $F$  is Faraday's constant,  $\Psi_0$  is the surface potential,  $R$  is the ideal gas constant, and  $T$  is temperature. Electrostatic SCMs have the benefit of taking into account the surface charge on a particle and producing equilibrium constants that are independent of the composition of the particle. However, as there is no experimental way to measure  $\Psi_0$ , it must be approximated from different models, such as the diffuse double-layer model or the triple-layer model (DAVIS et al., 1978; DZOMBAK and MOREL, 1990). Even with these models, estimation of the Coulombic term remains quite complex, especially for environmental samples and organic matter (DAVIS et al., 1998).

The need to quantify the electrostatic surface properties of a substrate is alleviated with non-electrostatic surface complexation models (NEMs). In this approach, the model does not account for surface electrical charge or its effect on sorption. The  $K_s$  values in these models implicitly include all chemical and electrostatic interactions. As a result, NEM equilibrium constants are conditional constants, valid only for the given solution conditions. These equilibrium constants may seem oversimplified, but they allow researchers to probe the mechanism of the sorptive process, rather than providing a rigorous thermodynamic description (SCHIFF and MARSHALL, 2011). NEMs are especially suited for studying moderately to strongly sorbing ions (such as the YREEs), where the free energy of sorption exceeds the electrostatic contribution (DAVIS and KENT, 1990). NEMs have been used to successfully model YREE sorption on basalt powder and quartz sand (TANG and JOHANNESSON, 2005; TERTRE et al., 2008), Pb and Cd sorption on soils

(SERRANO et al., 2009), and YREE sorption on iron hydroxides (QUINN et al., 2006a; SCHIJF and MARSHALL, 2011). DAVIS et al. (1998) also argued that because the surface charge behavior of complex environmental samples is not well understood, NEMs are a more appropriate choice over electrostatic SCMs for modeling metal sorption on organic matter.

Although NEMs have been used to describe metal sorption on bacteria, fungi, soils, etc. (FOWLE and FEIN, 1999; MARKAI et al., 2003; NAEEM et al., 2006; DEO et al., 2010; MISHRA et al., 2010), these studies have utilized chemical equilibrium programs (e.g. FITEQL) to model sorption data and provide best-fit parameters. Programs such as these solve a system of equilibrium reactions and mass balance equations to provide a numerical fit of the data, and they require detailed knowledge of all components in the system being studied, including metal-binding site concentrations, protonation constants, and all reactions taking place. Many of these details are not known for most types of organic matter, which makes it difficult to use this approach without making a number of simplifying assumptions.

The majority of sorption studies, including those that utilize FITEQL, titrate the sorbent with a metal solution at constant pH, an approach lending itself to a description with generic (e.g. Langmuir, Freundlich, Frumkin etc.) sorption isotherms (STUMM and MORGAN, 1996). These studies regard sorption as a bulk partitioning of the metal between the solution and the surface. Isotherms are fit to log-log plots of the degree of metal sorption as a function of dissolved metal concentrations, using site densities and conditional surface complexation constants as adjustable parameters. This is useful for complex organic substrates since the surface is treated as a generic, homogeneous

compartment for sorbed metals. However, due to this simplified description of the system, sorption isotherms have two major disadvantages (DAVIS and KENT, 1990). First, because the surface is treated as a single, bulk compartment for metal sorption with fixed independent sites, sorption isotherms cannot reveal stoichiometric information about surface or solution reactions, which means that such models cannot provide any insight into the actual sorption mechanism. Second, sorption isotherms require that the titration is continued until the majority of surface sites is saturated, which means that the system may no longer be at equilibrium. Changing the dissolved metal concentration in an experiment also makes it difficult to maintain experimental conditions like ionic strength, or to measure total metal concentrations ( $[M]_{\text{init}}$ ) at any given pH.

An alternative to FITEQL or partition isotherms is to use an analytical function, derived from first principles and mass balance equations, that is able to predict metal sorption onto a surface as a function of solution conditions. In such an approach sorption is measured as a function of pH (which is easily measured at a given point) rather than metal concentration. This approach has been used successfully to describe YREE sorption on hydrous ferric oxides under a variety of different temperature, ionic strength and pH conditions (QUINN et al., 2006a, b, c; SCHIJF and MARSHALL, 2011). The benefit of this approach is that the results can provide detailed information about the underlying mechanisms of metal sorption. The model used here is derived in a similar manner, and is able to predict YREE sorption on *U. lactuca* as a function of pH at three different ionic strengths.

### 3.3. Materials and Methods

YREE-*U. lactuca* sorption experiments were conducted as a function of pH at three ionic strengths (0.05 M, 0.5 M and 5.0 M NaCl). The experimental setup, materials preparations, and procedures are described in sections 2.3.1 and 2.3.2. For all sorption experiments, ICP-MS analysis was used to determine dissolved YREE concentrations in each sample. This procedure is described in section 2.3.5. Additional details concerning a reversibility experiment and the method for calculating distribution coefficients are included below.

#### *3.3.1. Reversibility experiment*

As chemical equilibrium models require that the processes being studied are in equilibrium and fully reversible (DAVIS and KENT, 1990), a reversibility experiment was conducted in the same manner as the sorption experiments. YREE sorption on the dried *U. lactuca* standard in a 0.5 M NaCl solution was measured after titrating the solution to select pH points from ~3 to 8. For the first half of the experiment, pH was gradually adjusted upwards with NaOH. YREE sorption was then reversed by gradually lowering the pH with HCl. Samples were taken after a 6-hour equilibration at each pH point, filtered with 0.22  $\mu\text{m}$  membrane filters, and analyzed for YREE concentration via ICP-MS.

#### *3.3.2. Calculating distribution coefficients*

Distribution coefficients from the sorption experiments were calculated with the colloid correction equation (Eq. 2.12) as described in section 2.4.3. This correction

utilized ultracentrifuge data to correct apparent YREE dissolved concentrations to produce truly dissolved YREE concentrations,  $[M]_{\text{corr}}$ . The corrected dissolved YREE concentrations were then used to calculate  $K_S$  values according to the equation:

$$K_S = \frac{[M]_{\text{init}} - [M]_{\text{corr}}}{[M]_{\text{corr}} \times [S]_T} \quad (3.1)$$

where  $[M]_{\text{init}}$  is the initial YREE concentration in solution before any *U. lactuca* addition,  $[M]_{\text{corr}}$  is the truly dissolved YREE concentration at the time of sampling (calculated from Eq. 2.12), and  $[S]_T$  is the total site concentration, taken to be the sum of L1, L2, and L3 from SCHIJF and EBLING (2010),  $\approx 1.6 \text{ mmol} \cdot \text{g}^{-1}$  *U. lactuca* (dry weight), the most likely candidates for metal sorption in the pH range studied ( $\text{pK}_a(\text{L}_1) \sim 3.9$ ,  $\text{pK}_a(\text{L}_2) \sim 6.1$ ,  $\text{pK}_a(\text{L}_3) \sim 9.4$ ).

### 3.4. Results and Discussion

#### *3.4.1. Reversibility experiment*

Sorption for all YREEs on *U. lactuca* was fully reversible by adjusting solution pH (Fig. 3.1 illustrates this for La) in 0.5 M NaCl. Similar reversibility experiments have been used before to demonstrate the validity of NEMs for metal sorption on bacterial cells (FOWLE and FEIN, 2000; NGWENYA et al., 2009). As full reversibility is an inherent assumption in any chemical equilibrium model, the reversible nature of YREE sorption on *U. lactuca* supports the use of a NEM for this system as well. The experiment also points to the mechanism of YREE sorption on *U. lactuca*, which could conceivably occur by internalization of metal ions into the cell interior. However, this would likely not be a reversible process and therefore a surface complexation model would not be applicable

for the system. The full reversibility seen in the experiment suggests that ion-exchange is occurring with functional groups on *U. lactuca*'s cell walls. This confirms results seen in several other studies where dehydrated *U. lactuca* tissue is treated as a cation-exchange resin (HAMDY, 2000; ZEROUAL et al., 2003) and metal uptake is fully reversible after treatment with strong acid.

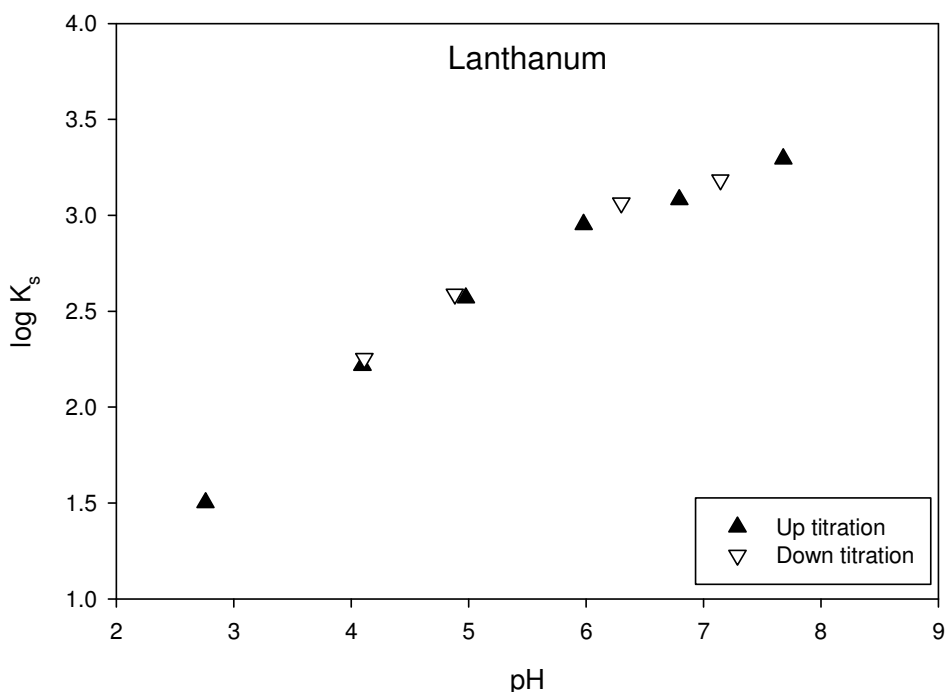


**Figure 3.1.** Reversibility experiment performed in 0.5 M NaCl on *U. lactuca* dried standard. Closed triangles represent samples taken after increasing solution pH, while open triangles are samples taken after decreasing solution pH. Note that both sets of samples follow the same sorption curve.

### 3.4.2. The non-electrostatic surface complexation model: derivation and fits

The reversibility experiment demonstrates equilibrium behavior for YREE sorption on *U. lactuca* over the pH range studied, so a non-electrostatic surface complexation model (NEM) was developed to describe the sorption process. Given support for the presence of three acidic functional groups from potentiometric titrations

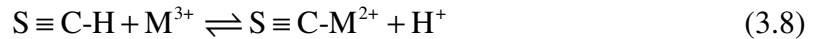
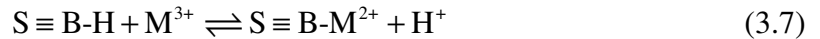
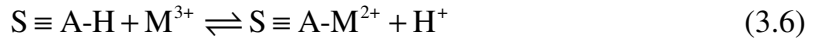
of *U. lactuca* (SCHIJF and EBLING, 2010), the model derived here considers YREE interactions with three monoprotic functional groups as well. The protonated forms of these groups are written as  $S\equiv A-H$ ,  $S\equiv B-H$  and  $S\equiv C-H$ , and can protonate and deprotonate according to the reactions:



With corresponding acid dissociation constants  $K_x$  (where x refers to site A, B or C):

$$K_x = \frac{[S\equiv X^-][H^+]}{[S\equiv X-H]} \quad (3.5)$$

YREE interaction with the surface will be considered through sorption on these three groups. Sorption of free metal ( $M^{3+}$ ) onto each of these groups (written as  $S\equiv X-M^{2+}$ ) is represented by the reactions:



and corresponding complexation constants  $\beta_x$ :

$$\beta_x = \frac{[S\equiv X-M^{2+}][H^+]}{[S\equiv X-H][M^{3+}]} \quad (3.9)$$

Under the solution conditions used in these experiments (0.05, 0.5 and 5.0 M NaCl, pH 2.7 – 8.5), there are significant YREE interactions with  $Cl^-$  and  $OH^-$  ions, resulting in dissolved  $MCl^{2+}$  and  $MOH^{2+}$  species (KLUNGNESS and BYRNE, 2000; LUO and BYRNE, 2001). While the extent of  $MCl^{2+}$  complexation is not pH dependent and

remains constant for a given ionic strength ( $MCl^{2+}$  complexation constants,  $_{Cl}\beta_1(M)$  are given in Table 3.1),  $MOH^{2+}$  formation is pH dependent:



This reaction becomes significant at the upper end of the pH range used in these experiments, where at pH 8.4  $MOH^{2+}$  makes up about 13% of total dissolved La and 84% of total dissolved Lu. YREE hydrolysis is represented by hydrolysis constants ( $\beta_1^*$ ):

$$\beta_1^*(M) = \frac{[MOH^{2+}][H^+]}{[M^{3+}]} \quad (3.11)$$

Values for all YREE hydrolysis constants are given in Table 3.1, and were calculated for each ionic strength from KLUNGNESS and BYRNE (2000). Given that a significant portion of dissolved metal is actually present as  $MCl^{2+}$  over all pHs and  $MOH^{2+}$  at high pH,  $_{Cl}\beta_1$  and  $\beta_1^*$  values were used to correct dissolved metal concentrations in the denominator of the  $K_S$  calculation (Eq. 3.1):

$$[M]_{corr} = [M^{3+}] + [MOH] + [MCl] = [M^{3+}] \left( 1 + \beta_1^* [H^+]^{-1} + {}_{Cl}\beta_1 [Cl^-] \right) \quad (3.12)$$

$$[M^{3+}] = \frac{[M]_{corr}}{\left( 1 + \beta_1^* [H^+]^{-1} + {}_{Cl}\beta_1 [Cl^-] \right)} \quad (3.13)$$

$$K_S = \frac{[M]_{mit} - [M]_{corr}}{\frac{[M]_{corr}}{\left( 1 + \beta_1^* [H^+]^{-1} + {}_{Cl}\beta_1 [Cl^-] \right)} \times [S]_T} \quad (3.14)$$

Because  $MCl^{2+}$  formation is not pH dependent,  $MCl^{2+}$  sorption cannot be distinguished from  $M^{3+}$  sorption in the model, where pH is the only experimental variable. However  $MOH^{2+}$  species are likely to interact with the surface at high pH.  $MOH^{2+}$  sorption is therefore considered with site C, which would be the final site to fully

deprotonate:



represented by the complexation constant

$$\beta_c^* = \frac{[\text{S} \equiv \text{C-MOH}^+][\text{H}^+]}{[\text{S} \equiv \text{C-H}][\text{MOH}^{2+}]} = \frac{[\text{S} \equiv \text{C-MOH}^+][\text{H}^+]^2}{[\text{S} \equiv \text{C-H}][\text{M}^{3+}]\beta_1^*} \quad (3.16)$$

Total metal concentration on the surface (S-M) is equal to the sum of  $\text{S} \equiv \text{A-M}^{2+}$ ,  $\text{S} \equiv \text{B-M}^{2+}$ ,  $\text{S} \equiv \text{C-M}^{2+}$  and  $\text{S} \equiv \text{C-MOH}^+$ , which can be expressed by substituting terms from Eqs. (3.9) and (3.16):

$$\begin{aligned} [\text{S-M}] = & \beta_A [\text{M}^{3+}][\text{S} \equiv \text{A-H}][\text{H}^+]^{-1} + \beta_B [\text{M}^{3+}][\text{S} \equiv \text{B-H}][\text{H}^+]^{-1} \\ & + {}_1\beta_c [\text{M}^{3+}][\text{S}_C\text{H}][\text{H}^+]^{-1} + \beta_c^* \beta_1^* [\text{M}^{3+}][\text{S} \equiv \text{C-H}][\text{H}^+]^{-2} \end{aligned} \quad (3.17)$$

The distribution coefficient ( $K_S$ ) can then be expressed in terms of the total site concentration  $[\text{S}]_T$ , total sorbed metal  $[\text{S-M}]$ , and free metal concentration  $[\text{M}^{3+}]$ :

$$K_S = \frac{[\text{S-M}]}{[\text{M}^{3+}] \times [\text{S}]_T} = \frac{[\text{S} \equiv \text{A-M}^{2+}] + [\text{S} \equiv \text{B-M}^{2+}] + [\text{S} \equiv \text{C-M}^{2+}] + [\text{S} \equiv \text{C-MOH}^+]}{[\text{M}^{3+}] \times (\text{A}_T + \text{B}_T + \text{C}_T)} \quad (3.18)$$

where  $[\text{S}]_T$  is the sum of the total concentrations of sites A, B and C:

$$[\text{S}]_T = \text{A}_T + \text{B}_T + \text{C}_T \quad (3.19)$$

which can be rearranged with terms from Eq. (3.5) to give:

$$\text{A}_T = [\text{S} \equiv \text{A-H}] + [\text{S} \equiv \text{A}^-] = [\text{S} \equiv \text{A-H}] \left( K_A [\text{H}^+]^{-1} + 1 \right) \quad (3.20)$$

$$\text{B}_T = [\text{S} \equiv \text{B-H}] + [\text{S} \equiv \text{B}^-] = [\text{S} \equiv \text{B-H}] \left( K_B [\text{H}^+]^{-1} + 1 \right) \quad (3.21)$$

$$\text{C}_T = [\text{S} \equiv \text{C-H}] + [\text{S} \equiv \text{C}^-] = [\text{S} \equiv \text{C-H}] \left( K_C [\text{H}^+]^{-1} + 1 \right) \quad (3.22)$$

Terms from Eqs. (3.17) and (3.20) – (3.22) can be substituted into Eq. (3.18):

$$K_S = \frac{\beta_A [M^{3+}] [S \equiv A-H] [H^+]^{-1} + \beta_B [M^{3+}] [S \equiv B-H] [H^+]^{-1}}{[M^{3+}] \times (A_T + B_T + C_T)} + \frac{\beta_C [M^{3+}] [S \equiv C-H] [H^+]^{-1} + \beta_C^* \beta_1^* [M^{3+}] [S \equiv C-H] [H^+]^{-2}}{[M^{3+}] \times (A_T + B_T + C_T)} \quad (3.23)$$

and rearranged to give

$$K_S = \left( \frac{1}{(A_T + B_T + C_T)} \right) \times \left( \frac{\beta_A A_T [H^+]^{-1}}{(1 + K_A [H^+]^{-1})} + \frac{\beta_B B_T [H^+]^{-1}}{(1 + K_B [H^+]^{-1})} + \frac{\beta_C C_T [H^+]^{-1} + \beta_C^* \beta_1^* C_T [H^+]^{-2}}{(1 + K_C [H^+]^{-1})} \right) \quad (3.24)$$

By assuming ratios ( $R_1$  and  $R_2$ ) of total group concentrations where

$$R_1 = \frac{B_T}{A_T} \text{ and } R_2 = \frac{C_T}{A_T}$$

Eq. (3.24) further reduces to:

$$K_S = \left( \frac{1}{(1 + R_1 + R_2)} \right) \times \left( \frac{\beta_A [H^+]^{-1}}{(1 + K_A [H^+]^{-1})} + \frac{\beta_B R_1 [H^+]^{-1}}{(1 + K_B [H^+]^{-1})} + \frac{\beta_C R_2 [H^+]^{-1} + \beta_C^* \beta_1^* R_2 [H^+]^{-2}}{(1 + K_C [H^+]^{-1})} \right) \quad (3.25)$$

When Eq. (3.25) is converted into its logarithmic form the final model is obtained, where values of  $\log K_S$  plotted as a function of pH should conform to the relation

$$\log K_S = \log \left( \frac{R \times 10^{pH}}{(1 + 10^{pH - pK_A})} + \frac{R \times 10^{pH + \beta_2}}{(1 + 10^{pH - pK_B})} + \frac{R (10^{pH + \beta_3} + 10^{2 \times pH + \beta_3^*})}{(1 + 10^{pH - pK_C})} \right) \quad (3.26)$$

where

$$R = \frac{\beta_A}{1 + R_1 + R_2} \quad (3.27)$$

$$\beta_2 = \log\left(\frac{\beta_B \times R_1}{\beta_A}\right) \quad (3.28)$$

$$\beta_3 = \log\left(\frac{\beta_C \times R_2}{\beta_A}\right) \quad (3.29)$$

$$\beta_3^* = \log\left(\frac{\beta_C^* \times \beta_1^* \times R_2}{\beta_A}\right) \quad (3.30)$$

Because distribution coefficients were calculated with a sum of the site densities for sites A, B and C, all of which had values of  $\sim 5 \times 10^{-4} \text{ mol}\cdot\text{g}^{-1}$  (SCHIFF and EBLING, 2010), the ratio terms  $R_1$  and  $R_2 \approx 1$ . Values of  $\beta_x$  can then be calculated by reducing Eqs. (3.27) – (3.30):

$$\beta_A = 3 \times R \quad (3.31)$$

$$\beta_B = 10^{\beta_2} \times \beta_A \quad (3.32)$$

$$\beta_C = 10^{\beta_3} \times \beta_A \quad (3.33)$$

$$\beta_C^* = \frac{10^{\beta_3^*} \times \beta_A}{\beta_1^*} \quad (3.34)$$

Fits of  $\log K_S$  and pH data (Tables 3.4 – 3.5) were achieved with Eq. (3.26) for 0.5 M and 5 M ionic strengths. Low pH data ( $< 3$ ) had to be excluded from the fits due to the gap in the data coverage between pH 2.7 and pH 4, which resulted in poor fits at low pH. Fresh *U. lactuca* data, which did not follow the sorption trend seen for BCR-279, were also excluded from the fits. Initial regressions where  $R$ ,  $\beta_2$ ,  $\beta_3$ ,  $\beta_3^*$  and the  $\text{p}K_x$  values were left as free parameters resulted in poorly constrained fits. However the  $\text{p}K_x$  values from these fits, though they had relatively high standard errors, resulted in

approximately the same the  $pK_a$  values obtained by SCHIJF and EBLING (2010). To constrain Eq. (3.26), the  $pK_x$  parameters were fixed to the SCHIJF and EBLING  $pK_a$  values (shown in Table 3.2). This approach sufficiently constrained the fits to four free parameters. Best-fit results of Eq. (3.26) (with fixed  $pK_x$  values) to  $\log K_S$  vs. pH data are shown in Table 3.6 for the 0.5 and 5.0 M data.

The 0.05 M ionic strength data did not provide sufficient resolution to independently fit all three functional groups, so a modified version of Eq. (3.26) was used, where YREE sorption with groups A and B are represented by a single term with a combined  $pK_a$  ( $pK_a$ ):

$$\log K_S = \log \left( \frac{R \times 10^{pH}}{(1 + 10^{pH - pK_a})} + \frac{R (10^{pH + \beta_3} + 10^{2 \times pH + \beta_3^*})}{(1 + 10^{pH - pK_C})} \right) \quad (3.35)$$

For these fits,  $R$ ,  $\beta_3$ ,  $\beta_3^*$  and the  $pK_x$  values were initially left as free parameters in the model. These fits were poorly constrained, so the number of free parameters was reduced by fixing  $pK_C$  to 9.43, the third group  $pK_a$  value obtained by SCHIJF and EBLING (2010). Best fit parameters for fits of Eq. (3.35) (with  $pK_C$  fixed at 9.43) to  $\log K_S$  vs. pH data (Table 3.3) are shown in Table 3.7 for 0.05 M data.

Fig. 3.2 shows NEM fits for Sm at all ionic strengths. Excellent fits were obtained for all YREEs with high  $r^2$  values ( $> 0.98$  for most elements) and low standard errors (Tables 3.6 – 3.7). As opposed to the linear regressions (Fig. 2.9), the NEM model is able to fit the non-linearity of the data, especially the points at high pH. These high-pH points are dominated by interaction with group C, which includes a term for  $MOH^{2+}$  interactions ( $\beta_C^*$ ). Early fits of the data considered the possibility that only  $MOH^{2+}$  complexes (and no free metal) were interacting with group C, resulting in a term of order  $[H^+]^2$  for the third

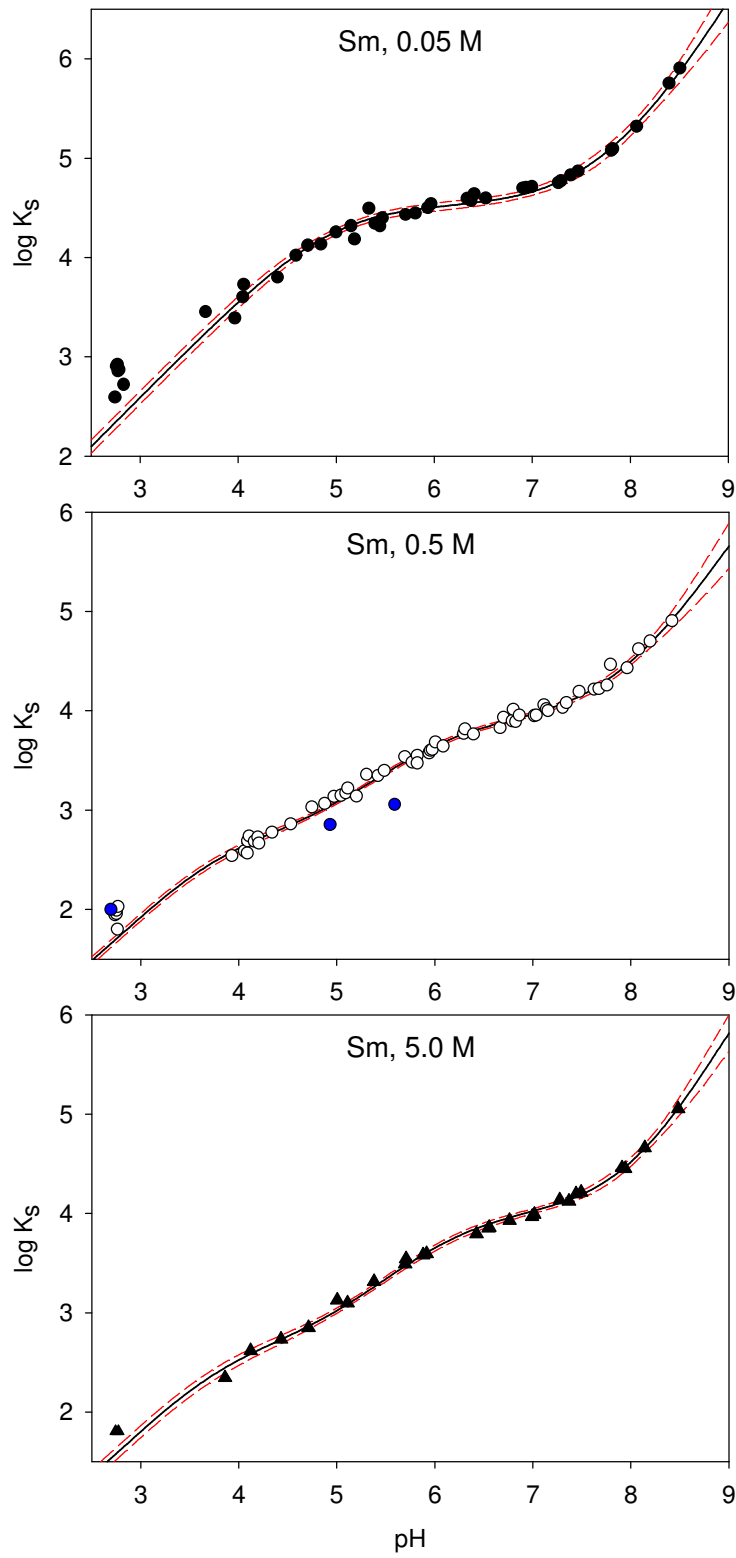
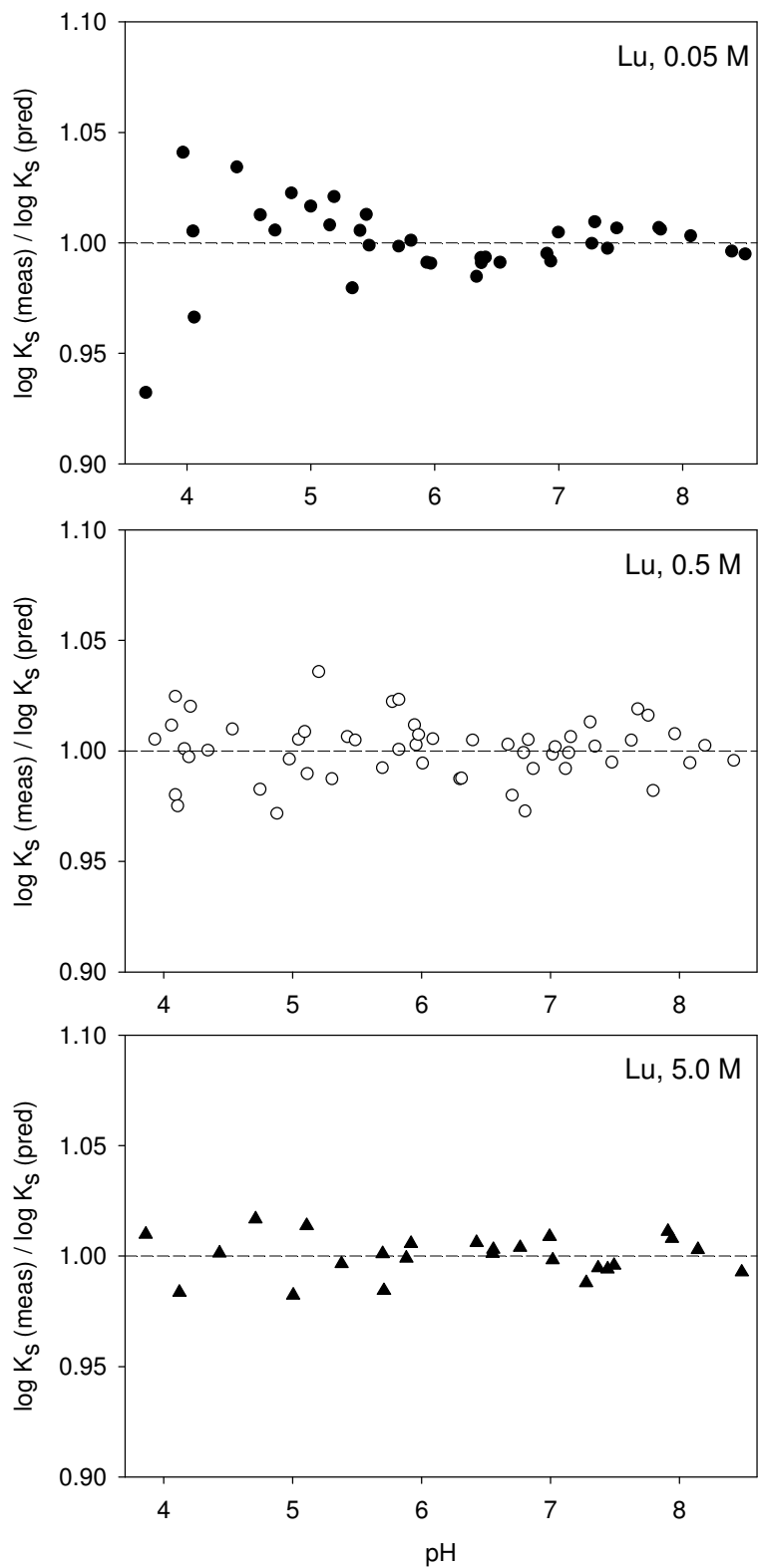


Figure 3.2. Regressions of  $\log K_S$  vs. pH data for Samarium using the NEM (Eq. 3.26 and 3.35). Low pH data (< 3) and fresh *U. lactuca* samples (blue circles) were not included in the fits. Dashed red lines represent 95% confidence intervals.



**Figure 3.3. Ratios of measured to predicted values of  $\log K_S$  for Lu, shown as a function of pH. Predicted values were calculated using Eq. (3.26) (0.5 and 5.0 M data), Eq. (3.35) (0.05 M data) and best-fit parameters from Table 3.6 – 3.7.**

term of Eq. (3.26) (second term of Eq. 3.35). However, these modified models gave significantly worse fits than Eqs. (3.26) or (3.35), implying that group C sorbs both free and hydrolyzed metal.

Ratios of measured to model-predicted  $\log K_s$  values, calculated with best-fit parameters in Table 3.6 – 3.7, are shown for Lu in Fig. 3.3. Ratios are generally randomly distributed around the mean (mean=1.000 for each ionic strength) and are within analytical error (< 5%), confirming the validity of the model. There is a slight increase in scatter at lower pH (< 5), caused by weaker YREE sorption which leads to error magnification as  $[M]_{\text{corr}}$  approaches  $[M]_{\text{init}}$  in the numerator of Eq. (3.1). For the lowest ionic strength, ratios are somewhat less randomly scattered, especially around pH 5. The increased scatter could be an artifact of the colloid correction, which completely reversed sorption trends at high pH in the 0.05 M data. Colloid-bound metal comprised more than 50% of the size fraction < 0.22  $\mu\text{m}$  above pH 5, which is where the scatter in Fig. 3.3 is less random.

Three distribution coefficients from the fresh *U. lactuca* experiment are shown for comparison to BCR-279 in Fig. 3.2 (blue circles). These data were not corrected for colloid-metal interactions as the fresh tissue sample showed little evidence of colloid formation (Ch. 2). Distribution coefficients for the fresh tissue are lower than those for BCR-279, suggesting that there was decreased sorption on the fresh tissue relative to the dried standard. This could be due to larger variation in the properties of the fresh tissue as compared the homogenized dried standard, though it is difficult to make any real comparisons with only one sample. The natural variability seen in the fresh tissue is the main reason why a dried *U. lactuca* standard was chosen for the majority of the

experiments rather than fresh biomass. The BCR-279 standard offered a consistent, reproducible form of the tissue that was easily obtained without the need for specimen collection or culturing, as was required for the fresh tissue. The dried standard was also easier to consistently weigh and transfer into solution, and many other metal sorption experiments use dried organic samples as opposed to fresh biomass (for example, TEXIER et al., 2000; TURNER et al., 2007, 2008).

#### *3.4.3. Interpretation of NEM best-fit parameters*

Due to the chemical coherence of the YREEs, patterns of YREE stability constants can be used as diagnostic tools to determine the type of YREE complexes formed on a surface. The gradual decrease in ionic radii across the series gives rise to regular, distinctive shapes of stability constants that are indicative of a certain type of YREE interaction. As a result, patterns are sensitive to YREE complexation with specific functional groups, and can be used to determine the identity of unknown functional groups on a surface by comparing them to known stability constants for dissolved YREE solution complexes, such as YREE complexation with carboxylates or hydroxide. For example, a broad maximum centered near Sm is diagnostic of an acetate-like group. In linear free-energy relations (LFER), stability constants for dissolved and surface functional groups are plotted against one another for comparison, to infer similarities or differences between the structures of two YREE complexes. This technique has been used not only to provide insights into YREE sorption mechanisms (QUINN et al., 2006b; SCHIJF and MARSHALL, 2011), but also to calculate sets of YREE stability constants from only one or two measured values (BYRNE and LI, 1995).

Using Eqs. (3.31) – (3.34), YREE stability constants for each functional group were calculated from the best-fit parameters in Table 3.6. These values are shown in Table 3.8 and plotted in Fig. 3.4. Three distinct patterns emerge from these figures, representing YREE binding to groups A, B, and C. The first functional group (group A) shows preference for the middle YREEs, indicated by higher  $\log \beta_A$  values centered on Sm. This feature is characteristic of YREE-acetate complexation, whose complexation constants ( $\log \text{OAc}\beta_1$ ) are plotted for comparison in Fig. 3.4 (KOLAT and POWELL, 1962). LFER between  $\log \text{OAc}\beta_1$  and  $\log \beta_A$  are shown in Fig. 3.5, suggesting that the structure of the first group is acetate-like and thus probably a carboxylate. Carboxylate groups typically have  $\text{pK}_a$  values in the range of  $\sim 3 - 5$ , which is in good agreement with the  $\text{pK}_a$  value for L1 found by Schijf and Ebling (2010) and used in the NEM fits for group A ( $\text{pK}_A \sim 4$ , Table 3.2).

The third functional group (group C) shows preferential binding for the heavy YREEs, where  $\log \beta_C$  increases with increasing atomic number (Fig. 3.4). The pattern is very similar to that for YREE-hydroxide complexation, shown for comparison in Fig. 3.4 (KLUNGNESS and BYRNE, 2000). LFER confirms this correlation ( $r^2 \sim 0.97$ ), shown in Fig. 3.5 and suggests the presence of a phenol. Phenols are common functional groups on organic matter and are purported to participate in YREE sorption (POURRET and MARTINEZ, 2009). YREE binding to a hydroxide on a phenol would likely resemble the stability constant pattern for dissolved YREE hydroxide complexation. Similarities between stability constants for YREE complexation with surface hydroxyl groups and YREE complexation with dissolved hydroxide is well documented for various oxide minerals (QUINN et al., 2004; SCHIJF and MARSHALL, 2011). The high  $\text{pK}_a$  of group C

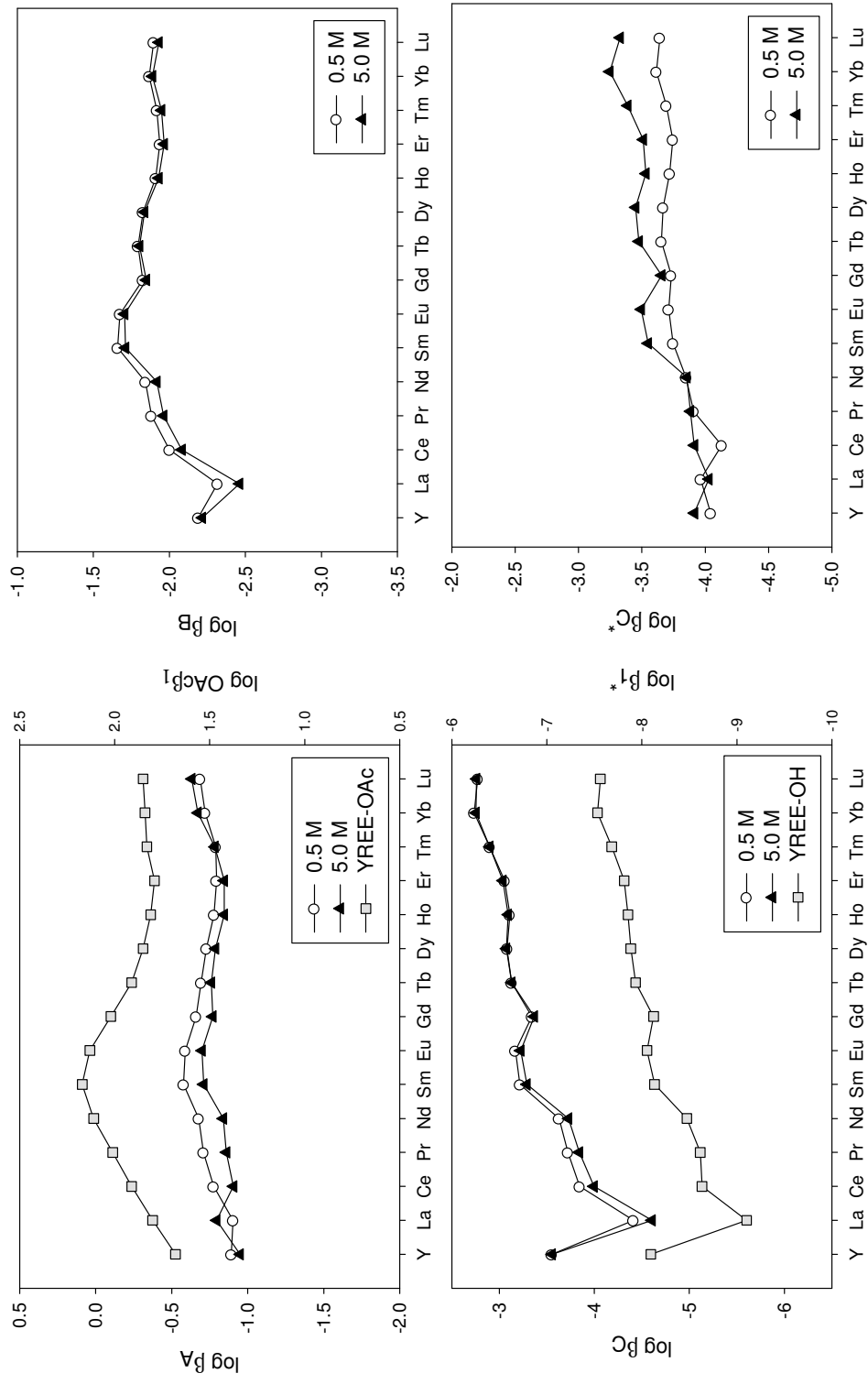


**Figure 3.4. Functional group stability constants for  $M^{3+}$  complexation with groups A, B, and C (log  $\beta_A$ , log  $\beta_B$  and log  $\beta_C$ , respectively) and  $MOH^{2+}$  complexation with group C (log  $\beta_{C^*}$ ) across the YREE series. Each panel depicts complexation with one group, shown for 0.5 and 5.0 M ionic strengths. YREE complexation with hydroxide (YREE-OH) and acetate (YREE-OAc) are shown for comparison.**

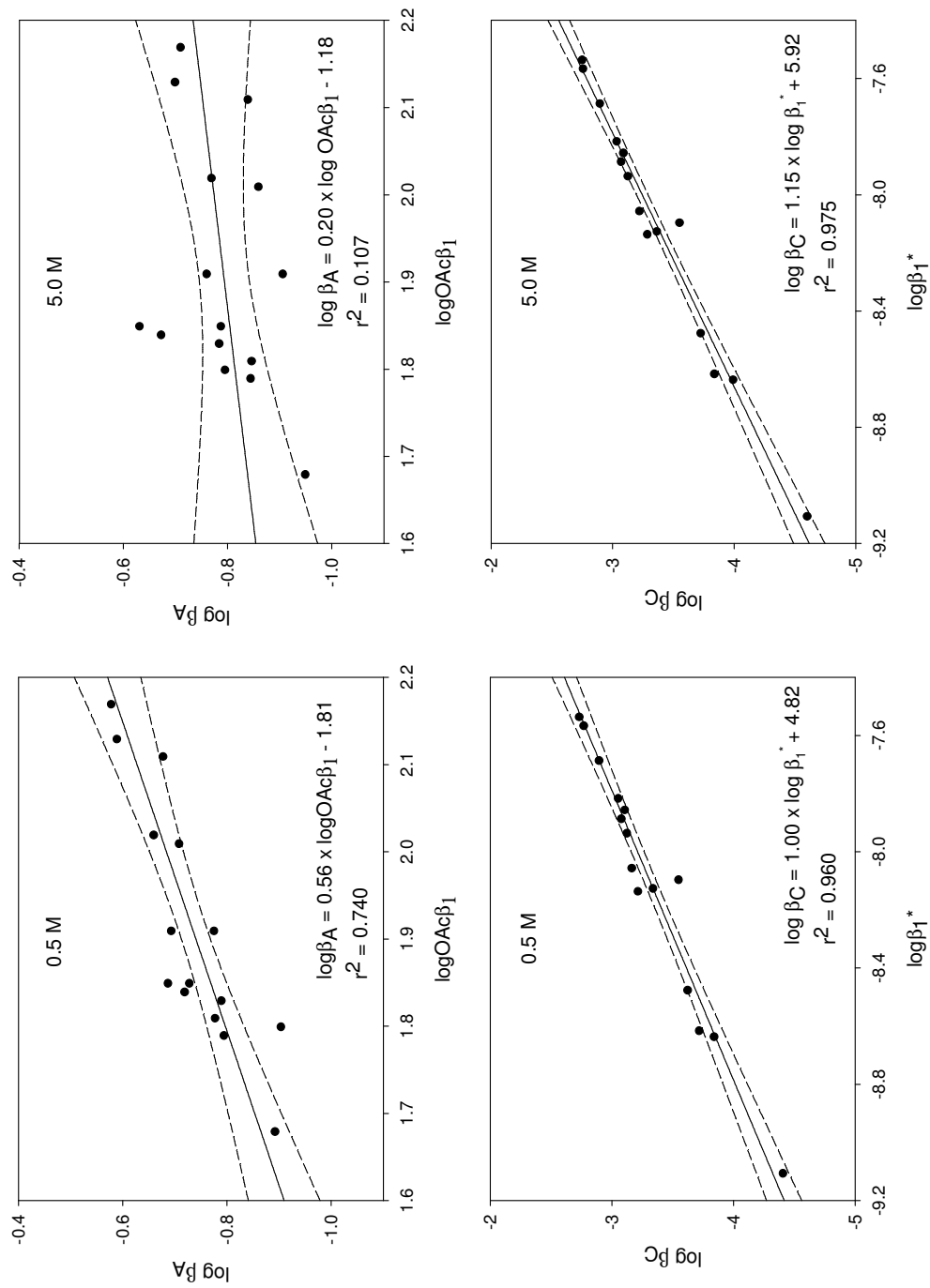


**Figure 3.5. Linear free-energy relations (LFER) between group A ( $\log \beta_A$ ) and acetate ( $\log \text{OAc}\beta_1$ ) stability constants and group C ( $\log \beta_C$ ) and hydroxide ( $\log \beta_1^*$ ) stability constants for 0.5 and 5.0 M ionic strengths. Dashed lines represent 95% confidence intervals.**

( $pK_C \sim 9$ ) also supports the presence of a phenol, which typically have  $pK_a$  values of  $\sim 9 - 10$ . Most studies have attributed high  $pK_a$  groups to amines (for example GONZALEZ-DAVILA et al., 1995; YEE et al., 2004), but phenols and amines share similar  $pK_a$  values and cannot be well distinguished by spectroscopic techniques (such as Extended X-ray Absorption Fine Structure). The unique chemical properties of the YREEs and the pattern of stability constants make it possible to distinguish these two groups, and group C here clearly suggests YREE binding to a phenol group. It is also more likely that the YREEs would bind with a phenol rather than an amine because the YREEs generally have a lower affinity for nitrogen-bearing groups.

Stability constants for  $MOH^{2+}$  binding to group C ( $\log \beta_C^*$ ) have a similar pattern to free-metal binding to group C, though the trend is somewhat suppressed, which could be due to different surface affinities for the  $MOH^{2+}$  vs. the  $M^{3+}$  species. It is likely that the free metal will have a slightly higher affinity for the surface due to its higher charge (3+) and smaller ionic radius.

The second functional group stability constant pattern ( $\log \beta_B$ ) did not match that of any known YREE complexation constants, but it is possible that group B is a phosphate complex. Unfortunately, there is no published pattern of measured YREE-phosphate stability constants available for comparison. Phosphate is a component of cell membrane phospholipids, and other work with microbial biomass have attributed mid- $pK_a$  groups ( $pK_{a,s} \sim 6$ ) to a phosphate complex (BOYANOV et al., 2003; NGWENYA et al., 2003; HA et al., 2010; MISHRA et al., 2010). Phosphate groups typically have  $pK_a$  values in the range of  $\sim 6 - 7$ , which fit well with the  $pK_B$  ( $\sim 6$ ) used in the NEM fits.

The similarity between  $\log OAc\beta_1$  and  $\log \beta_A$  is greater for 0.5 M than 5.0 M,

which is likely due to the higher  $\text{Na}^+$  concentration in the 5.0 M experiments (Fig. 3.5). Increased  $\text{Na}^+$  concentrations may suppress sorption by forming an electric double-layer at the surface of the algae, shielding its negative charge and thereby lowering its overall affinity for the positively charged YREEs. This would lead to the  $\log \beta_A$  pattern being suppressed at higher ionic strength, and a poorer correlation with  $\log \text{OAc}\beta_1$  than in 0.5 M NaCl. This relation somewhat holds true for  $\log \beta_B$  and  $\log \beta_C$  patterns as well, where stability constants are slightly higher in 0.5 M relative to 5.0 M ionic strength. However the effect is less pronounced for groups B and C than for group A, presumably because YREE sorption with each of the functional groups is affected differently by ionic strength.

#### *3.4.4. The modified low-ionic-strength NEM*

YREE stability constants calculated from the modified NEM (Eq. 3.35) are shown in Fig. 3.6 for YREE sorption with the combined groups A and B ( $\log \beta_a$ ), and free metal and hydrolyzed metal sorption on group C ( $\log \beta_C$  and  $\log \beta_C^*$ ). As with group A in the full model (Eq. 3.26), complexation with the combined groups A and B ( $\log \beta_a$ ) in the modified NEM also follows an acetate-like pattern across the YREE series ( $r^2 = 0.89$ , Fig. 3.7). The  $\text{pK}_a$  value of the combined groups, which was left free in the fits, averaged slightly higher than the value found in Schijf and Ebling (2010) (4.79 found in the NEM fits vs. 4.06 found in the potentiometric titrations). This is likely a result of influence from the B group. If this is the case, then the  $\text{pK}_a$  of 4.79 would be a combination of the  $\text{pK}_a$  from the first two groups resolved in the full NEM model ( $\text{pK}_A \sim 4$ ,  $\text{pK}_B \sim 6$ ). Evidence for this theory is also seen in the  $\text{pK}_a$  trend across the YREE series (Table 3.7),

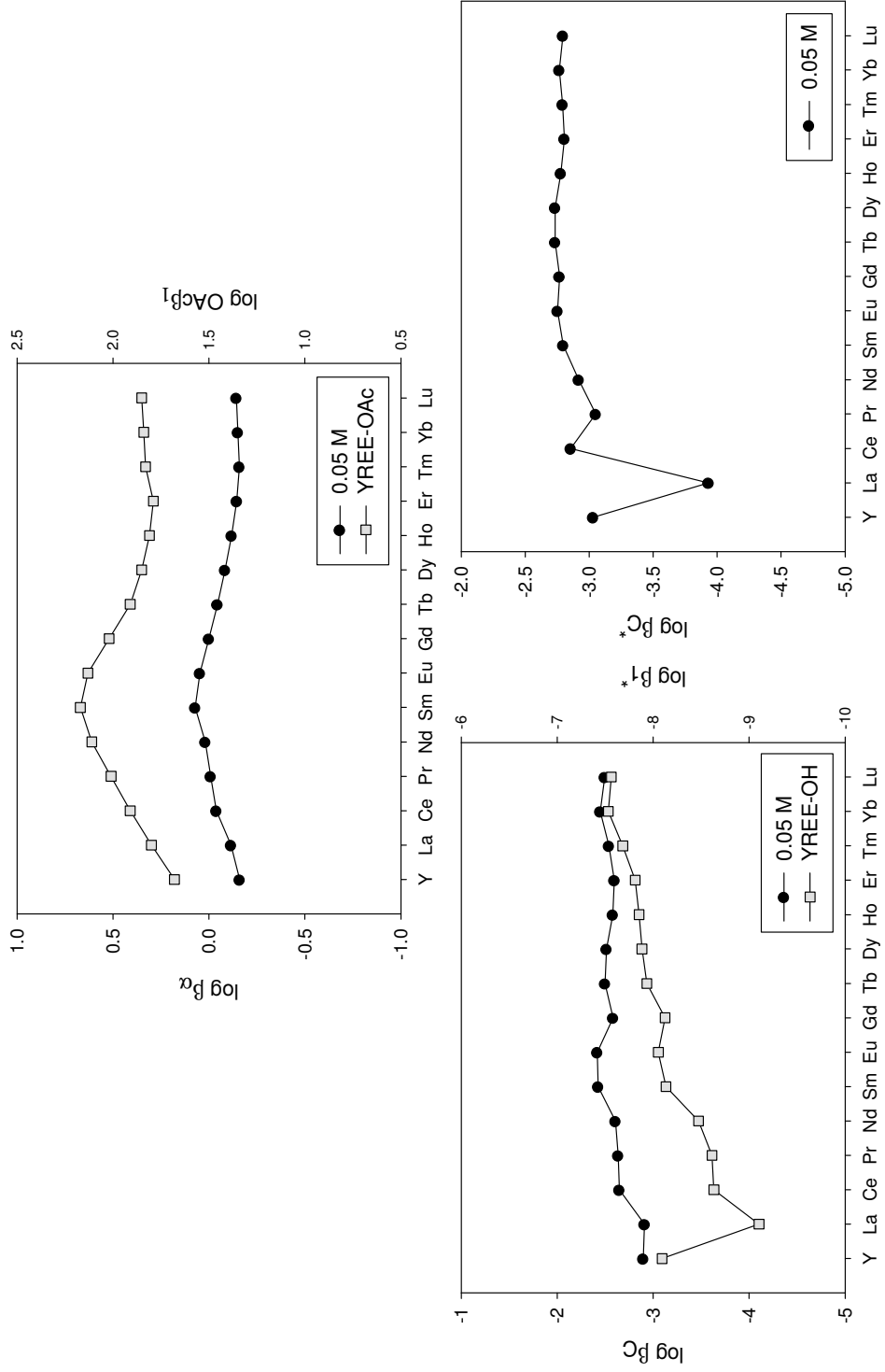


**Figure 3.6.** Functional group stability constants for  $M^{3+}$  complexation with groups A and B ( $\log \beta_A$ , group C ( $\log \beta_C$ ) and  $MOH^{2+}$  complexation with group C ( $\log \beta_C^*$ ) across the YREE series in 0.05 M NaCl. YREE complexation with hydroxide (YREE-OH) and acetate (YREE-OAc) and shown for comparison. Dashed lines represent 95% confidence intervals.

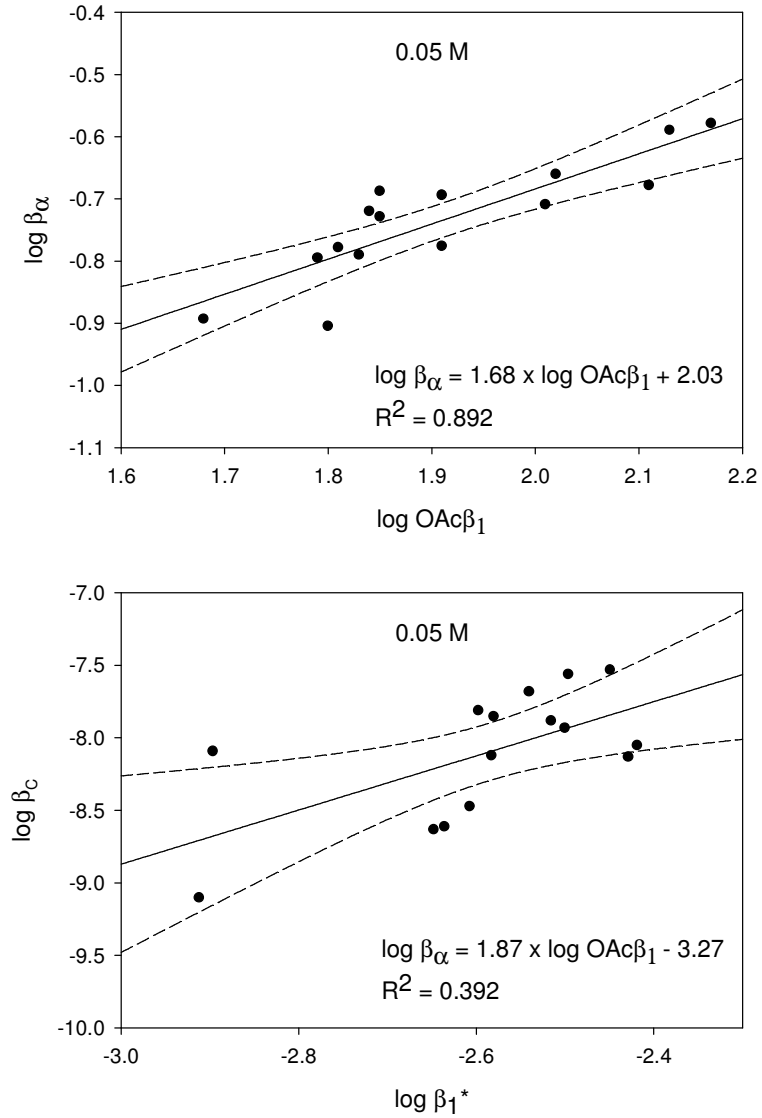


**Figure 3.7. Linear free-energy relations (LFER) between groups A and B ( $\log \beta_a$ ) and acetate ( $\log \text{OAc}\beta_1$ ) stability constants and group C ( $\log \beta_c$ ) and hydroxide ( $\log \beta_1^*$ ) stability constants for 0.05 M ionic strength.**

where the  $\text{pK}_{a\text{s}}$  for the light REEs (La – Eu) are higher than the  $\text{pK}_{a\text{s}}$  for the heavy REEs (Gd – Lu). Because acid dissociation constants only describe protonation and deprotonation of a surface, they should remain constant for a given ionic strength and should not change as a function of the metal being sorbed. The variation with YREE suggests that the heavy YREEs, whose  $\text{pK}_{a\text{s}}$  values are slightly lower than the light

YREEs, are preferentially sorbing with group A over the unresolved group B and vice versa.

The second group resolved in the modified NEM (group C) was assigned the same  $pK_a$  as group C in the full model (9.43). Attempts to fit Eq. (3.35) with  $pK_C$  fixed at 6.24 were unsuccessful, and leaving  $pK_C$  as a free parameter resulted in  $pK_C$  values of  $\sim 9$ . This suggests that the modified NEM is able to resolve the third group independent of group B in the full NEM. The complexation pattern for  $\log \beta_C$  in the 0.05 M fits does not match the YREE-hydroxide pattern as well as  $\log \beta_C$  in the full model, though the correlation ( $r^2 = 0.39$ , Fig. 3.7) and  $pK_C$  (9.4) still supports the presence of a phenol group. The pattern of stability constants for sorption of  $MOH^{2+}$  on group C is similar to the pattern for  $M^{3+}$  sorption with group C (Fig. 3.6), repeating the trend seen for  $MOH^{2+}$  sorption on group C in 0.5 and 5.0 M NaCl (Fig. 3.4).

It is somewhat unclear why the NEM could not resolve all three groups in the low ionic strength data set. Initially, it seems that with less  $Na^+$  competition for binding sites in solution, it would be possible to resolve more functional groups at a lower ionic strength. Clearly this was not the case, as a modified NEM with two terms was necessary to obtain acceptable fits of the 0.05 M data, whereas the higher ionic strengths required a three-site model. The three-site model matches the findings in SCHIJF and EBLING (2010) quite well, and each set of experiments produced the same  $pK_a$  values. The 0.05 M model is essentially a simplified version of the full three-site model in the sense that the first term is some mixture of groups A and B. There are two possible reasons for this. First, the ionic strength effects are likely different for each functional group which could be causing the  $\beta_A$  and  $\beta_B$  values to overlap at low ionic strength. If  $\beta_A$  is suppressed at high

ionic strength (as indicated by the 5.0 M data in Fig. 3.4. and 3.5.), then at low ionic strength  $\beta_A$  would be much higher and may overlap with  $\beta_B$ , which likely would not change much at low ionic strength as there was little suppression of  $\beta_B$  values between 0.5 and 5.0 M ionic strength. In effect, this would cause groups A and B to appear to “merge” in the log  $K_S$  vs. pH data, making it difficult for the model to resolve them into separate groups.

The second reason for the difference between the data sets could be due to the colloid correction equation, which had the most significant effect on the 0.05 M data. The correction had the largest effect on log  $K_S$  values above pH ~5, which is just below the  $pK_a$  for group B. The colloid correction model, which was derived from only 6 data points (Fig. 2.3), was not a perfect representation of the system and could be causing the loss of resolution in the 0.05 M log  $K_S$  data. These six points also provided a relatively low pH resolution (~1 pH unit) for the colloid model as compared to the data used to fit the NEM, which likely explains why only two sites were resolved in the colloid data and three sites were resolved with the NEM. However, because the colloid correction model’s primary purpose was to provide a numerical description, rather than a mechanistic explanation of YREE–colloid interactions, including a third group could not significantly improve those fits, which already have high  $r^2$  values and low standard errors (Table 2.3).

### 3.5. Potential benefits of the NEM for biomonitoring and bioremediation efforts

Because it has such a high affinity for trace metals, *U. lactuca* has been widely studied for its potential use as a biomonitor, where scientists have hoped to determine ambient metal concentrations by measuring metal concentrations on *U. lactuca* tissue

(PHILLIPS, 1977; SEELIGER and EDWARDS, 1977; RAINBOW, 1995; BROWN et al., 1999; LEE and WANG, 2001). The need to determine the correlation between these two quantities has been recognized for some time (SEELIGER and EDWARDS, 1977), but authors have only speculated on the factors that could influence such correlations, such as temperature, salinity, or pH (PHILLIPS, 1977). Biomonitoring efforts must be founded on a thorough understanding of *U. lactuca*'s sorptive properties and be able to predict how sorption is affected by solution conditions. The NEM provides a partial answer to this problem, as it is able to predict the extent of metal sorption on *U. lactuca* as a function of pH at three different ionic strengths. Scientists could utilize the model for biomonitoring efforts by predicting metal behavior in ambient water if pH, ionic strength, and the sorbed metal concentration on *U. lactuca* are known. The model covers a wide range of salinity conditions including not only seawater, but also fresh water to brines. Though *U. lactuca* will not grow for extended periods in fresh water or brines, the model does suggest how salinity variations will affect metal sorption. Estuaries, where salinity fluctuations are common, are a typical habitat for *U. lactuca* and the model could be useful for biomonitoring studies conducted in these areas.

Additionally, materials engineers and scientists have tested dried *U. lactuca* for its potential as a biosorbent to remove toxic metals from aquatic environments (ZEROUAL et al., 2003; SUZUKI et al., 2005; HERRERO et al., 2006; EL-SIKAILY et al., 2007). These remediation efforts would be best served with a thorough understanding of the mechanisms behind metal sorption with dried biomass, a goal which this study helps to inform. The NEM could be used by such studies to predict the extent of sorption by *U. lactuca* packed-bed columns under different pH and ionic strength conditions. As with

biomonitoring studies, results here confirm that *U. lactuca* would be an effective biosorbent under a wide range of environmental conditions and aquatic environments including seawater, freshwater and brines.

### 3.6. Conclusions

YREE sorption on *U. lactuca* appears to occur through passive, reversible sorption with functional groups on the cell walls. The processes modeled here are completely reversible over the pH range studied, which validates the use of an equilibrium surface complexation model to describe YREE sorption. A NEM was able to accurately describe YREE sorption on *U. lactuca* by assuming the presence of three monoprotic functional groups with  $pK_{as}$  of ~4, 6 and 9. The model also included a term to describe YREE-hydroxide sorption with the third functional group, which becomes important at  $pH > 7$ .

Ionic strength effects are seen in many aspects of the data analysis. Linear regressions of distribution coefficients as a function of pH suggested that  $Na^+$  ions suppress sorption at higher ionic strengths (Ch. 2), and this suppression is also seen in the stability constants, where  $\log \beta_x$  patterns are suppressed at 5.0 M ionic strength relative to 0.5 M ionic strength, especially for group A. The lowest ionic strength data were unable to independently resolve groups A and B, so a modified NEM was used where the first two groups are represented by a combined term. This could be the result of different ionic strength effects on the different groups, causing  $\beta_A$  and  $\beta_B$  values to overlap. The need for a modified NEM could also be an artifact of the colloid correction, which had the greatest effect on the 0.05 M  $\log K_S$  data above pH 5.

The unique chemistry of the YREEs allows for measurements of the entire 15-element series to be used to identify metal-complexing functional groups. Stability constants for the first and third groups over the YREE series provide patterns that resemble YREE-acetate and YREE-hydroxide stability constants. LFER confirm the similarities, suggesting that the first functional group is a carboxylate and that the third functional group is a phenol. The second functional group's  $pK_a$  suggests that it may be a phosphate group. These functional group identities are consistent with metal-complexing functional groups found on other types of organic matter, where carboxyl and phosphate groups are often identified. Phenols are also common functional groups on organic matter, and the unique chemistry of the YREEs allowed for identifying the high  $pK_a$  group as a hydroxyl rather than an amine, a distinction that has been difficult to make in other metal sorption studies.

NEMs appear to be a practical approach for modeling metal sorption on organic surfaces. By deriving an analytical function from first principles, stability constants and  $pK_a$  values can be obtained that accurately describe metal sorption on complex organic matter. The approach used here may be applicable to describing metal sorption on other complex organic substrates, which would allow for a better understanding of trace-metal mobility and geochemistry in natural environments. The NEM can also help inform bioremediation efforts that hope to use *U. lactuca* to sorb and remove toxic metals from contaminated environments. Biomonitoring studies which have attempted to correlate *U. lactuca* metal concentrations to those in the surrounding water will also benefit, in that the NEM can provide specific predictions for metal sorption based on solution pH and ionic strength.

### 3.7. Concluding remarks and future work

Given that relatively little is understood about trace metal sorption on organic matter, this thesis provides some answers to questions surrounding this topic, especially with respect to marine organic matter. The research objectives were designed to answer basic thermodynamic questions about the nature of the YREE sorption on *U. lactuca* and to provide general insights into the metal sorption mechanisms. While the results are specific to YREE sorption on *U. lactuca*, the broader conclusions could be expanded for other type-A metal cations and for other types of marine organic matter.

The first research objective, to determine how distribution coefficients vary as a function of pH, was answered in a number of different ways. Ionic strength and pH were clearly essential variables in determining the extent of sorption, and sorption was found to increase with increasing pH. This behavior is typical of metal cation sorption with organic surfaces, and repeats results found for metal cation sorption on bacterial and fungal biomass (FOWLE and FEIN, 1999; NAEEM et al., 2006). Increasing ionic strength generally suppressed sorption while low ionic strength enhanced it, where distribution coefficients were highest at 0.05 M ionic strength and lowest for 5.0 M ionic strength. This result is also verified in the stability constants, which are largest at low ionic strength and weakest at high ionic strength.

The second research objective was to develop a surface complexation model to describe YREE sorption on *U. lactuca*. The NEM (Eq. 3.26) is able to predict  $\log K_s$  values as a function of pH at the three ionic strengths studied. The model not only provides excellent fits of the data, but unlike previous work with chemical equilibrium programs such as FITEQL, Eq. (3.26) is an analytical function that provides mechanistic

information about the system. Three monoprotic functional groups are present on the algal surface, where both free metal and hydrolyzed metal participate in sorption. This result also verifies conclusions in SCHIJF and EBLING (2010) finding the same number of functional groups, the same proton stoichiometry, and the same  $pK_a$  values.

The final research objective was to use YREE patterns of stability constants to help determine the identity of *U. lactuca*'s functional groups. While this technique is a powerful one, the results are ultimately inferential in that a YREE pattern provides evidence for the presence of a functional group, but cannot conclusively determine a functional group's structure. The LFERs suggest the presence of a carboxyl and phenol group, which are consistent with the known composition of organic matter, known functional group  $pK_a$  values, and YREE chemical properties. However, the results ultimately cannot provide definitive structures for groups A and C. The technique is also limited in that if a YREE complexation constant pattern has not been measured for the type of functional group present, it cannot be identified (as was the case for group B). Nevertheless, LFERs for the YREEs provide important evidence for the presence of certain functional groups over others in the same  $pK_a$  range, as is the case for phenol and amine groups.

One common method for determining functional group identities is to use spectroscopic techniques such as EXAFS in conjunction with metal sorption experiments (NGWENYA et al., 2009; MISHRA et al., 2010). Both approaches will generally compliment and inform one another so that together they offer a comprehensive picture of the thermodynamic and the structural properties of the system. EXAFS data provides information about a metal's local bonding structure, such as interatomic distances and

coordination numbers. This information is used to determine the specific structure of a metal binding functional group. Though EXAFS has been used in many metal sorption studies, it is difficult to distinguish light atoms that are close to one another on the periodic table, such as nitrogen and oxygen. This is especially problematic for organic matter, which is dominated by C, N, O, P and S, all of which are difficult to distinguish from one another with EXAFS. Preliminary EXAFS data for YREE sorption on *U. lactuca* at pH 6.5 suggested the presence of phosphate complexes (STRAKA and SCHIFF, 2009), though a larger, more robust data set would be necessary to conclusively determine the functional group structure. Furthermore, EXAFS analysis for the YREEs relative to other trace metals are particularly complicated, and future EXAFS work for metal sorption on *U. lactuca* would likely benefit from using elements such as Cu or Zn.

Future work could also include expanding *U. lactuca* sorption studies to other toxic metals of concern, such as Cd and Hg. Unlike the YREEs, Cd and Hg are B-type metals and may have different affinities for the surface or interact with different functional groups. The technique and approach used in this project could also be applicable to other types of organic matter or other organisms, where the YREEs could be used as diagnostic tools to determine possible site identities. Such information will better inform a general knowledge of metal cycling, geochemistry, and interactions with organic matter.

### 3.8. Data tables

**Table 3.1. YREE hydrolysis constants ( $\log \beta_1^*$ ) and YREE-chloride stability constants ( $\log {}_c\beta_1$ ) calculated for I = 0.05, 0.5 and 5.0 M ionic strength (KLUNGNESS and BYRNE, 2000; LUO and BYRNE, 2001).**

|    | $\log \beta_1^*$ |       |       | $\log {}_c\beta_1$ |        |        |
|----|------------------|-------|-------|--------------------|--------|--------|
|    | 0.05 M           | 0.5 M | 5.0 M | 0.05 M             | 0.5 M  | 5.0 M  |
| Y  | -8.00            | -8.09 | -8.13 | 0.155              | -0.326 | -0.760 |
| La | -9.01            | -9.10 | -9.14 | 0.155              | -0.326 | -0.760 |
| Ce | -8.54            | -8.63 | -8.67 | 0.155              | -0.326 | -0.760 |
| Pr | -8.52            | -8.61 | -8.65 | 0.155              | -0.326 | -0.760 |
| Nd | -8.38            | -8.47 | -8.51 | 0.155              | -0.326 | -0.760 |
| Sm | -8.04            | -8.13 | -8.17 | 0.155              | -0.326 | -0.760 |
| Eu | -7.96            | -8.05 | -8.09 | 0.155              | -0.326 | -0.760 |
| Gd | -8.03            | -8.12 | -8.16 | 0.155              | -0.326 | -0.760 |
| Tb | -7.84            | -7.93 | -7.97 | 0.155              | -0.326 | -0.760 |
| Dy | -7.79            | -7.88 | -7.92 | 0.155              | -0.326 | -0.760 |
| Ho | -7.76            | -7.85 | -7.89 | 0.155              | -0.326 | -0.760 |
| Er | -7.72            | -7.81 | -7.85 | 0.155              | -0.326 | -0.760 |
| Tm | -7.59            | -7.68 | -7.72 | 0.155              | -0.326 | -0.760 |
| Yb | -7.44            | -7.53 | -7.57 | 0.155              | -0.326 | -0.760 |
| Lu | -7.47            | -7.56 | -7.60 | 0.155              | -0.326 | -0.760 |

**Table 3.2. Acid dissociation constants as determined from potentiometric titrations of BCR-279 (SCHIJF and EBLING, 2010). These values were used to constrain NEM fits (Eq. 3.25 for 0.5 and 5.0 M data, Eq. 3.34 for 0.05 M data).**

| Ionic strength | $pK_A$ | $pK_B$ | $pK_C$ |
|----------------|--------|--------|--------|
| 0.05 M         | 4.061  | 6.244  | 9.433  |
| 0.5 M          | 3.795  | 6.004  | 9.367  |
| 5.0 M          | 3.847  | 6.168  | 9.464  |

**Table 3.3. Log  $K_S$  values in 0.05 M ionic strength, calculated using Eq. (3.1) and corrected for  $\text{MOH}^{2+}$  and  $\text{MCl}^{2+}$  complexation (Eq. 3.14). <sup>a</sup> Samples not included in NEM fits.**

| pH                | Y    | La   | Ce   | Pr   | Nd   | Sm   | Eu   | Gd   | Tb   | Dy   | Ho   | Er   | Tm   | Yb   | Lu   |
|-------------------|------|------|------|------|------|------|------|------|------|------|------|------|------|------|------|
| 2.75 <sup>a</sup> | 2.45 | 2.49 | 2.53 | 2.54 | 2.56 | 2.59 | 2.57 | 2.53 | 2.51 | 2.49 | 2.48 | 2.47 | 2.47 | 2.48 | 2.50 |
| 2.76 <sup>a</sup> | 2.72 | 2.78 | 2.84 | 2.85 | 2.87 | 2.90 | 2.88 | 2.84 | 2.81 | 2.79 | 2.76 | 2.75 | 2.75 | 2.77 | 2.78 |
| 2.77 <sup>a</sup> | 2.75 | 2.79 | 2.86 | 2.87 | 2.88 | 2.92 | 2.90 | 2.85 | 2.82 | 2.80 | 2.78 | 2.77 | 2.77 | 2.79 | 2.80 |
| 2.78 <sup>a</sup> | 2.67 | 2.72 | 2.78 | 2.80 | 2.81 | 2.85 | 2.83 | 2.78 | 2.74 | 2.72 | 2.70 | 2.68 | 2.69 | 2.70 | 2.72 |
| 2.79 <sup>a</sup> | 2.68 | 2.72 | 2.78 | 2.81 | 2.83 | 2.87 | 2.84 | 2.80 | 2.77 | 2.74 | 2.72 | 2.71 | 2.70 | 2.72 | 2.74 |
| 2.84 <sup>a</sup> | 2.49 | 2.54 | 2.60 | 2.64 | 2.66 | 2.72 | 2.70 | 2.64 | 2.61 | 2.57 | 2.56 | 2.54 | 2.54 | 2.57 | 2.58 |
| 3.67              | 3.19 | 3.25 | 3.34 | 3.37 | 3.39 | 3.45 | 3.43 | 3.37 | 3.33 | 3.29 | 3.25 | 3.22 | 3.21 | 3.23 | 3.23 |
| 3.97              | 3.11 | 3.18 | 3.27 | 3.31 | 3.33 | 3.39 | 3.36 | 3.30 | 3.26 | 3.22 | 3.17 | 3.15 | 3.13 | 3.15 | 3.14 |
| 4.05              | 3.30 | 3.38 | 3.47 | 3.51 | 3.54 | 3.60 | 3.57 | 3.50 | 3.46 | 3.41 | 3.36 | 3.33 | 3.31 | 3.32 | 3.32 |
| 4.06              | 3.44 | 3.52 | 3.61 | 3.65 | 3.67 | 3.73 | 3.70 | 3.63 | 3.59 | 3.55 | 3.50 | 3.47 | 3.45 | 3.46 | 3.46 |
| 4.41              | 3.45 | 3.54 | 3.66 | 3.70 | 3.73 | 3.80 | 3.76 | 3.69 | 3.64 | 3.59 | 3.53 | 3.49 | 3.47 | 3.48 | 3.47 |
| 4.60              | 3.64 | 3.76 | 3.88 | 3.93 | 3.95 | 4.02 | 3.98 | 3.91 | 3.85 | 3.80 | 3.73 | 3.69 | 3.66 | 3.66 | 3.65 |
| 4.72              | 3.72 | 3.84 | 3.98 | 4.03 | 4.05 | 4.12 | 4.08 | 4.00 | 3.95 | 3.89 | 3.82 | 3.77 | 3.75 | 3.75 | 3.74 |
| 4.85              | 3.71 | 3.84 | 3.98 | 4.04 | 4.06 | 4.13 | 4.10 | 4.00 | 3.96 | 3.89 | 3.82 | 3.77 | 3.74 | 3.75 | 3.73 |
| 5.00              | 3.78 | 3.94 | 4.09 | 4.15 | 4.17 | 4.25 | 4.21 | 4.11 | 4.06 | 3.99 | 3.91 | 3.85 | 3.82 | 3.83 | 3.81 |
| 5.16              | 3.85 | 4.01 | 4.16 | 4.22 | 4.24 | 4.31 | 4.28 | 4.18 | 4.13 | 4.06 | 3.98 | 3.93 | 3.90 | 3.91 | 3.88 |
| 5.19              | 3.82 | 3.94 | 4.05 | 4.09 | 4.12 | 4.18 | 4.16 | 4.08 | 4.04 | 3.98 | 3.92 | 3.88 | 3.85 | 3.85 | 3.84 |
| 5.34              | 4.01 | 4.19 | 4.35 | 4.40 | 4.42 | 4.49 | 4.45 | 4.35 | 4.30 | 4.23 | 4.14 | 4.09 | 4.05 | 4.06 | 4.04 |
| 5.40              | 3.91 | 4.06 | 4.19 | 4.24 | 4.27 | 4.34 | 4.31 | 4.22 | 4.17 | 4.11 | 4.03 | 3.98 | 3.95 | 3.97 | 3.94 |
| 5.45              | 3.89 | 4.04 | 4.17 | 4.22 | 4.24 | 4.31 | 4.28 | 4.19 | 4.15 | 4.09 | 4.01 | 3.96 | 3.94 | 3.94 | 3.92 |
| 5.47              | 3.95 | 4.11 | 4.25 | 4.30 | 4.32 | 4.39 | 4.36 | 4.27 | 4.22 | 4.16 | 4.08 | 4.03 | 4.00 | 4.00 | 3.98 |
| 5.71              | 3.96 | 4.12 | 4.27 | 4.33 | 4.35 | 4.43 | 4.40 | 4.29 | 4.25 | 4.19 | 4.10 | 4.05 | 4.03 | 4.04 | 4.02 |
| 5.81              | 3.95 | 4.12 | 4.28 | 4.34 | 4.36 | 4.44 | 4.41 | 4.29 | 4.25 | 4.19 | 4.11 | 4.06 | 4.03 | 4.04 | 4.02 |
| 5.94              | 4.00 | 4.17 | 4.33 | 4.40 | 4.41 | 4.50 | 4.47 | 4.34 | 4.31 | 4.25 | 4.16 | 4.11 | 4.08 | 4.10 | 4.07 |
| 5.97              | 4.02 | 4.20 | 4.37 | 4.44 | 4.45 | 4.54 | 4.50 | 4.37 | 4.33 | 4.26 | 4.17 | 4.12 | 4.09 | 4.11 | 4.08 |
| 6.34              | 4.06 | 4.23 | 4.41 | 4.48 | 4.49 | 4.59 | 4.56 | 4.41 | 4.39 | 4.33 | 4.24 | 4.19 | 4.18 | 4.20 | 4.17 |
| 6.38              | 4.04 | 4.22 | 4.41 | 4.47 | 4.49 | 4.58 | 4.55 | 4.40 | 4.38 | 4.31 | 4.22 | 4.17 | 4.15 | 4.18 | 4.14 |
| 6.38              | 4.03 | 4.20 | 4.39 | 4.46 | 4.47 | 4.57 | 4.53 | 4.39 | 4.37 | 4.30 | 4.22 | 4.17 | 4.16 | 4.18 | 4.15 |
| 6.41              | 4.04 | 4.24 | 4.44 | 4.52 | 4.53 | 4.64 | 4.59 | 4.43 | 4.40 | 4.33 | 4.23 | 4.18 | 4.16 | 4.19 | 4.15 |
| 6.53              | 4.06 | 4.22 | 4.41 | 4.48 | 4.49 | 4.59 | 4.56 | 4.42 | 4.40 | 4.34 | 4.25 | 4.20 | 4.20 | 4.22 | 4.19 |
| 6.91              | 4.15 | 4.31 | 4.51 | 4.58 | 4.59 | 4.69 | 4.66 | 4.51 | 4.50 | 4.44 | 4.36 | 4.31 | 4.32 | 4.36 | 4.32 |
| 6.94              | 4.17 | 4.31 | 4.51 | 4.58 | 4.59 | 4.70 | 4.67 | 4.52 | 4.52 | 4.46 | 4.38 | 4.34 | 4.34 | 4.39 | 4.36 |
| 7.00              | 4.13 | 4.29 | 4.51 | 4.58 | 4.59 | 4.71 | 4.68 | 4.51 | 4.51 | 4.45 | 4.36 | 4.32 | 4.32 | 4.38 | 4.33 |
| 7.27              | 4.27 | 4.35 | 4.55 | 4.61 | 4.62 | 4.75 | 4.73 | 4.59 | 4.62 | 4.58 | 4.51 | 4.48 | 4.52 | 4.59 | 4.55 |
| 7.30              | 4.26 | 4.37 | 4.57 | 4.62 | 4.64 | 4.77 | 4.75 | 4.60 | 4.62 | 4.58 | 4.51 | 4.47 | 4.50 | 4.57 | 4.53 |
| 7.40              | 4.36 | 4.42 | 4.63 | 4.67 | 4.69 | 4.83 | 4.82 | 4.68 | 4.71 | 4.68 | 4.62 | 4.59 | 4.63 | 4.72 | 4.67 |
| 7.47              | 4.36 | 4.43 | 4.66 | 4.70 | 4.73 | 4.86 | 4.86 | 4.71 | 4.74 | 4.72 | 4.64 | 4.62 | 4.66 | 4.75 | 4.70 |
| 7.81              | 4.64 | 4.59 | 4.84 | 4.87 | 4.90 | 5.07 | 5.09 | 4.95 | 5.04 | 5.03 | 4.97 | 4.96 | 5.04 | 5.16 | 5.10 |
| 7.83              | 4.67 | 4.62 | 4.87 | 4.88 | 4.92 | 5.09 | 5.11 | 4.97 | 5.06 | 5.05 | 5.00 | 4.98 | 5.06 | 5.18 | 5.13 |
| 8.07              | 4.93 | 4.75 | 5.05 | 5.05 | 5.10 | 5.32 | 5.35 | 5.22 | 5.35 | 5.35 | 5.31 | 5.31 | 5.41 | 5.55 | 5.49 |
| 8.40              | 5.41 | 5.05 | 5.42 | 5.40 | 5.48 | 5.75 | 5.81 | 5.69 | 5.85 | 5.87 | 5.84 | 5.84 | 5.97 | 6.12 | 6.07 |
| 8.51              | 5.58 | 5.14 | 5.55 | 5.52 | 5.61 | 5.90 | 5.97 | 5.85 | 6.02 | 6.05 | 6.02 | 6.03 | 6.15 | 6.32 | 6.26 |

**Table 3.4. Distribution coefficients in 0.5 M ionic strength, calculated using Eq. (3.1) and corrected for  $\text{MOH}^{2+}$  and  $\text{MCl}^{2+}$  complexation (Eq. 3.14). <sup>a</sup>Samples not included in NEM fits. <sup>b</sup>Fresh *U. lactuca* tissue samples.**

| pH                  | Y    | La   | Ce   | Pr   | Nd   | Sm   | Eu   | Gd   | Tb   | Dy   | Ho   | Er   | Tm   | Yb   | Lu   |
|---------------------|------|------|------|------|------|------|------|------|------|------|------|------|------|------|------|
| 2.70 <sup>a,b</sup> | 1.54 | 1.65 | 1.75 | 1.75 | 1.76 | 1.91 | 1.91 | 1.86 | 1.78 | 1.72 | 1.64 | 1.60 | 1.57 | 1.76 | 1.89 |
| 2.74 <sup>a</sup>   | 1.61 | 1.31 | 1.66 | 1.61 | 1.69 | 1.85 | 1.84 | 1.78 | 1.79 | 1.69 | 1.72 | 1.72 | 1.71 | 1.89 | 1.95 |
| 2.74 <sup>a</sup>   | 1.61 | 1.57 | 1.80 | 1.74 | 1.76 | 1.90 | 1.91 | 1.84 | 1.81 | 1.78 | 1.73 | 1.72 | 1.77 | 1.89 | 1.94 |
| 2.76 <sup>a</sup>   | 1.65 | 1.59 | 1.75 | 1.75 | 1.78 | 1.86 | 1.87 | 1.81 | 1.77 | 1.78 | 1.72 | 1.72 | 1.76 | 1.88 | 1.94 |
| 2.76 <sup>a</sup>   | 1.58 | 1.50 | 1.74 | 1.75 | 1.76 | 1.89 | 1.88 | 1.82 | 1.81 | 1.78 | 1.71 | 1.75 | 1.77 | 1.89 | 1.96 |
| 2.77 <sup>a</sup>   | 1.25 | 1.11 | 1.46 | 1.45 | 1.51 | 1.70 | 1.71 | 1.57 | 1.55 | 1.55 | 1.46 | 1.44 | 1.56 | 1.70 | 1.79 |
| 2.77 <sup>a</sup>   | 1.68 | 1.64 | 1.73 | 1.72 | 1.82 | 1.93 | 1.93 | 1.86 | 1.83 | 1.82 | 1.78 | 1.80 | 1.87 | 1.93 | 1.99 |
| 3.93                | 2.08 | 2.04 | 2.20 | 2.28 | 2.31 | 2.44 | 2.43 | 2.34 | 2.32 | 2.29 | 2.24 | 2.22 | 2.25 | 2.32 | 2.36 |
| 4.06                | 2.12 | 2.08 | 2.26 | 2.34 | 2.36 | 2.49 | 2.49 | 2.38 | 2.36 | 2.34 | 2.30 | 2.28 | 2.30 | 2.38 | 2.40 |
| 4.09                | 2.13 | 2.08 | 2.24 | 2.31 | 2.35 | 2.47 | 2.46 | 2.36 | 2.36 | 2.33 | 2.28 | 2.26 | 2.28 | 2.35 | 2.38 |
| 4.09                | 2.26 | 2.22 | 2.37 | 2.44 | 2.47 | 2.59 | 2.59 | 2.50 | 2.50 | 2.45 | 2.39 | 2.39 | 2.41 | 2.48 | 2.50 |
| 4.11                | 2.28 | 2.25 | 2.42 | 2.50 | 2.53 | 2.64 | 2.63 | 2.55 | 2.54 | 2.51 | 2.46 | 2.45 | 2.45 | 2.51 | 2.52 |
| 4.16                | 2.23 | 2.15 | 2.34 | 2.41 | 2.43 | 2.59 | 2.57 | 2.48 | 2.47 | 2.43 | 2.37 | 2.36 | 2.37 | 2.44 | 2.47 |
| 4.20                | 2.26 | 2.21 | 2.41 | 2.46 | 2.49 | 2.63 | 2.62 | 2.52 | 2.51 | 2.47 | 2.41 | 2.39 | 2.40 | 2.48 | 2.50 |
| 4.21                | 2.22 | 2.15 | 2.32 | 2.41 | 2.45 | 2.57 | 2.55 | 2.46 | 2.45 | 2.41 | 2.36 | 2.34 | 2.36 | 2.43 | 2.44 |
| 4.35                | 2.31 | 2.26 | 2.44 | 2.52 | 2.56 | 2.68 | 2.67 | 2.59 | 2.57 | 2.54 | 2.48 | 2.45 | 2.46 | 2.53 | 2.55 |
| 4.54                | 2.37 | 2.31 | 2.50 | 2.59 | 2.63 | 2.76 | 2.75 | 2.65 | 2.64 | 2.61 | 2.54 | 2.53 | 2.53 | 2.59 | 2.60 |
| 4.75                | 2.55 | 2.52 | 2.68 | 2.77 | 2.80 | 2.93 | 2.92 | 2.82 | 2.81 | 2.77 | 2.71 | 2.69 | 2.70 | 2.76 | 2.76 |
| 4.88                | 2.65 | 2.59 | 2.76 | 2.83 | 2.86 | 2.97 | 2.96 | 2.89 | 2.89 | 2.86 | 2.82 | 2.80 | 2.81 | 2.86 | 2.86 |
| 4.94 <sup>a,b</sup> | 2.46 | 2.60 | 2.74 | 2.81 | 2.84 | 2.93 | 2.90 | 2.80 | 2.74 | 2.66 | 2.58 | 2.53 | 2.51 | 2.56 | 2.57 |
| 4.98                | 2.60 | 2.57 | 2.76 | 2.86 | 2.90 | 3.04 | 3.02 | 2.90 | 2.90 | 2.86 | 2.79 | 2.77 | 2.78 | 2.84 | 2.83 |
| 5.05                | 2.59 | 2.54 | 2.71 | 2.87 | 2.89 | 3.05 | 3.04 | 2.92 | 2.91 | 2.87 | 2.79 | 2.77 | 2.78 | 2.84 | 2.84 |
| 5.10                | 2.61 | 2.58 | 2.80 | 2.89 | 2.93 | 3.07 | 3.06 | 2.94 | 2.93 | 2.89 | 2.81 | 2.79 | 2.80 | 2.87 | 2.86 |
| 5.12                | 2.68 | 2.63 | 2.84 | 2.94 | 2.99 | 3.12 | 3.11 | 2.98 | 2.98 | 2.95 | 2.88 | 2.85 | 2.86 | 2.93 | 2.93 |
| 5.21                | 2.57 | 2.54 | 2.76 | 2.86 | 2.90 | 3.04 | 3.03 | 2.90 | 2.90 | 2.86 | 2.79 | 2.76 | 2.78 | 2.85 | 2.84 |
| 5.31                | 2.78 | 2.76 | 2.98 | 3.08 | 3.11 | 3.26 | 3.24 | 3.11 | 3.12 | 3.08 | 3.00 | 2.97 | 2.99 | 3.05 | 3.04 |
| 5.43                | 2.81 | 2.76 | 2.97 | 3.08 | 3.11 | 3.25 | 3.23 | 3.11 | 3.12 | 3.08 | 3.01 | 2.98 | 3.00 | 3.06 | 3.05 |
| 5.49                | 2.84 | 2.77 | 3.00 | 3.12 | 3.15 | 3.30 | 3.28 | 3.16 | 3.16 | 3.13 | 3.05 | 3.03 | 3.04 | 3.11 | 3.09 |
| 5.60 <sup>a,b</sup> | 2.76 | 2.86 | 3.07 | 3.17 | 3.20 | 3.34 | 3.30 | 3.16 | 3.13 | 3.06 | 2.96 | 2.92 | 2.91 | 2.96 | 2.94 |
| 5.70                | 2.96 | 2.90 | 3.15 | 3.25 | 3.29 | 3.44 | 3.43 | 3.30 | 3.32 | 3.28 | 3.21 | 3.19 | 3.21 | 3.28 | 3.26 |
| 5.78                | 2.94 | 2.87 | 3.11 | 3.20 | 3.24 | 3.38 | 3.37 | 3.25 | 3.26 | 3.23 | 3.16 | 3.13 | 3.16 | 3.21 | 3.20 |
| 5.83                | 3.01 | 2.92 | 3.16 | 3.26 | 3.30 | 3.45 | 3.44 | 3.32 | 3.34 | 3.31 | 3.24 | 3.22 | 3.25 | 3.31 | 3.30 |
| 5.83                | 2.92 | 2.84 | 3.09 | 3.19 | 3.22 | 3.37 | 3.36 | 3.23 | 3.26 | 3.23 | 3.16 | 3.14 | 3.17 | 3.24 | 3.22 |
| 5.95                | 3.02 | 2.92 | 3.18 | 3.28 | 3.31 | 3.47 | 3.46 | 3.34 | 3.36 | 3.34 | 3.26 | 3.25 | 3.28 | 3.35 | 3.33 |
| 5.96                | 3.04 | 2.94 | 3.19 | 3.30 | 3.34 | 3.50 | 3.49 | 3.36 | 3.39 | 3.36 | 3.29 | 3.28 | 3.31 | 3.38 | 3.36 |
| 5.98                | 3.05 | 2.95 | 3.20 | 3.31 | 3.35 | 3.51 | 3.50 | 3.37 | 3.39 | 3.36 | 3.29 | 3.28 | 3.31 | 3.38 | 3.36 |
| 6.01                | 3.09 | 3.00 | 3.27 | 3.37 | 3.41 | 3.58 | 3.57 | 3.43 | 3.46 | 3.43 | 3.35 | 3.33 | 3.37 | 3.44 | 3.42 |
| 6.09                | 3.09 | 2.97 | 3.23 | 3.33 | 3.38 | 3.54 | 3.53 | 3.40 | 3.43 | 3.41 | 3.34 | 3.33 | 3.37 | 3.44 | 3.42 |
| 6.30                | 3.22 | 3.06 | 3.34 | 3.45 | 3.49 | 3.67 | 3.66 | 3.53 | 3.57 | 3.55 | 3.49 | 3.49 | 3.53 | 3.60 | 3.58 |
| 6.31                | 3.18 | 3.05 | 3.36 | 3.48 | 3.52 | 3.71 | 3.70 | 3.55 | 3.60 | 3.58 | 3.49 | 3.48 | 3.53 | 3.61 | 3.58 |
| 6.40                | 3.17 | 3.03 | 3.32 | 3.43 | 3.47 | 3.66 | 3.65 | 3.50 | 3.55 | 3.53 | 3.45 | 3.44 | 3.50 | 3.58 | 3.56 |
| 6.67                | 3.21 | 3.01 | 3.34 | 3.46 | 3.50 | 3.72 | 3.71 | 3.55 | 3.62 | 3.61 | 3.54 | 3.54 | 3.61 | 3.70 | 3.68 |

**Table 3.4 (cont.).**

| pH   | Y    | La   | Ce   | Pr   | Nd   | Sm   | Eu   | Gd   | Tb   | Dy   | Ho   | Er   | Tm   | Yb   | Lu   |
|------|------|------|------|------|------|------|------|------|------|------|------|------|------|------|------|
| 6.71 | 3.33 | 3.13 | 3.44 | 3.56 | 3.61 | 3.82 | 3.82 | 3.66 | 3.73 | 3.71 | 3.65 | 3.65 | 3.71 | 3.80 | 3.78 |
| 6.79 | 3.29 | 3.08 | 3.40 | 3.52 | 3.57 | 3.79 | 3.78 | 3.62 | 3.69 | 3.68 | 3.61 | 3.61 | 3.68 | 3.77 | 3.74 |
| 6.81 | 3.38 | 3.17 | 3.51 | 3.63 | 3.67 | 3.90 | 3.89 | 3.72 | 3.80 | 3.79 | 3.71 | 3.72 | 3.79 | 3.88 | 3.85 |
| 6.83 | 3.28 | 3.08 | 3.40 | 3.51 | 3.56 | 3.78 | 3.77 | 3.61 | 3.68 | 3.67 | 3.59 | 3.60 | 3.67 | 3.76 | 3.73 |
| 6.87 | 3.34 | 3.14 | 3.47 | 3.58 | 3.62 | 3.84 | 3.83 | 3.67 | 3.74 | 3.73 | 3.66 | 3.67 | 3.74 | 3.83 | 3.80 |
| 7.02 | 3.36 | 3.09 | 3.45 | 3.55 | 3.60 | 3.83 | 3.83 | 3.67 | 3.76 | 3.76 | 3.69 | 3.70 | 3.78 | 3.87 | 3.84 |
| 7.04 | 3.37 | 3.11 | 3.44 | 3.56 | 3.61 | 3.83 | 3.83 | 3.68 | 3.75 | 3.75 | 3.69 | 3.70 | 3.77 | 3.86 | 3.84 |
| 7.12 | 3.40 | 3.16 | 3.51 | 3.64 | 3.69 | 3.93 | 3.93 | 3.76 | 3.84 | 3.84 | 3.76 | 3.77 | 3.85 | 3.95 | 3.91 |
| 7.14 | 3.46 | 3.18 | 3.51 | 3.62 | 3.67 | 3.89 | 3.89 | 3.74 | 3.82 | 3.82 | 3.76 | 3.77 | 3.84 | 3.92 | 3.90 |
| 7.16 | 3.37 | 3.12 | 3.46 | 3.58 | 3.63 | 3.87 | 3.87 | 3.70 | 3.79 | 3.78 | 3.72 | 3.72 | 3.80 | 3.90 | 3.87 |
| 7.31 | 3.43 | 3.14 | 3.48 | 3.60 | 3.65 | 3.89 | 3.88 | 3.73 | 3.82 | 3.82 | 3.76 | 3.77 | 3.85 | 3.94 | 3.92 |
| 7.35 | 3.53 | 3.21 | 3.54 | 3.66 | 3.71 | 3.93 | 3.94 | 3.80 | 3.88 | 3.88 | 3.84 | 3.85 | 3.92 | 4.00 | 3.98 |
| 7.48 | 3.61 | 3.27 | 3.63 | 3.74 | 3.79 | 4.03 | 4.03 | 3.89 | 3.98 | 3.98 | 3.93 | 3.94 | 4.01 | 4.10 | 4.07 |
| 7.63 | 3.66 | 3.27 | 3.63 | 3.74 | 3.79 | 4.02 | 4.03 | 3.91 | 4.00 | 4.01 | 3.96 | 3.98 | 4.05 | 4.12 | 4.10 |
| 7.68 | 3.64 | 3.29 | 3.63 | 3.74 | 3.80 | 4.02 | 4.02 | 3.89 | 3.98 | 3.98 | 3.93 | 3.95 | 4.01 | 4.08 | 4.06 |
| 7.76 | 3.65 | 3.26 | 3.63 | 3.74 | 3.80 | 4.03 | 4.04 | 3.92 | 4.01 | 4.02 | 3.97 | 3.98 | 4.05 | 4.13 | 4.11 |
| 7.80 | 3.83 | 3.43 | 3.81 | 3.93 | 3.99 | 4.23 | 4.24 | 4.10 | 4.21 | 4.21 | 4.16 | 4.17 | 4.24 | 4.31 | 4.29 |
| 7.97 | 3.76 | 3.34 | 3.70 | 3.84 | 3.90 | 4.14 | 4.16 | 4.03 | 4.14 | 4.14 | 4.10 | 4.11 | 4.19 | 4.26 | 4.24 |
| 8.08 | 3.94 | 3.58 | 3.90 | 4.02 | 4.08 | 4.29 | 4.30 | 4.19 | 4.29 | 4.29 | 4.24 | 4.25 | 4.31 | 4.39 | 4.36 |
| 8.20 | 3.91 | 3.57 | 3.90 | 4.04 | 4.10 | 4.32 | 4.33 | 4.21 | 4.31 | 4.31 | 4.25 | 4.26 | 4.33 | 4.41 | 4.38 |
| 8.43 | 4.06 | 3.60 | 3.96 | 4.09 | 4.16 | 4.40 | 4.41 | 4.31 | 4.43 | 4.44 | 4.39 | 4.41 | 4.48 | 4.54 | 4.53 |

**Table 3.5. Log  $K_S$  values in 5.0 M ionic strength, calculated using Eq. (3.1) and corrected for  $\text{MOH}^{2+}$  and  $\text{MCl}^{2+}$  complexation (Eq. 3.14). <sup>a</sup> Samples not included in NEM fits.**

| pH                | Y    | La   | Ce   | Pr   | Nd   | Sm   | Eu   | Gd   | Tb   | Dy   | Ho   | Er   | Tm   | Yb   | Lu   |
|-------------------|------|------|------|------|------|------|------|------|------|------|------|------|------|------|------|
| 2.74 <sup>a</sup> | 1.69 | 1.68 | 1.76 | 1.66 | 1.71 | 1.81 | 1.88 | 1.84 | 1.85 | 1.82 | 1.76 | 1.78 | 1.85 | 2.04 | 2.09 |
| 2.77 <sup>a</sup> | 1.64 | 1.54 | 1.68 | 1.62 | 1.66 | 1.81 | 1.80 | 1.73 | 1.73 | 1.67 | 1.71 | 1.77 | 1.90 | 2.03 | 2.09 |
| 3.86              | 2.08 | 2.08 | 2.08 | 2.15 | 2.19 | 2.35 | 2.36 | 2.28 | 2.29 | 2.27 | 2.21 | 2.24 | 2.31 | 2.42 | 2.47 |
| 4.12              | 2.39 | 2.40 | 2.41 | 2.47 | 2.49 | 2.62 | 2.62 | 2.54 | 2.58 | 2.55 | 2.50 | 2.49 | 2.55 | 2.63 | 2.66 |
| 4.43              | 2.41 | 2.47 | 2.47 | 2.54 | 2.57 | 2.74 | 2.75 | 2.65 | 2.68 | 2.64 | 2.57 | 2.56 | 2.60 | 2.71 | 2.74 |
| 4.71              | 2.47 | 2.58 | 2.56 | 2.65 | 2.68 | 2.85 | 2.86 | 2.75 | 2.79 | 2.75 | 2.68 | 2.66 | 2.69 | 2.79 | 2.80 |
| 5.00              | 2.74 | 2.81 | 2.85 | 2.93 | 2.96 | 3.13 | 3.14 | 3.03 | 3.05 | 3.02 | 2.94 | 2.92 | 2.95 | 3.04 | 3.03 |
| 5.11              | 2.63 | 2.72 | 2.80 | 2.87 | 2.91 | 3.10 | 3.11 | 2.97 | 3.01 | 2.97 | 2.88 | 2.85 | 2.89 | 2.99 | 2.98 |
| 5.38              | 2.89 | 2.90 | 3.01 | 3.10 | 3.13 | 3.31 | 3.32 | 3.20 | 3.22 | 3.19 | 3.11 | 3.08 | 3.12 | 3.20 | 3.18 |
| 5.70              | 3.04 | 2.99 | 3.18 | 3.27 | 3.31 | 3.49 | 3.50 | 3.37 | 3.41 | 3.38 | 3.29 | 3.26 | 3.30 | 3.38 | 3.35 |
| 5.71              | 3.12 | 3.06 | 3.24 | 3.33 | 3.37 | 3.54 | 3.55 | 3.43 | 3.47 | 3.44 | 3.35 | 3.33 | 3.36 | 3.44 | 3.42 |
| 5.88              | 3.16 | 3.05 | 3.26 | 3.36 | 3.40 | 3.58 | 3.59 | 3.47 | 3.51 | 3.48 | 3.40 | 3.38 | 3.42 | 3.49 | 3.47 |
| 5.92              | 3.16 | 3.05 | 3.27 | 3.37 | 3.41 | 3.59 | 3.60 | 3.47 | 3.51 | 3.49 | 3.40 | 3.38 | 3.42 | 3.49 | 3.47 |
| 6.43              | 3.34 | 3.11 | 3.42 | 3.54 | 3.58 | 3.79 | 3.80 | 3.67 | 3.73 | 3.71 | 3.64 | 3.62 | 3.67 | 3.76 | 3.74 |
| 6.55              | 3.41 | 3.15 | 3.48 | 3.59 | 3.63 | 3.85 | 3.86 | 3.73 | 3.80 | 3.78 | 3.71 | 3.70 | 3.76 | 3.84 | 3.82 |
| 6.56              | 3.38 | 3.14 | 3.46 | 3.58 | 3.63 | 3.86 | 3.87 | 3.72 | 3.79 | 3.78 | 3.70 | 3.69 | 3.75 | 3.84 | 3.82 |
| 6.76              | 3.46 | 3.20 | 3.53 | 3.65 | 3.70 | 3.93 | 3.94 | 3.80 | 3.88 | 3.86 | 3.79 | 3.78 | 3.84 | 3.94 | 3.92 |
| 6.99              | 3.53 | 3.21 | 3.54 | 3.67 | 3.72 | 3.97 | 3.98 | 3.84 | 3.93 | 3.93 | 3.86 | 3.87 | 3.94 | 4.05 | 4.03 |
| 7.02              | 3.56 | 3.22 | 3.56 | 3.69 | 3.74 | 3.99 | 4.01 | 3.87 | 3.97 | 3.97 | 3.91 | 3.91 | 3.99 | 4.11 | 4.09 |
| 7.28              | 3.75 | 3.34 | 3.69 | 3.82 | 3.88 | 4.14 | 4.17 | 4.03 | 4.15 | 4.16 | 4.11 | 4.12 | 4.21 | 4.33 | 4.31 |
| 7.37              | 3.73 | 3.28 | 3.65 | 3.78 | 3.84 | 4.12 | 4.16 | 4.01 | 4.15 | 4.17 | 4.12 | 4.14 | 4.24 | 4.38 | 4.36 |
| 7.44              | 3.80 | 3.36 | 3.72 | 3.85 | 3.91 | 4.20 | 4.23 | 4.09 | 4.22 | 4.24 | 4.19 | 4.21 | 4.32 | 4.46 | 4.42 |
| 7.49              | 3.82 | 3.37 | 3.73 | 3.86 | 3.93 | 4.22 | 4.25 | 4.11 | 4.25 | 4.27 | 4.22 | 4.24 | 4.35 | 4.50 | 4.46 |
| 7.91              | 4.09 | 3.48 | 3.91 | 4.03 | 4.11 | 4.46 | 4.51 | 4.35 | 4.55 | 4.58 | 4.53 | 4.56 | 4.71 | 4.90 | 4.84 |
| 7.94              | 4.11 | 3.48 | 3.88 | 4.01 | 4.09 | 4.45 | 4.51 | 4.35 | 4.56 | 4.60 | 4.56 | 4.60 | 4.76 | 4.96 | 4.90 |
| 8.14              | 4.34 | 3.57 | 4.06 | 4.16 | 4.25 | 4.66 | 4.73 | 4.56 | 4.81 | 4.86 | 4.82 | 4.87 | 5.04 | 5.26 | 5.19 |
| 8.48              | 4.75 | 3.79 | 4.31 | 4.43 | 4.55 | 5.05 | 5.15 | 4.97 | 5.27 | 5.34 | 5.31 | 5.37 | 5.58 | 5.83 | 5.76 |

Table 3.6. Best-fit parameters for  $\log K_S$  vs. pH data (Tables 3.4 – 3.5) using the NEM (Eq. 3.25) for 0.5 and 5.0 M data, with  $\log K_X$  values set equal to those found in Table 3.3.

| YREE | 0.5 M NaCl    |              |              |             | 5.0 M NaCl |               |              |              |             |       |
|------|---------------|--------------|--------------|-------------|------------|---------------|--------------|--------------|-------------|-------|
|      | R             | $\beta_2$    | $\beta_3$    | $\beta_3^*$ | $r^2$      | R             | $\beta_2$    | $\beta_3$    | $\beta_3^*$ | $r^2$ |
| Y    | 0.043 ± 0.002 | -1.30 ± 0.03 | -2.66 ± 0.05 | -11.2 ± 0.2 | 0.993      | 0.037 ± 0.003 | -1.27 ± 0.05 | -2.61 ± 0.07 | -11.1 ± 0.2 | 0.994 |
| La   | 0.041 ± 0.002 | -1.41 ± 0.04 | -3.51 ± 0.15 | -12.2 ± 0.4 | 0.977      | 0.053 ± 0.005 | -1.66 ± 0.08 | -3.81 ± 0.35 | -12.3 ± 0.5 | 0.958 |
| Ce   | 0.056 ± 0.003 | -1.23 ± 0.03 | -3.07 ± 0.08 | -12.0 ± 0.4 | 0.988      | 0.041 ± 0.004 | -1.18 ± 0.06 | -3.09 ± 0.16 | -11.6 ± 0.3 | 0.988 |
| Pr   | 0.065 ± 0.003 | -1.17 ± 0.03 | -3.01 ± 0.08 | -11.8 ± 0.3 | 0.989      | 0.046 ± 0.004 | -1.10 ± 0.05 | -2.98 ± 0.13 | -11.6 ± 0.3 | 0.991 |
| Nd   | 0.070 ± 0.003 | -1.16 ± 0.03 | -2.95 ± 0.07 | -11.6 ± 0.3 | 0.990      | 0.048 ± 0.004 | -1.08 ± 0.05 | -2.89 ± 0.12 | -11.5 ± 0.3 | 0.993 |
| Sm   | 0.088 ± 0.004 | -1.08 ± 0.03 | -2.64 ± 0.05 | -11.3 ± 0.2 | 0.993      | 0.065 ± 0.005 | -1.00 ± 0.05 | -2.58 ± 0.08 | -11.0 ± 0.1 | 0.996 |
| Eu   | 0.086 ± 0.004 | -1.09 ± 0.03 | -2.58 ± 0.05 | -11.2 ± 0.2 | 0.994      | 0.067 ± 0.005 | -1.01 ± 0.05 | -2.53 ± 0.08 | -10.8 ± 0.1 | 0.996 |
| Gd   | 0.073 ± 0.003 | -1.17 ± 0.03 | -2.68 ± 0.05 | -11.2 ± 0.1 | 0.993      | 0.057 ± 0.004 | -1.08 ± 0.05 | -2.60 ± 0.08 | -11.0 ± 0.1 | 0.996 |
| Tb   | 0.067 ± 0.003 | -1.10 ± 0.03 | -2.43 ± 0.04 | -10.9 ± 0.1 | 0.995      | 0.058 ± 0.004 | -1.04 ± 0.05 | -2.37 ± 0.06 | -10.6 ± 0.1 | 0.997 |
| Dy   | 0.062 ± 0.003 | -1.10 ± 0.03 | -2.35 ± 0.04 | -10.8 ± 0.1 | 0.995      | 0.054 ± 0.003 | -1.05 ± 0.05 | -2.29 ± 0.06 | -10.5 ± 0.1 | 0.997 |
| Ho   | 0.055 ± 0.003 | -1.13 ± 0.03 | -2.33 ± 0.04 | -10.8 ± 0.1 | 0.995      | 0.047 ± 0.003 | -1.08 ± 0.05 | -2.25 ± 0.05 | -10.5 ± 0.1 | 0.997 |
| Er   | 0.053 ± 0.003 | -1.14 ± 0.03 | -2.26 ± 0.04 | -10.8 ± 0.1 | 0.995      | 0.048 ± 0.003 | -1.12 ± 0.05 | -2.19 ± 0.05 | -10.5 ± 0.1 | 0.998 |
| Tm   | 0.054 ± 0.003 | -1.13 ± 0.04 | -2.11 ± 0.03 | -10.6 ± 0.1 | 0.996      | 0.055 ± 0.003 | -1.16 ± 0.04 | -2.11 ± 0.04 | -10.3 ± 0.1 | 0.998 |
| Yb   | 0.063 ± 0.003 | -1.15 ± 0.04 | -2.02 ± 0.03 | -10.4 ± 0.1 | 0.997      | 0.071 ± 0.004 | -1.22 ± 0.04 | -2.08 ± 0.04 | -10.1 ± 0.1 | 0.999 |
| Lu   | 0.068 ± 0.003 | -1.21 ± 0.04 | -2.09 ± 0.03 | -10.5 ± 0.1 | 0.997      | 0.078 ± 0.004 | -1.30 ± 0.04 | -2.13 ± 0.04 | -10.3 ± 0.1 | 0.999 |

Table 3.7. Best-fit parameters for log  $K_S$  vs. pH data (Table 3.3) using the modified NEM (Eq. 3.34) for 0.05 M data, with log  $K_C$  set equal to 9.433.

| YREE | 0.05 M NaCl |              |             |             |       |
|------|-------------|--------------|-------------|-------------|-------|
|      | R           | $B_3$        | $B_3^*$     | $pK_a$      | $r^2$ |
| Y    | 0.23 ± 0.02 | -2.74 ± 0.07 | -10.9 ± 0.1 | 4.62 ± 0.05 | 0.987 |
| La   | 0.26 ± 0.02 | -2.80 ± 0.07 | -12.9 ± 4.3 | 4.77 ± 0.04 | 0.979 |
| Ce   | 0.31 ± 0.02 | -2.61 ± 0.07 | -11.5 ± 0.3 | 4.87 ± 0.05 | 0.982 |
| Pr   | 0.33 ± 0.02 | -2.63 ± 0.08 | -11.7 ± 0.4 | 4.91 ± 0.05 | 0.980 |
| Nd   | 0.35 ± 0.03 | -2.63 ± 0.08 | -11.4 ± 0.3 | 4.90 ± 0.05 | 0.982 |
| Sm   | 0.40 ± 0.03 | -2.50 ± 0.07 | -11.0 ± 0.2 | 4.93 ± 0.05 | 0.984 |
| Eu   | 0.37 ± 0.03 | -2.47 ± 0.07 | -10.9 ± 0.1 | 4.92 ± 0.05 | 0.986 |
| Gd   | 0.33 ± 0.02 | -2.58 ± 0.07 | -10.9 ± 0.1 | 4.83 ± 0.04 | 0.987 |
| Tb   | 0.30 ± 0.02 | -2.46 ± 0.07 | -10.6 ± 0.1 | 4.83 ± 0.05 | 0.989 |
| Dy   | 0.27 ± 0.02 | -2.43 ± 0.06 | -10.5 ± 0.1 | 4.79 ± 0.05 | 0.990 |
| Ho   | 0.25 ± 0.02 | -2.46 ± 0.06 | -10.5 ± 0.1 | 4.73 ± 0.05 | 0.990 |
| Er   | 0.24 ± 0.02 | -2.45 ± 0.06 | -10.5 ± 0.1 | 4.70 ± 0.05 | 0.990 |
| Tm   | 0.23 ± 0.02 | -2.38 ± 0.06 | -10.3 ± 0.1 | 4.68 ± 0.05 | 0.991 |
| Yb   | 0.24 ± 0.02 | -2.30 ± 0.06 | -10.2 ± 0.1 | 4.68 ± 0.05 | 0.992 |
| Lu   | 0.24 ± 0.02 | -2.35 ± 0.06 | -10.2 ± 0.1 | 4.64 ± 0.05 | 0.992 |

Table 3.8. Calculated YREE stability constants for  $M^{3+}$  complexation with groups A, B, and C ( $\log \beta_A$ ,  $\log \beta_B$  and  $\log \beta_C$ , respectively) and  $MOH^{2+}$  complexation with group C ( $\log \beta_C^*$ ). No  $\log \beta_B$  values are shown for 0.05 M ionic strength, whose model equation (Eq. 3.34) included only group C and a combined term for groups A and B ( $\log \beta_n$ ).

| YREE | 0.05 M         |                |                  | 0.5 M          |                |                | 5.0 M          |                |                |                  |       |
|------|----------------|----------------|------------------|----------------|----------------|----------------|----------------|----------------|----------------|------------------|-------|
|      | $\log \beta_n$ | $\log \beta_C$ | $\log \beta_C^*$ | $\log \beta_A$ | $\log \beta_B$ | $\log \beta_C$ | $\log \beta_A$ | $\log \beta_B$ | $\log \beta_C$ | $\log \beta_C^*$ |       |
| Y    | -0.159         | -2.90          | -3.03            | -0.88          | -2.22          | -3.45          | -4.04          | -0.95          | -2.22          | -3.56            | -3.91 |
| La   | -0.115         | -2.91          | -3.93            | -0.90          | -2.33          | -4.29          | -3.97          | -0.80          | -2.46          | -4.61            | -4.03 |
| Ce   | -0.038         | -2.65          | -2.86            | -0.77          | -2.01          | -3.78          | -4.13          | -0.91          | -2.08          | -4.00            | -3.91 |
| Pr   | -0.009         | -2.64          | -3.05            | -0.71          | -1.89          | -3.64          | -3.91          | -0.86          | -1.96          | -3.84            | -3.88 |
| Nd   | 0.018          | -2.61          | -2.92            | -0.67          | -1.86          | -3.53          | -3.85          | -0.84          | -1.92          | -3.73            | -3.85 |
| Sm   | 0.071          | -2.43          | -2.80            | -0.57          | -1.68          | -3.12          | -3.75          | -0.71          | -1.71          | -3.29            | -3.55 |
| Eu   | 0.047          | -2.42          | -2.75            | -0.58          | -1.70          | -3.06          | -3.71          | -0.70          | -1.71          | -3.23            | -3.50 |
| Gd   | 0.0003         | -2.58          | -2.77            | -0.65          | -1.85          | -3.22          | -3.73          | -0.77          | -1.85          | -3.37            | -3.66 |
| Tb   | -0.044         | -2.50          | -2.73            | -0.68          | -1.83          | -3.00          | -3.65          | -0.76          | -1.80          | -3.13            | -3.48 |
| Dy   | -0.084         | -2.52          | -2.73            | -0.72          | -1.86          | -2.96          | -3.67          | -0.79          | -1.84          | -3.07            | -3.45 |
| Ho   | -0.119         | -2.58          | -2.78            | -0.76          | -1.95          | -2.99          | -3.72          | -0.85          | -1.93          | -3.09            | -3.53 |
| Er   | -0.145         | -2.60          | -2.81            | -0.78          | -1.98          | -2.95          | -3.74          | -0.85          | -1.97          | -3.04            | -3.51 |
| Tm   | -0.159         | -2.54          | -2.79            | -0.78          | -1.96          | -2.80          | -3.69          | -0.78          | -1.95          | -2.90            | -3.39 |
| Yb   | -0.151         | -2.45          | -2.77            | -0.70          | -1.93          | -2.63          | -3.62          | -0.67          | -1.89          | -2.75            | -3.25 |
| Lu   | -0.143         | -2.50          | -2.80            | -0.67          | -1.96          | -2.67          | -3.64          | -0.63          | -1.93          | -2.76            | -3.33 |

## Bibliography

- Benoit, G., Oktaymarshall, S. D., Cantu, A., Hood, E. M., Coleman, C. H., Corapcioglu, M. O., and Santschi, P. H., 1994. Partitioning of Cu, Pb, Ag, Zn, Fe, Al, and Mn between filter-retained particles, colloids, and solution in 6 Texas estuaries. *Marine Chemistry* **45**, 307-336.
- Boyanov, M. I., Kelly, S. D., Kemner, K. M., Bunker, B. A., Fein, J. B., and Fowle, D. A., 2003. Adsorption of cadmium to *Bacillus subtilis* bacterial cell walls: a pH-dependent X-ray absorption fine structure spectroscopy study. *Geochimica et Cosmochimica Acta* **67**, 3299-3311.
- Brown, G. E. and Parks, G. A., 2001. Sorption of trace elements on mineral surfaces: Modern perspectives from spectroscopic studies, and comments on sorption in the marine environment. *International Geology Review* **43**, 963-1073.
- Brown, M. T., Hodgkinson, W. M., and Hurd, C. L., 1999. Spatial and temporal variations in the copper and zinc concentrations of two green seaweeds from Otago Harbour, New Zealand. *Marine Environmental Research* **47**, 175-184.
- Buffle, J., Perret, D., and Newman, M., 1992. The use of filtration and ultrafiltration for size fractionation of aquatic particles, colloids, and macromolecules. In: Buffle, J. and Leeuwen, H. P. v. Eds.), *Environmental Particles*. Lewis Publishers, Boca Raton, FL.
- Byrne, R. H. and Kim, K. H., 1990. Rare-earth element scavenging in seawater. *Geochimica et Cosmochimica Acta* **54**, 2645-2656.
- Byrne, R. H. and Li, B. Q., 1995. Comparative complexation behavior of the rare-earths. *Geochimica et Cosmochimica Acta* **59**, 4575-4589.
- Byrne, R. H. and Sholkovitz, E. R., 1996. Chapter 158 Marine chemistry and geochemistry of the lanthanides. In: Karl A. Gschneidner, J. and LeRoy, E. Eds.), *Handbook on the Physics and Chemistry of Rare Earths*. Elsevier, Amsterdam.
- Cosden, J. M., Schijf, J., and Byrne, R. H., 2003. Fractionation of Platinum Group Elements in Aqueous Systems: Comparative Kinetics of Palladium and Platinum Removal from Seawater by *Ulva lactuca* L. *Environmental Science & Technology* **37**, 555-560.
- Davis, J. A., Coston, J. A., Kent, D. B., and Fuller, C. C., 1998. Application of the Surface Complexation Concept to Complex Mineral Assemblages. *Environmental Science & Technology* **32**, 2820-2828.
- Davis, J. A., James, R. O., and Leckie, J. O., 1978. Surface Ionization and Complexation at Oxide-Water Interface. 1. Computation of Electrical Double-Layer Properties in Simple Electrolytes. *Journal of Colloid and Interface Science* **63**, 480-499.
- Davis, J. A. and Kent, D. B., 1990. Surface Complexation Modeling in Aqueous Geochemistry. In: Michael F. Hochella, J. and White, A. F. Eds.), *Mineral-Water Interface Geochemistry*. Mineralogical Society of America, Washington, DC.
- Deo, R. P., Songkasiri, W., Rittmann, B. E., and Reed, D. T., 2010. Surface Complexation of Neptunium(V) onto Whole Cells and Cell Components of *Shewanella* alga: Modeling and Experimental Study. *Environmental Science & Technology* **44**, 4930-4935.
- Dickinson, D. M. J., Jones, R. G. W., and Davenport, J., 1982. Osmotic Adaptation of

- Ulva Lactuca* Under Fluctuating Salinity Regimes. *Planta* **155**, 409-415.
- Ding, S., Liang, T., Zhang, C., Yan, J., and Zhang, Z., 2005. Accumulation and fractionation of rare earth elements (REEs) in wheat: controlled by phosphate precipitation, cell wall absorption and solution complexation. *J. Exp. Bot.* **56**, 2765-2775.
- Dzombak, D. A. and Morel, F., 1990. *Surface Complexation Modeling: Hydrous Ferric Oxide*. John Wiley & Sons, Inc., New York.
- El-Sikaily, A., El Nemr, A., Khaled, A., and Abdelwehab, O., 2007. Removal of toxic chromium from wastewater using green alga *Ulva lactuca* and its activated carbon. *Journal of Hazardous Materials* **148**, 216-228.
- Fein, J. B., Boily, J. F., Yee, N., Gorman-Lewis, D., and Turner, B. F., 2005. Potentiometric titrations of *Bacillus subtilis* cells to low pH and a comparison of modeling approaches. *Geochimica et Cosmochimica Acta* **69**, 1123-1132.
- Fowle, D. A. and Fein, J. B., 1999. Competitive adsorption of metal cations onto two gram positive bacteria: Testing the chemical equilibrium model. *Geochimica et Cosmochimica Acta* **63**, 3059-3067.
- Fowle, D. A. and Fein, J. B., 2000. Experimental measurements of the reversibility of metal-bacteria adsorption reactions. *Chemical Geology* **168**, 27-36.
- Gadd, G. M., 1990. Chapter 11. Fungi and Yeasts for Metal Accumulation. In: Ehrlich, H. L. and Brierley, C. L. Eds.), *Microbial Mineral Recovery*. McGraw Hill Pub. Co., New York.
- Gaudry, A., Zeroual, S., Gaie-Levrel, F., Moskura, M., Boujral, F. Z., El Moursli, R. C., Guessous, A., Mouradi, A., Givernaud, T., and Delmas, R., 2007. Heavy metals pollution of the Atlantic marine environment by the Moroccan phosphate industry, as observed through their bioaccumulation in *Ulva lactuca*. *Water Air and Soil Pollution* **178**, 267-285.
- Ghorpade, S. M., 2010. Interactions between natural organic matter composition and mercury transport in a boreal watershed. M. Sc. thesis, University of Maryland.
- Goldberg, E. D., Baker, M., and Fox, D. L., 1952. Microfiltration in Oceanographic Research. 1. Marine Sampling with the Molecular Filter. *Journal of Marine Research* **11**, 194-204.
- Gonzalez-Davila, M., Santana-Casiano, J. M., Perez-Pena, J., and Millero, F. J., 1995. Binding of Cu(II) to the Surface and Exudates of the Alga *Dunaliella tertiolecta* in Seawater. *Environmental Science & Technology* **29**, 289-301.
- Greene, B. and Darnall, D. W., 1990. Chapter 12. Microbial Oxygenic Photoautotrophs for Metal-Ion Binding. In: Ehrlich, H. L. and Brierley, C. L. Eds.), *Microbial Mineral Recovery*. McGraw Hill Pub. Co., New York.
- Guiry, M. D. and Guiry, G. M., 2010. AlgaeBase. National University of Ireland, Galway.
- Guo, L. D., Santschi, P. H., and Warnken, K. W., 2000. Trace metal composition of colloidal organic material in marine environments. *Marine Chemistry* **70**, 257-275.
- Gustafsson, O. and Gschwend, P. M., 1997. Aquatic colloids: Concepts, definitions, and current challenges. *Limnology and Oceanography* **42**, 519-528.
- Ha, J., Gélabert, A., Spormann, A. M., and Brown Jr, G. E., 2010. Role of extracellular polymeric substances in metal ion complexation on *Shewanella oneidensis*: Batch

- uptake, thermodynamic modeling, ATR-FTIR, and EXAFS study. *Geochimica et Cosmochimica Acta* **74**, 1-15.
- Hamdy, A. A., 2000. Removal of Pb<sup>2+</sup> by Biomass of Marine Algae. *Current Microbiology* **41**, 239-245.
- Harden, V. P. and Harris, J. O., 1953. The isoelectric point of bacterial cells. *Journal of Bacteriology* **65**, 198-202.
- Haug, A., 1976. The influence of borate and calcium on the gel formation of a sulfated polysaccharide from *Ulva lactuca*. *Acta Chemica Scandinavica B* **30**, 562-566.
- Herrero, R., Cordero, B., Lodeiro, P., Rey-Castro, C., and Sastre de Vicente, M. E., 2006. Interactions of cadmium(II) and protons with dead biomass of marine algae *Fucus* sp. *Marine Chemistry* **99**, 106-116.
- Ho, Y. B., 1990. *Ulva lactuca* as bioindicator of metal contamination in intertidal waters in Hong Kong. *Hydrobiologia* **203**, 73-81.
- Jannasch, H. W., Honeyman, B. D., Balistrieri, L. S., and Murray, J. W., 1988. Kinetics of Trace-element Uptake by Marine Particles. *Geochimica et Cosmochimica Acta* **52**, 567-577.
- Kapoor, A. and Viraraghavan, T., 1997. Heavy metal biosorption sites in *Aspergillus niger*. *Bioresource Technology* **61**, 221-227.
- Kloareg, B., Demarty, M., and Mabeau, S., 1987. Ion-Exchange Properties of Isolated Cell Walls of Brown Algae: The Interstitial Solution. *Journal of Experimental Botany* **38**, 1652-1662.
- Klungness, G. D. and Byrne, R. H., 2000. Comparative hydrolysis behavior of the rare earths and yttrium: the influence of temperature and ionic strength. *Polyhedron* **19**, 99-107.
- Kolat, R. S. and Powell, J. E., 1962. Acetate complexes of the rare earth and several transition metal ions. *Inorganic Chemistry* **1**, 293-296.
- Kulik, D. A., Aja, S. U., Sinitsyn, V. A., and Wood, S. A., 2000. Acid-base surface chemistry and sorption of some lanthanides on K<sup>+</sup>-saturated marblehead illite: II. A multisite-surface complexation modeling. *Geochimica et Cosmochimica Acta* **64**, 195-213.
- Lau, T. C., Ang, P. O., and Wong, P. K., 2003. Development of seaweed biomass as a biosorbent for metal ions. *Water Science and Technology* **47**, 49-54.
- Lead, J. R., Hamilton-Taylor, J., Davison, W., and Harper, M., 1999. Trace metal sorption by natural particles and coarse colloids. *Geochimica et Cosmochimica Acta* **63**, 1661-1670.
- Lee, W.-Y. and Wang, W.-X., 2001. Metal accumulation in the green macroalga *Ulva fasciata*: effects of nitrate, ammonium and phosphate. *The Science of the Total Environment* **278**, 11-22.
- Loder, T. C. and Liss, P. S., 1985. Control by Organic Coatings of the Surface-Charge of Estuarine Suspended Particles. *Limnology and Oceanography* **30**, 418-421.
- Loughnane, C. J., McIvor, L. M., Rindi, F., Stengel, D. B., and Guiry, M. D., 2008. Morphology, *rbcL* phylogeny and distribution of distromatic *Ulva* (Ulvophyceae, Chlorophyta) in Ireland and southern Britain. *Phycologia* **47**, 416-429.
- Luo, Y. R. and Byrne, R. H., 2000. The ionic strength dependence of rare earth and yttrium fluoride complexation at 25 °C. *Journal of Solution Chemistry* **29**, 1089-1099.

- Luo, Y. R. and Byrne, R. H., 2001. Yttrium and Rare Earth Element Complexation by Chloride Ions at 25°C. *Journal of Solution Chemistry* **30**, 837-845.
- Luo, Y. R. and Byrne, R. H., 2004. Carbonate complexation of yttrium and the rare earth elements in natural waters. *Geochimica et Cosmochimica Acta* **68**, 691-699.
- Luo, Y. X. and Millero, F. J., 2004. Effects of temperature and ionic strength on the stabilities of the first and second fluoride complexes of yttrium and the rare earth elements. *Geochimica et Cosmochimica Acta* **68**, 4301-4308.
- Markai, S., Andres, Y., Montavon, G., and Grambow, B., 2003. Study of the interaction between europium (III) and *Bacillus subtilis*: fixation sites, biosorption modeling and reversibility. *Journal of Colloid and Interface Science* **262**, 351-361.
- Mills, G. L. and Quinn, J. G., 1981. Isolation of dissolved organic matter and copper organic complexes from estuarine waters using reverse phase liquid chromatography *Marine Chemistry* **10**, 93-102.
- Mishra, B., Boyanov, M., Bunker, B. A., Kelly, S. D., Kemner, K. M., and Fein, J. B., 2010. High- and low-affinity binding sites for Cd on the bacterial cell walls of *Bacillus subtilis* and *Shewanella oneidensis*. *Geochimica et Cosmochimica Acta* **74**, 4219-4233.
- Morel, F. M. and Gschwend, P. M., 1987. The Role of Colloids in the Partitioning of Solutes in Natural Waters. In: Stumm, W. (Ed.), *Aquatic Surface Chemistry: Chemical Processes at the Particle-Water Interface*. John Wiley & Sons, New York.
- Naeem, A., Woertz, J. R., and Fein, J. B., 2006. Experimental Measurement of Proton, Cd, Pb, Sr, and Zn Adsorption Onto the Fungal Species *Saccharomyces Cerevisiae*. *Environmental Science & Technology* **40**, 5724-5729.
- Nasr, A. H. and Aleem, A. A., 1948. Ecological studies of some marine algae from Alexandria. *Hydrobiologia* **1**, 251-281.
- Ngwenya, B. T., Mosselmans, J. F. W., Magennis, M., Atkinson, K. D., Tourney, J., Olive, V., and Ellam, R. M., 2009. Macroscopic and spectroscopic analysis of lanthanide adsorption to bacterial cells. *Geochimica et Cosmochimica Acta* **73**, 3134-3147.
- Ngwenya, B. T., Sutherland, I. W., and Kennedy, L., 2003. Comparison of the acid-base behaviour and metal adsorption characteristics of a gram-negative bacterium with other strains. *Applied Geochemistry* **18**, 527-538.
- Norris, J. N., 2010. Marine Algae of the Northern Gulf of California: Chlorophyta and Phaeophyceae. *Smithsonian Contributions to Botany* **94**, 31-36.
- Nyffeler, U. P., Li, Y. H., and Santschi, P. H., 1984. A Kinetic Approach to Describe Trace-Element Distribution Between Particles and Solution in Natural Aquatic Systems. *Geochimica et Cosmochimica Acta* **48**, 1513-1522.
- Ohta, A. and Kawabe, I., 2000. Rare earth element partitioning between Fe oxyhydroxide precipitates and aqueous NaCl solutions doped with NaHCO<sub>3</sub>: Determinations of rare earth element complexation constants with carbonate ions. *Geochemical Journal* **34**, 439-454.
- Pankow, J. F. and McKenzie, S. W., 1991. Parameterizing the Equilibrium Distribution of Chemicals between the Dissolved, Solid Particulate Matter, and Colloidal Matter Compartments in Aqueous Systems. *Environmental Science & Technology* **25**, 2046-2053.

- Pearson, R. G., 1963. Hard and Soft Acids and Bases. *Journal of the American Chemical Society* **85**, 3533-3539.
- Percival, E., 1979. The polysaccharides of green, red and brown seaweeds: Their basic structure, biosynthesis and function. *British Phycological Journal* **14**, 103-117.
- Percival, E. and Wold, J. K., 1963. The Acid Polysaccharide from the Green Seaweed *Ulva lactuca*. Part II. The Site of the Ester Sulphate. *Journal of Chemical Society*, 5459 - 5468.
- Phillips, D. J. H., 1977. The use of biological indicator organisms to monitor trace metal pollution in marine and estuarine environments—A review. *Environmental Pollution* **13**, 281-317.
- Pourret, O. and Martinez, R. E., 2009. Modeling lanthanide series binding sites on humic acid. *Journal of Colloid and Interface Science* **330**, 45-50.
- Quinn, K. A., Byrne, R. H., and Schijf, J., 2004. Comparative Scavenging of Yttrium and the Rare Earth Elements in Seawater: Competitive Influences of Solution and Surface Chemistry. *Aquatic Geochemistry* **10**, 59-80.
- Quinn, K. A., Byrne, R. H., and Schijf, J., 2006a. Sorption of yttrium and rare earth elements by amorphous ferric hydroxide: Influence of pH and ionic strength. *Marine Chemistry* **99**, 128-150.
- Quinn, K. A., Byrne, R. H., and Schijf, J., 2006b. Sorption of yttrium and rare earth elements by amorphous ferric hydroxide: Influence of solution complexation with carbonate. *Geochimica et Cosmochimica Acta* **54**, 4151-4165.
- Quinn, K. A., Byrne, R. H., and Schijf, J., 2006c. Sorption of Yttrium and Rare Earth Elements by Amorphous Ferric Hydroxide: Influence of Temperature. *Environmental Science & Technology* **41**, 541-546.
- Rainbow, P. S., 1995. Biomonitoring of heavy metal availability in the marine environment. *Marine Pollution Bulletin* **31**, 183-192.
- Ren, H. M., Liu, H. J., Qu, J. H., Berg, M., Qi, W. X., and Xu, W., 2010. The influence of colloids on the geochemical behavior of metals in polluted water using as an example Yongdingxin River, Tianjin, China. *Chemosphere* **78**, 360-367.
- Ritchie, R. J. and Larkum, A. W. D., 1982. Ion Exchange Fluxes of the Cell Walls of *Enteromorpha intestinalis* (L.). *Journal of Experimental Botany* **33**, 140-153.
- Sari, A. and Tuzen, M., 2008. Biosorption of Pb(II) and Cd(II) from aqueous solution using green alga (*Ulva lactuca*) biomass. *Journal of Hazardous Materials* **152**, 302-308.
- Sawyer, C. N., 1965. The sea lettuce problem in Boston Harbor. *Journal of the Water Pollution Control Federation* **37**, 1122-1133.
- Schiewer, S. and Volesky, B., 1996. Modeling multi-metal ion exchange in biosorption. *Environmental Science & Technology* **30**, 2921-2927.
- Schiewer, S. and Wong, M. H., 2000. Ionic strength effects in biosorption of metals by marine algae. *Chemosphere* **41**, 271-282.
- Schijf, J. and Byrne, R. H., 1999. Determination of stability constants for the mono- and difluoro-complexes of Y and the REE, using a cation-exchange resin and ICP-MS. *Polyhedron* **18**, 2839-2844.
- Schijf, J. and Byrne, R. H., 2001. Stability constants for mono- and dioxalato-complexes of Y and the REE, potentially important species in groundwaters and surface freshwaters. *Geochimica et Cosmochimica Acta* **65**, 1037-1046.

- Schijf, J. and Byrne, R. H., 2004. Determination of  $\beta_1$  for yttrium and the rare earth elements at  $I=0.66\text{ m}$  and  $T=25\text{ }^\circ\text{C}$  - Implications for YREE solution speciation in sulfate-rich waters. *Geochimica et Cosmochimica Acta* **68**, 2825-2837.
- Schijf, J. and Ebling, A. M., 2010. Investigation of the Ionic Strength Dependence of *Ulva lactuca* Acid Functional Group  $\text{pK}_{\text{as}}$  by Manual Alkalimetric Titrations. *Environmental Science & Technology* **44**, 1644-1649.
- Schijf, J. and Marshall, K., 2011. YREE sorption on hydrous ferric oxide in 0.5 M NaCl solutions: A model extension. *Marine Chemistry* **123**, 32-43.
- Scott, G. T. and Hayward, H. R., 1953. Metabolic factors influencing the sodium and potassium distribution in *Ulva lactuca*. *The Journal of General Physiology* **36**, 659-671.
- Seeliger, U. and Edwards, P., 1977. Correlation coefficients and concentration factors of copper and lead in seawater and benthic algae. *Marine Pollution Bulletin* **8**, 16-19.
- Serrano, S., O'Day, P. A., Vlassopoulos, D., Garcia-Gonzalez, M. T., and Garrido, F., 2009. A surface complexation and ion exchange model of Pb and Cd competitive sorption on natural soils. *Geochimica et Cosmochimica Acta* **73**, 543-558.
- Shannon, R., 1976. Revised effective ionic radii and systematic studies of interatomic distances in halides and chalcogenides. *Acta Crystallographica Section A* **32**, 751-767.
- Sheng, P. X., Ting, Y.-P., Chen, J. P., and Hong, L., 2004. Sorption of lead, copper, cadmium, zinc, and nickel by marine algal biomass: characterization of biosorptive capacity and investigation of mechanisms. *Journal of Colloid and Interface Science* **275**, 131-141.
- Smith, R. M. and Martell, A. E., 2004. *NIST Critically Selected Stability Constants of Metal Complexes Database - Version 8.0*. National Institute of Standards and Technology, Gaithersburg, MD.
- Stanley, J. K. and Byrne, R. H., 1990. The influence of solution chemistry on REE uptake by *Ulva lactuca* L. in seawater. *Geochimica et Cosmochimica Acta* **54**, 1587-1595.
- Straka, A. M. and Schijf, J., 2009. An Extended X-Ray Absorption Fine Structure (EXAFS) Study of YREE sorption on *Ulva lactuca* L. *Geological Society of America Abstracts with Programs* **41**, 328.
- Stroes-Gascoyne, S., Kramer, J. R., and Snodgrass, W. J., 1986. A new model describing the adsorption of copper on  $\text{MnO}_2$ . *Environmental Science & Technology* **20**, 1047-1050.
- Stumm, W., Huang, C. P., and Jenkins, S. R., 1970. Specific Chemical Interaction Affecting Stability of Dispersed Systems. *Croatica Chemica Acta* **42**, 223-244.
- Stumm, W. and Morgan, J. J., 1996. *Aquatic Chemistry: Chemical Equilibria and Rates in Natural Waters*. John Wiley & Sons, Inc., New York.
- Sugimura, Y. and Suzuki, Y., 1988. A high-temperature catalytic oxidation method for the determination of non-volatile dissolved organic carbon in seawater by direct injection of a liquid sample. *Marine Chemistry* **24**, 105-131.
- Suzuki, Y., Kametani, T., and Maruyama, T., 2005. Removal of heavy metals from aqueous solution by nonliving *Ulva* seaweed as biosorbent. *Water Research* **39**, 1803-1808.

- Tang, J. W. and Johannesson, K. H., 2005. Adsorption of rare earth elements onto Carrizo sand: Experimental investigations and modeling with surface complexation. *Geochimica et Cosmochimica Acta* **69**, 5247-5261.
- Tertre, E., Hofmann, A., and Berger, G., 2008. Rare earth element sorption by basaltic rock: Experimental data and modeling results using the "Generalised Composite approach". *Geochimica et Cosmochimica Acta* **72**, 1043-1056.
- Texier, A.-C., Andrès, Y., Illemassene, M., and Le Cloirec, P., 2000. Characterization of lanthanide ions binding sites in the cell wall of *Pseudomonas aeruginosa*. *Environmental Science & Technology* **34**, 610-615.
- Tsezos, M. and Volesky, B., 1982a. The Mechanism of Thorium Biosorption by *Rhizopus arrhizus*. *Biotechnology and Bioengineering* **24**, 955-969.
- Tsezos, M. and Volesky, B., 1982b. The Mechanism of Uranium Biosorption by *Rhizopus arrhizus*. *Biotechnology and Bioengineering* **24**, 385-401.
- Turner, A., Lewis, M. S., Shams, L., and Brown, M. T., 2007. Uptake of platinum group elements by the marine macroalga, *Ulva lactuca*. *Marine Chemistry* **105**, 271-280.
- Turner, A., Pedroso, S. S., and Brown, M. T., 2008. Influence of salinity and humic substances on the uptake of trace metals by the marine macroalga, *Ulva lactuca*: Experimental observations and modelling using WHAM. *Marine Chemistry* **110**, 176-184.
- Vignati, D. A. L., Camusso, M., and Dominik, J., 2005. Estimation of the truly dissolved concentrations of Cd, Cu, Ni, and Zn in contrasting aquatic environments with a simple empirical model. *Ecological Modelling* **184**, 125-139.
- Wang, D., Wang, C., Zhao, G., Wei, Z., Tao, Y., and Liang, X., 2001. Composition, Characteristic and Activity of Rare Earth Element-Bound Polysaccharide from Tea. *Bioscience, Biotechnology, and Biochemistry* **65**, 1987-1992.
- Wang, W.-X. and Dei, R. C. H., 1999. Kinetic measurements of metal accumulation in two marine macroalgae. *Marine Biology* **135**, 11-23.
- Webster, E. A. and Gadd, G. M., 1996a. Cadmium replaces calcium in the cell wall of *Ulva lactuca*. *BioMetals* **9**, 241-244.
- Webster, E. A. and Gadd, G. M., 1996b. Perturbation of monovalent cation composition in *Ulva lactuca* by cadmium, copper and zinc. *BioMetals* **9**, 51-56.
- Webster, E. A., Murphy, A. J., Chudek, J. A., and Gadd, G. M., 1997. Metabolism-independent binding of toxic metals by *Ulva lactuca*: cadmium binds to oxygen-containing groups, as determined by NMR. *BioMetals* **10**, 105-117.
- Wei, Z., Hong, F., Yin, M., Li, H., Hu, F., Zhao, G., and Wong, J., 2005a. Structural differences between light and heavy rare earth element binding chlorophylls in naturally grown fern *Dicranopteris linearis*. *Biological Trace Element Research* **106**, 279-297.
- Wei, Z., Hong, F., Yin, M., Li, H., Hu, F., Zhao, G., and WoonchungWong, J., 2005b. Subcellular and molecular localization of rare earth elements and structural characterization of yttrium bound chlorophyll a in naturally grown fern *Dicranopteris dichotoma*. *Microchemical Journal* **80**, 1-8.
- Weich, R. G., Lundberg, P., Vogel, H. J., and Jensén, P., 1989. Phosphorus-31 NMR studies of cell wall-associated calcium-phosphates in *Ulva lactuca*. *Plant Physiology* **90**, 230-236.
- Wen, L.-S., Stordal, M. C., Tang, D., Gill, G. A., and Santschi, P. H., 1996. An ultraclean

- cross-flow ultrafiltration technique for the study of trace metal phase speciation in seawater. *Marine Chemistry* **55**, 129-152.
- Wong, M. H., Kwok, T. T., and Ho, K. C., 1982. Heavy metals in *Ulva lactuca* collected within Tolo Harbour, an almost landlocked sea. *Hydrobiological Bulletin* **16**, 223-230.
- Xue, H. B., Stumm, W., and Sigg, L., 1988. The Binding of Heavy-Metals to Algal Surfaces. *Water Research* **22**, 917-926.
- Yee, N., Benning, L. G., Phoenix, V. R., and Ferris, F. G., 2004. Characterization of metal-cyanobacteria sorption reactions: A combined macroscopic and infrared spectroscopic investigation. *Environmental Science & Technology* **38**, 775-782.
- Yoon, Y.-Y., Martin, J.-M., and Cotté, M. H., 1999. Dissolved trace metals in the Western Mediterranean Sea: total concentration and fraction isolated by C18 Sep-Pak technique. *Marine Chemistry* **66**, 129-148.
- Zeroual, Y., Moutaouakkil, A., Dzairi, F. Z., Talbi, M., Chung, P. U., Lee, K., and Blaghen, M., 2003. Biosorption of mercury from aqueous solution by *Ulva lactuca* biomass. *Bioresource Technology* **90**, 349-351.